

# **The role of *p*-coumaric acid on physiological and biochemical response of chia seedling under salt stress**

**Mbukeni Andrew Nkomo**

A thesis submitted in partial fulfilment of the requirements for the degree of Philosophiae Doctor in the Department of Biotechnology, University of the Western Cape



UNIVERSITY *of the*  
WESTERN CAPE

Supervisor: Dr. Ashwil Klein

Co-supervisor: Prof. Marshall Keyster

**December 2020**

# UNIVERSITY GENERAL PLAGIARISM DECLARATION



## FACULTY OF NATURAL SCIENCE GENERAL PLAGIARISM DECLARATION

**Name:** Mbukeni Andrew Nkomo

**Student number:** 2870274

1. I, Mbukeni Andrew Nkomo, declare that this thesis entitled: **The role of *p*-coumaric acid on physiological and biochemical response of chia seedling under salt stress**, is my own work.
2. I know what plagiarism entails, namely to use another's work and to present it as my own without attributing the sources in the correct way. (Refer to University Calendar part 1 for definition)
3. I know that plagiarism is a punishable offence because it constitutes theft.
4. I understand the plagiarism policy of the Faculty of Natural Science of the University of the Western Cape.

-----  
Signature

-----09/12/2020-----

Date

**KEYWORDS**

Antioxidant enzymes

Ascorbate peroxidase

Chia

Chlorophyll

Glycine betaine

Lipid peroxidation

*p*-Coumaric acid

Peroxidase

Photosynthesis

Piperonylic acid

Plant proteomics

Proline

Pseudocereals

Reactive oxygen species

Salt stress

Superoxide radical

Superoxide dismutase

Osmoprotectant

Oxidative stress



## GENERAL ABSTRACT

### THE ROLE OF *p*-COUMARIC ACID ON PHYSIOLOGICAL AND BIOCHEMICAL RESPONSE OF CHIA SEEDLING UNDER SALT STRESS

**M.A Nkomo**

PhD Thesis, Department of Biotechnology, University of the Western Cape

The role of phenolic acids in mitigating salt stress tolerance have been well documented. However, there are contradicting reports on the effect of exogenously applied phenolic acids on the growth and development of various plants species. A general trend was observed where phenolic acids were shown to inhibit plant growth and development, with the exception of a few documented cases. One of these such cases is presented in this thesis. This study investigates the role of exogenously applied *p*-coumaric acid (*p*-CA) on physio-biochemical and molecular responses of chia seedlings under salt stress. This study is divided into three parts. *Part one (Chapter 3) focuses on the impact of exogenous p-coumaric acid on the growth and development of chia seedlings.*

In this section, chia seedlings were supplemented with exogenous *p*-CA and the various biochemical and plant growth parameters were measured. The results showed that exogenous *p*-CA enhanced the growth of chia seedlings. An increase in chlorophyll, proline and superoxide oxide contents were also observed in the *p*-CA treatment relative to the control. We suggested that the increase in chia seedling growth could possibly be via the activation of reactive oxygen species-signalling pathway involving  $O_2^-$  under the control of proline accumulation (Chapter 3). Given the allopathy, nature of *p*-coumaric acid it is noteworthy that the response observed in this study may be species dependent, as contrasting responses have been reported in other plant species.



*Part two (Chapter 4) of this study investigates the influence of piperonylic acid (an inhibitor of endogenous p-coumaric acid) on the growth and development of chia seedlings.*

In trying to illustrate whether *p*-CA does play a regulatory role in enhancing pseudocereal plant growth, we treated chia seedlings with the irreversible inhibitor of C4H enzyme, to inhibit the biosynthesis of endogenous *p*-CA. In this section, chia seedlings were treated with piperonylic acid and changes in plant growth, ROS-induced oxidative damage, *p*-CA content and antioxidant capacity was monitored. Inhibition of endogenous *p*-CA restricted chia seedling growth by enhancing ROS-induced oxidative damage as seen for increased levels of superoxide, hydrogen peroxide and the extent of lipid peroxidation. Although an increase in antioxidant activity was observed in response to piperonylic acid, this increase was not sufficient to scavenge the ROS molecules to prevent oxidative damage and ultimate cellular death manifested as reduced plant growth. The results presented in this section support our hypothesis that *p*-CA play an important regulatory role in enhancing chia seedling growth and development as shown in Chapter 3.

*Part three (Chapter 5) seeks to identify and functionally characterise p-coumaric acid induced putative protein biomarkers under salt stress conditions in chia seedlings.*

Previous studies have shown that *p*-CA reversing the negative effect caused by NaCl-induced salt stress. While these studies were able to demonstrate the involvement of *p*-CA in promoting plant growth under salt stress conditions, they focussed primarily on the physiological aspect, which lacks in-depth biochemical and molecular analysis (ionomic and proteomic data) which could help in detecting the genes/proteins involved in salt stress tolerance mechanisms. A comparative ionomics and proteomic study was conducted, with the aim of elucidating the pivotal roles of essential macro elements and/or key protein markers involved in *p*-CA induced salt stress tolerance in chia seedlings. With the exception of Na, all the other macro elements were decreased in the salt treatment. Contrary to what was observed for the salt treatment most

of the macro elements were increased in the *p*-CA treatment. However, the addition of exogenous *p*-CA to salt stressed seedlings showed an increase in essential macro elements such as Mg and Ca which have been shown to play a key role in plant growth and development. In the proteomic analysis we identified 907 proteins associated with shoots across all treatments. Interestingly, only eight proteins were conserved amongst all treatments. A total of 79 proteins were unique to the *p*-CA, 26 to the combination treatment (NaCl + *p*-CA) and only two proteins were unique to the salt stress treatment. The unique proteins identified in each of the treatments were functionally characterised to various subcellular compartments and biological processes. Most of the positively identified proteins were localised to the chloroplast and plays key roles in photosynthesis, transportation, stress responses and signal transduction pathways. Moreover, the protein biomarkers identified in this study (especially in the *p*-CA treatment) are putative candidates for genetic improvement of salt stress tolerance in plants.

*The work reported in Chapter 3 has been published in a peer-reviewed journal [M Nkomo, A Gokul, M Keyster, A Klein (2019) Exogenous p-Coumaric Acid Improves Salvia hispanica L. Seedling Shoot Growth. Plants 8 (12), 546].*

**December 2020**

## THESIS SYNOPSIS

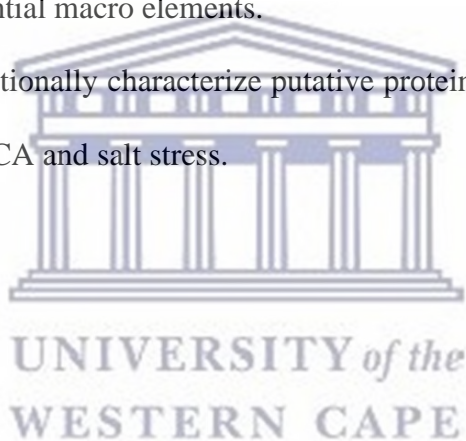
This synopsis, provides a brief overview of this research and summarily outlines the major aims of this study. This thesis is presented in seven chapters. **Chapter 1** (Literature review) explores and coherently presents existing information around the subject under study. It further provides a justification for this research; the questions driving the research and outlines the importance of this study. **Chapter 2** (Methods and Materials) describes the materials and methods which were followed in partaking this research. **Chapter 3** describes the role of exogenous *p*-coumaric acid in improving chia seedling growth possibly via activation of a ROS signalling pathway involving  $O_2^-$  under the control of proline accumulation. This work was recently published in *Plants* (an MDPI Journal). **Chapter 4** describes the role of piperonylic acid (an coumarate-4-hydroxylase inhibitor) on the growth and biochemical responses of chia plants. Piperonylic acid is an irreversible inhibitor of the enzyme (C<sub>4</sub>H) that produces *p*-coumaric acid. The work presented in this chapter supports our argument that *p*-coumaric acid is directly involved in enhancing growth promotion of chia plants. **Chapter 5**, seeks to identify and functionally characterise *p*-coumaric acid induced putative protein biomarkers under salt stress conditions in chia seedlings. **Chapter 6** summarises the outcomes and conclusion remarks drawn throughout the thesis, while highlighting the important aspects that could open avenues towards future and further research studies. **Chapter 7** compiles the literature cited throughout the thesis.

## AIMS AND OBJECTIVES OF THIS STUDY

The aim of this study was to investigate the role of exogenous *p*-coumaric acid on the physiological and molecular responses of chia plants under salt stress conditions.

The objectives of this study were to:

- i. Investigate the role of exogenously *p*-CA in chia plant growth.
- ii. Determine the effect of *p*-CA inhibition (using piperonylic acid) in chia seedling growth and mineral nutrient accumulation.
- iii. Investigate the role of applied *p*-CA in modulating chia seedlings during long-term by studying essential macro elements.
- iv. Identify and functionally characterize putative proteins bio-markers in chia shoots in response to *p*-CA and salt stress.



## **DEDICATION**

**Dedicated to my late father Buti Zachariah Nkomo and Uncle Vuyani**

**Comfort Sibeko.**



**To My Daughter Mabatho I went through this process so as to motivate you that you can accomplish anything in life as long as you set your mind to**

**it.**

**I LOVES YOU**

## ACKNOWLEDGEMENTS

Firstly, I would like to thank my **Ancestors** for giving me the strength, guidance and providing the direct link to **Umvelibanzi** whom without I am nothing.

Secondly, I would like to extend a special thanks to the **Good Dr.** (my promoter) **Dr. Ashwil Klein** for the support and wisdom you had instilled in me through my journey as a post graduate student. **Prof. Marshall Keyster** your guidance and mentorship as a co-promotor is also noted and highly appreciated.

I would like to acknowledge my mother (**Nomfusi Nkomo**) and (**The Lebatlang family**), for their endless love, support they have given to my daughter “**Mmabatho Nkomo**” throughout my absents as a post graduate student.

**Dr Royla Minnies-Ndimba, Nokuthula Nkomo, Khaya Sibeko, Zintle Kolo, “the Late” Allison Mhlakaza (Nozulu)** and many more that I couldn’t count, without your financial support this study would have never been completed.

It would be unfair to **name my friends** and live the rest of the people out, so I would rather thank the entire Plant Omics Laboratory and the Department of Biotechnology both past and present members for intellectual conversation and constructive criticism that I have receive throughout the years.

Lastly, thank you to the University of the Western Cape, GrainSA, the National Research Foundation (NRF) and the Agricultural Research Council (ARC).



## LIST OF TABLES

Table 2.1. List of chemicals and suppliers.....	20
Table 2.2 List of buffers and stock solutions prepared for this study .....	23
Table 3.1. Chlorophyll and osmolyte concentration in chia seedling shoots in response to <i>p</i> -coumaric acid. Data represent the means ( $\pm$ SE) of six independent experiments and different letters per row indicate the mean values that are significant different at $p \leq 0.05$ using the Tukey-Kramer test. ....	41
Table 4.1. Content of essential macro elements in the shoots of chia seedlings. Macro elements data expressed in $\text{mg.g}^{-1}$ FW, presented by the means $\pm$ SE ( $n = 3$ ). The blue arrow represents an increase in macro elements, while the red arrow represents a decrease when comparing the <i>p</i> -CA treatment to the control. ....	55
Table 5.1. The differences in mineral contents ( $\text{mg.g}^{-1}$ FW) in response to <i>p</i> -CA, salt stress and a combination of <i>p</i> -CA and salt stress. The data that represents the mean $\pm$ SE in same column with dissimilar letters are significant at $p \leq 0.05$ . The blue arrow shows an increase in mineral content, while the red arrow represents a decrease and the star sign shows that no significant difference was observed when compared to the control. ....	67
Table 5.2. Shoot protein concentrations of chia seedlings in response to different treatments .....	68
<b>Table 5.3.</b> Representative of unique protein isoforms identified in the combined treatment .	75

## LIST OF FIGURES

- Figure 1.1. *Salvia hispanica* L. (chia) plants grown in the field.....5
- Figure 1.2. Synthesis of aromatic amino acids via the pentose phosphate pathway (PPP). Oxidative PPP provides a precursor erythrose-4-phosphate for the shikimate pathway. The shikimate pathway converts sugar phosphates into aromatic amino acids such as phenylalanine (Phe) and tyrosine (Tyr).....8
- Figure 1.3. The chemical structural difference between the benzoic and hydroxycinnamic phenolic compound.....9
- Figure 1.4. Biosynthetic pathways of *p*-coumaric acid. The phenylalanine route (PAL-C<sub>4</sub>H) describes the synthesis of *p*-coumaric acid in whereas the tyrosine route (PAL/TAL and TAL) describe its synthesis in microbes.....13
- Figure 1.5. Biosynthesis of hydroxycinnamic acids and their derivatives involved in lignin production in plants. The biosynthetic enzymes resulting in the biosynthesis of lignin precursors (monolignols) and lignins are: phenylalanine ammonia-lyase (PAL); tyrosine ammonia-lyase (TAL); cinnamate 4-hydroxylase (C<sub>4</sub>H); 4-hydroxycinnamate 3-hydroxylase (C<sub>3</sub>H); caffeic acid 3-O-methyltransferase (COMT); ferulate 5-hydroxylase (F<sub>5</sub>H); 4-coumarate (4CL): CoA ligase; coumaroyl-coenzyme A 3-hydroxylase (CCoA 3H); caffeoyl-coenzyme A O-methyltransferase (CCoA OMT); cinnamoyl-CoA reductase (CCR); and cinnamyl alcohol dehydrogenase (CAD).....13
- Figure 1.6. An illustration of the conventional polyacrylamide gel. A top ‘stacking’ gel containing a lower concentration of acrylamide facilitates entry of SDS-coated polypeptides into the ‘resolving’ gel where the bands separate according to molecular mass. Separation is shown by the different migration of bands (shown in red) within the gel.....16

Figure 3.1. Concentration dependant germination of chia seedlings. The white bar = 2 cm (A) Data represent the means ( $\pm$ SE) of three independent experiments and different letters indicate the mean values that are significantly different at  $p \leq 0.05$  using the Tukey Kramer test.....39

Figure 3.2. Representative chia seedling shoots under control and *p*-CA treatments (A). Shoot height (B), shoot fresh weight (C) and shoot dry weight (D) of chia seedlings treated with *p*-CA. Data represent the mean ( $\pm$ SE) from six independent experiments. Different letters represent statistical significance at  $p \leq 0.05$  (Tukey-Kramer test). .....40

Figure 3.3. Superoxide content (A), total SOD activity (B) and the activity of individual SOD isoforms (C) in control and *p*-CA treated chia seedlings. Data represent the mean ( $\pm$  SE) from six independent experiments. Different letters represent statistical significance at  $p \leq 0.05$  (Tukey-Kramer test).....42

Figure 3.4. Hydrogen peroxide content (A) and lipid peroxidation (B) in chia seedling shoots under control and *p*-CA treatment. Data represent the mean ( $\pm$  SE) six independent experiments. Different letters represent statistical significance at  $P \leq 0.05$  (Tukey-Kramer test). .....43

Figure 3.5. Schematic model of *p*-CA signalling in chia seedlings. Inhibition or scavenging (red lines). Activation or increase (green lines). Indirect activation or indirect increase (dashed green line). Did not occur in this study (blue crosses).....46

Figure 4.1. Exogenous PA restricts chia seedlings growth and *p*-CA content. Plant growth parameters include individual representatives of each treatment (A) shoot height (B), fresh weight (C), leaf area (D) and measurement of *p*-CA (E). Data represent the mean ( $\pm$ SE) from

six independent experiments. Different letters above the error bars indicate means that are statistically significantly different at 5% level of significance. ....51

Figure 4.2. The influence of PA on superoxide content (A) hydrogen peroxide content (B) and malondialdehyde content (C). The O<sub>2</sub>- content was measured using freshly harvested shoot material from chia seedlings. Data represent the mean ( $\pm$  SE) of six independent experiments. Means with different letters are significantly different from each other ( $p \leq 0.05$ ). ....52

Figure 4.3. PA increased proline content (A) and total SOD activity (B) in chia seedlings shoots. Data represent the mean ( $\pm$  SE) of six independent experiments. Different letters represent statistical significance at  $p \leq 0.05$ . ....53

Figure 4.4. Changes in shoot APX (A), CAT (B) and POD (C) activities in response to exogenous PA. Data represent the mean ( $\pm$  SE) of six independent experiments. Different letters represent statistical significance at  $p \leq 0.05$ . ....54

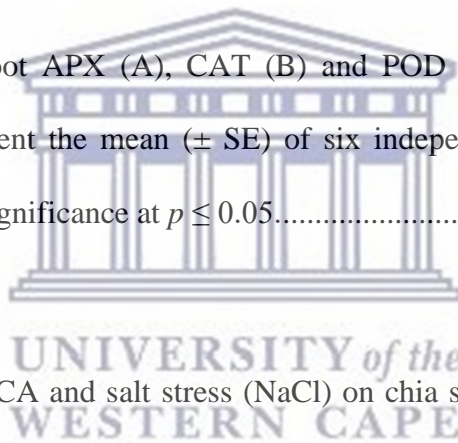


Figure 5.1. The effect of *p*-CA and salt stress (NaCl) on chia seedling growth and biomass. Changes in (A) shoot length of chia seedlings (left to right; Control, *p*-CA, NaCl and NaCl + *p*-CA) and (B) fresh weights and (C) dry weights was measured in response to the different treatments. Data represent the mean ( $\pm$ SE) from six independent experiments. Different letters represent statistical significance at  $P \leq 0.05$  (Tukey-Kramer test). ....65

Figure 5.2. One – dimensional shoots proteome profile of chia in response to *p*-CA and salt stress. Protein extracts (10  $\mu$ g) from different treatments were size fractionated on a 12 % denaturing 1D SDS polyacrylamide gel. Black arrows indicate differences that were visually observed. ....68

Figure 5.3. Total ion chromatograms of the system blank (A) and suitability mixture (B) injection.....69

Figure 5.4. The total ion chromatography LC MS analysis of chia seedlings treated with *p*-CA and NaCl-induced salt stress. A) Control, B) *p*-CA, C) NaCl and D) NaCl + *p*-CA. ....70

Figure 5.5. Detection of *p*-CA responsive protein on chia seedlings exposed to salt stress. A) Total number of proteins identified in the different treatments. B) Venn diagram illustrating the common and unique proteins identified in all treatments. ....71

Figure 5.6. Subcellular localisation of positively identified proteins expressed in chia shoots. ....72

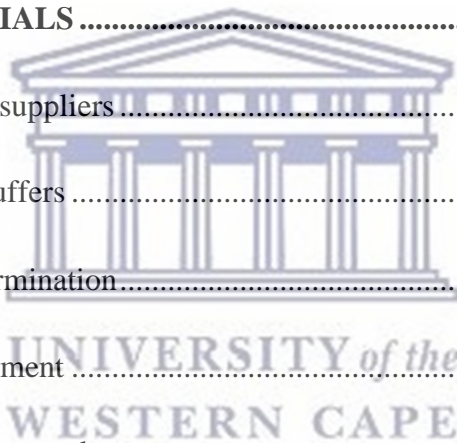
Figure 5.7. Identification and gene ontology classification of unique isoform proteins based on subcellular component. A) Protein isoforms identified in the *p*-CA treatment. B) Subcellular localisation of identified protein isoforms. C) Biological processes of proteins isoforms in *p*-CA treatment. D) Interaction network of unique protein isoforms in *p*-CA treatment. Red nodes represent identified protein isoforms. Blue line colour indicates protein interaction. Green nodes represent protein interaction from my inquiry database. ....74

<b>UNIVERSITY GENERAL PLAGIARISM DECLARATION.....</b>	<b>i</b>
<b>KEYWORDS.....</b>	<b>i</b>
<b>GENERAL ABSTRACT.....</b>	<b>iii</b>
<b>THESIS SYNOPSIS.....</b>	<b>vi</b>
<b>AIMS AND OBJECTIVES OF THIS STUDY .....</b>	<b>vii</b>
<b>DEDICATION.....</b>	<b>viii</b>
<b>ACKNOWLEDGEMENTS .....</b>	<b>ix</b>
<b>LIST OF TABLES .....</b>	<b>x</b>
<b>LIST OF FIGURES .....</b>	<b>xi</b>
<b>CHAPTER 1.....</b>	<b>1</b>
<b>LITERATURE REVIEW .....</b>	<b>1</b>
1.1 Introduction .....	1
1.2 Pseudocereals .....	3
1.3 Chia .....	4
<i>1.3.1. Botanical characteristics.....</i>	<i>4</i>
<i>1.3.2. Nutritional benefit.....</i>	<i>5</i>
<i>1.3.3. Health benefits.....</i>	<i>6</i>
1.4 Phenolic compounds .....	7
<i>1.4.1. Phenolic acid diversification and biosynthesis .....</i>	<i>8</i>
<i>1.4.2. Phenolic acids as plant signalling molecules.....</i>	<i>10</i>
<i>1.4.3. Phenolic acids and plant stress responses .....</i>	<i>10</i>





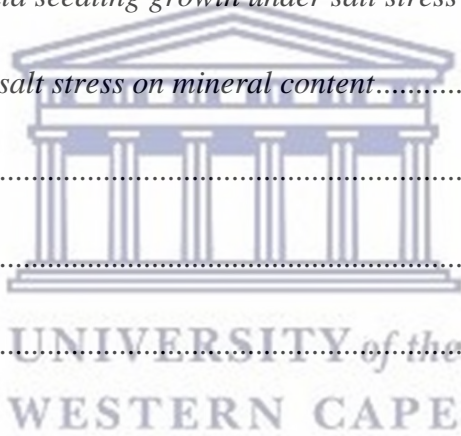
1.5. <i>p</i> -Coumaric acid in plants .....	12
1.5.1. <i>p</i> -Coumaric acid as an antioxidant .....	14
1.5.2 <i>p</i> -Coumaric acid in plant growth and development .....	14
1.6. Integrating multi-omics approaches for improving stress tolerance .....	15
1.6.1. Proteomics .....	15
1.6.2. Metabolomics/Ionomics .....	17
1.7. In summary .....	18
<b>CHAPTER 2 .....</b>	<b>20</b>
<b>METHODS AND MATERIALS .....</b>	<b>20</b>
2.1. List of chemicals and suppliers .....	20
2.2. Stock solutions and buffers .....	23
2.3. Evaluation of seed germination .....	26
2.4. Plant growth and treatment .....	26
2.5. Measurement of plant growth .....	27
2.6. Measurement of shoot chlorophyll content .....	27
2.7. Measurement of <i>p</i> -coumaric acid content .....	27
2.8. Protein extraction for biochemical analysis .....	27
2.9. Measurement of superoxide content .....	28
2.10. Measurement of hydrogen peroxide content .....	28
2.11. Determination of malondialdehyde (MDA) content .....	28
2.12. Measurement and detection of SOD activity .....	29



2.13. Measurement of total APX activity .....	29
2.14. Measurement of total CAT activity .....	30
2.15. Measurement of total POD activity .....	30
2.16. Determination of proline content .....	30
2.17. Determination of glycine betaine .....	31
2.18. Profiling the shoot proteome of chia seedlings .....	31
2.18.1. <i>Sample preparation for proteomic analysis</i> .....	31
2.18.2. <i>One dimensional polyacrylamide gel electrophoresis (1D PAGE)</i> .....	32
2.18.3. <i>Protein pellet solubilization</i> .....	32
2.18.4. <i>On-bead digest</i> .....	33
2.18.5. <i>Peptide fractionation and detection using LC-MS/MS</i> .....	34
2.18.6. <i>Protein validation and data analysis</i> .....	35
2.19. Statistical analysis .....	35
<b>CHAPTER 3</b> .....	<b>37</b>
<b>EXOGENOUS <i>p</i>-COUMARIC ACID IMPROVES CHIA SEEDLING SHOOT GROWTH</b> .....	<b>37</b>
3.1. Abstract .....	37
3.2. Introduction .....	37
3.3. Results .....	39
3.3.1. <i>p-CA alters chia germination percentage</i> .....	39
3.3.2. <i>p-CA improves chia seedling growth</i> .....	39
3.3.3. <i>The effect of exogenous p-CA on chlorophyll metabolism and osmolyte content</i> ..	40

3.3.4. <i>Effects of p-CA on superoxide radical and superoxide dismutase</i> .....	41
3.3.5. <i>Effects of exogenous application of p-CA on H<sub>2</sub>O<sub>2</sub> and its extent of lipid peroxidation</i> .....	42
3.4. Discussion .....	43
3.5. Conclusion.....	46
<b>CHAPTER 4.....</b>	<b>48</b>
<b>INHIBITION OF <i>p</i>-COUMARIC ACID ALTERS CHIA SEEDLING GROWTH, MINERAL CONTENT AND ROS SCAVENGING CAPACITY .....</b>	<b>48</b>
4.1. Abstract .....	48
4.2 Introduction .....	49
4.3. Results .....	50
4.3.1. <i>Inhibition of p-CA restricts chia plant growth</i> .....	50
4.3.2. <i>PA increases ROS accumulation and the extent of lipid peroxidation</i> .....	51
4.3.3. <i>Exogenous PA augments proline and total SOD in the shoots of chia seedlings</i> ...	52
4.3.4. <i>PA alters changes in hydrogen peroxide scavenging antioxidant enzyme activities</i> .....	53
4.3.5. <i>A survey of essential macro-elements in response to exogenous PA</i> .....	54
4.4. Discussion .....	55
4.4.1. <i>Inhibition of p-CA impairs growth and development in chia seedlings</i> .....	55
4.4.2. <i>PA augments ROS content and reduces membrane stability</i> .....	56
4.4.3. <i>PA augments proline accumulation</i> .....	57
4.4.4. <i>PA augments antioxidant enzymes</i> .....	58

4.4.5. <i>PA augments essential mineral content</i> .....	59
4.5. Conclusions .....	60
<b>CHAPTER 5</b> .....	<b>62</b>
<b><i>p</i>-COUMARIC ACID AND SALT STRESS DIFFERENTIAL ALTERS THE IONOMIC AND PROTEOMIC PROFILES OF CHIA SHOOTS</b> .....	<b>62</b>
5.1. Abstract .....	62
5.2. Introduction .....	63
5. 3. Results .....	64
5.3.1. <i>p-CA improves chia seedling growth under salt stress</i> .....	64
5.3.2. <i>Effects p-CA and salt stress on mineral content</i> .....	65
<i>a. Na content</i> .....	65
<i>b. K content</i> .....	66
<i>c. P content</i> .....	66
<i>d. Mg content</i> .....	66
5.3.3. <i>Separation and visualization of chia shoot proteome</i> .....	67
5.3.4 <i>Identification and subcellular localisation of shoot proteins using LC MS analysis</i> .....	69
5.3.5 <i>Functional characterisation of p-CA induced protein isoforms</i> .....	73
5.3.6 <i>Functional characterisation of p-CA induced protein isoforms under salt stress</i> ..	74
5.4. Discussion .....	75
5.4.1 <i>p-CA improves chia seedling shoot biomass under salt stress</i> .....	75
5.4.2. <i>Exogenous p-CA alters Mg and Ca elements under salt stress conditions</i> .....	76



5.4.3. Towards the proteomic mapping of p-CA induced salt stress tolerant .....	77
5.3.3. Protein isoforms identified in chia seedlings .....	78
a. Proteins isoforms associated with photosynthesis.....	78
b. Proteins Associated with Transport .....	79
c. Proteins isoforms associated with stress response and signal transduction.....	79
d. Other functional proteins.....	80
5.5. Conclusion.....	80
<b>CHAPTER 6.....</b>	<b>82</b>
<b>CONCLUDING REMARKS AND FUTURE OUTLOOK .....</b>	<b>82</b>
<b>CHAPTER 7.....</b>	<b>84</b>
<b>REFERENCES.....</b>	<b>84</b>
<b>SUPPLEMENTARY DATA.....</b>	<b>106</b>



# CHAPTER 1

## LITERATURE REVIEW

### 1.1 Introduction

The global food system has major impacts on the environment, which threatens food security and sustainability. Abiotic stress conditions including saline soils, greenhouse gas emissions, water abstraction, air pollution and loss of biodiversity are some of the major factors that negatively affect the environment (Pathak et al. 2012). Ensuring global food security is the second of 17 Sustainable Development Goals (SDG) adopted by the United Nations as part of its 2030 Agenda for Sustainable Development (Lee et al. 2016) but achieving this while reducing negative environmental impacts is one of the greatest challenge's humanity faced with. The drive towards a sustainable global food system will become more difficult with the constant increase in global population. Although the current global food supply (with timely distribution) is sufficient to feed the world's population to avoid hunger, food production must increase dramatically in the next decades (Berners-Lee et al. 2018). According to Food and Agriculture Organisation of the United Nations the global population will increases to  $\approx 9.7$  billion in 2050 (Berners-Lee et al. 2018). Economically important staple crops such maize, rice and wheat provides at least 30% of the food calories to more than 4.5 billion people in 94 developing countries. This include 900 million poor consumers for whom maize is the preferred staple. Approximately 67% of the total maize production in the developing world comes from low and lower middle-income countries (Weatherly et al. 2020). Therefore, maize plays an important role in the livelihoods of millions of poor farmers. The current global population is around 7.8 billion people and by 2050, the figure is expected to rise to approximately 9.3 billion. Between now and 2050, the demand for maize in the developing world will double (Rosegrant et al. 2009). The nature of the demand for maize is also changing.



Maize is an important food crop but over the past decade, its demand as livestock feed has grown tremendously. To add insult to injury, most of the traditional staple crops including maize are prone to environmental constraints such as high saline soils. Salt stress is one of the most brutal environmental factors limiting the yield of most crop plants due to their inherent sensitivity, resulting in extensive financial losses to the agricultural sector (Munns 2002; Munns and Tester 2008). In South Africa, salt stress effect is estimated at 31.4% of total arable land, to which 15% of the affected area is under irrigation (De Villiers et al. 2003). To overcome the overreliance on a few staple crops to feed the global population; there is a need to explore alternative food crops with comparable or superior nutritional characteristics, resilience to abiotic stresses to ensure food security and sustainability for the ever-growing global population. The emergence of pseudocereals as alternative or supplementary food source to the global food system will alleviate the overreliance on the more traditional cereal crops such as maize, wheat and rice (Joshi et al. 2019). Unlike the traditional staple crops, these underutilized, nutrient-rich crops are very resilient to harsh environments such as drought, salinity, extreme temperature and yield well with limited resources (Mabhaudhi et al. 2019). Pseudocereals are plants that produce fruits or seeds, which are used and consumed as grains, although they are classified as neither grasses nor true cereal grains. They are typically high in protein and other nutrients, gluten-free, and are considered whole grains (Comino et al. 2013). Pseudocereals produce starch-rich seeds that can be used in food applications similarly to cereal grains (Rodríguez et al. 2020). The most widely known representatives include chia, buckwheat, amaranth, quinoa, and canihua, which is less well known. All of these pseudocereals have good nutritional compositions, with high concentrations of essential amino acids, essential fatty acids, minerals, and some vitamins. Apart from its nutritional profiles, the regular consumption of pseudocereals promotes health benefits as reduced risk of cardiovascular disease, diabetes, anticarcinogenic effect, anti-inflammatory, and antimicrobial

(Gorinstein et al. 2002; Mir et al. 2018). These health benefits are attributed to the presence of isoflavonoids and phytosterols in the grain crops.

This chapter, will review the agricultural importance of pseudocereals (with reference to chia) as a potential nutritive supplement to the traditional cereals staple crops, by exploring to the impact of abiotic stress conditions on growth and production. In addition, this review will also highlight the role of phenolic compounds in regulating plant growth and development by exploring the mechanisms adopted by plants to cope under abiotic stress (salinity) conditions. Furthermore, different scientific approaches and strategies will be explored to improve our general understanding of the role of these vital compounds (phenolics) within plant systems.

## 1.2 Pseudocereals

Pseudocereals are defined as fruits or seeds of non-grass species that are consumed in the same way as cereal species. Pseudocereals are highly effective supplements with superior nutritional traits to conventional cereals. The protein contents and quality of pseudocereals (quinoa, chia, amaranths and buckwheat) are much higher than cereals, containing higher amounts of lysine, which is quite low in cereals. When considering digestibility, bioavailability of lysine and net protein utilisation, pseudocereal proteins are definitely better when compared to traditional staple cereal crops. The nutritive value of pseudocereals is very much competitive if not superior to conventional cereal crops. Apart from its high protein contents, pseudocereals have high amounts of unsaturated oils, dietary fiber (Mota et al. 2016; Tang et al. 2016) and are rich in a wide range of phenolic compounds such as flavonoids, phenolic acids, essential trace elements and vitamins. These compounds have been shown to play a significant role in reducing the risk of heart diseases, cancers, while improving brain function and promoting growth and development (Li and Zhang 2001; Gorinstein et al. 2002; Kalinova and Dadakova 2009). Pseudocereals have also shown a low allergenicity of gluten disease such as celiac disease (CD). Gorinstein et al. (2007), suggested that pseudocereals can be implemented into,

not only gluten sensitive individual's diets, but have also been recommended in children-meals as a replacement of crop products containing gluten traces (Gorinstein et al. 2007).

### **1.3 Chia**

*Salvia hispanica* L., commercially known as chia, was first cultivated in the 16th century by the pre-Columbian communities of Mexico and Guatemala (Ayerza and Coates 2005; Ixtaina et al. 2008; Sandoval – Oliveros and Paredes – Lopez 2012). Chia, is an annual herbaceous plant and member of the Lamiaceae family. The genus *Salvia* consists of approximately 900 species, that are widely distributed in several regions around the world, including Southern Africa, Central America, North and South America, and South-East Asia (Ixtaina et al. 2008; Mohd Ali et al. 2012). Chia is not only cultivated in the countries of its origin but in other territories such as Australia, Bolivia, Columbia, Peru, Argentina, America, and Europe. Although Mexico is recognized as the world's largest chia producer (Grancieri et al. 2019), Australia have made significant strides in the cultivation of this seed crop (Timilsena et al. 2016). Chia is regarded as a capable crop to be cultivated in arid and semiarid conditions like Australia, which has a similar climate to South Africa (Ixtaina et al. 2008; Mohd Ali et al. 2012; Reyes – Caudillo et al. 2008). This opens an avenue for South African growers to join in this growing market, as the current planting and production of chia seed oil are yet to meet the world market demand.

#### **1.3.1. Botanical characteristics**

Chia is cultivated for its seeds and produces white and purple flowers, which are 3 to 4 mm small and hermaphrodites. This plant can grow up to 2 meters tall and is sensitive to daylight (Mohd Ali et al. 2012). The leaves of chia plants are reverse petiolate and serrated, with size dimensions of 4-8 cm in length and 3-5 cm wide. A common feature of many lamiaceae species is that their leaves are squared, ribbed and hairy. Chia seeds are generally very small, oval-shaped, 2 mm long, 1 to 1.5 mm wide, and less than 1 mm thick (Grancieri

et al. 2019; Das 2018; Mohd Ali et al. 2012; Knez Hrnčič et al. 2018). The colour of the seed varies from black, grey, or black spotted to white. It has been established that there is no significant difference in the nutritional value of black and white colour chia seeds (Knez Hrnčič et al. 2018). Interestingly, a slight difference in the morphology of the two seeds were observed, with the white seeds being larger, thicker, and broader compared to black seeds. Chia can grow in poor soils that are not suitable for other grain species. This has sparked an interest in countries such as Argentina, Colombia, Ecuador, Peru, Bolivia, Paraguay and Australia to start cultivating chia for commercial purposes (Busilacchi et al. 2013).



Figure 1.1. *Salvia hispanica* L. (chia) plants grown in the field (Picture was taken by Brent Gnyp).

### 1.3.2. Nutritional benefit

Chia seeds have become one of the world's most recognizable foods based on their nutritional properties and medicinal values (Ullah et al. 2016; Das 2018; Mohd Ali et al. 2012; de Falco et al. 2017). When compared to the more traditional cereal staple crops, chia has a far superior nutritional profile. Despite their relatively small size, chia seeds are full of important nutrients and the high percentage of fatty acids (omega-3 fatty acids) present can be crucial for health, antioxidant, and antimicrobial activity (Ullah et al. 2016; Das 2018; Ixtaina et al. 2008; Reyes-

Caudillo et al. 2008; Ayerza 2016). In addition, these seeds are rich in antioxidants, high in fiber and other minerals such as iron, and calcium. Omega-3 is essential for growth and development, and has been recommended as a good source in baby food products (Gorinstein et al. 2007). Different parts of the chia plant are now commercially available for consumption as food supplement all over the world. When compared to other locally grown food crops such as canola and soybean, chia-based food products are slowly emerging as an alternative food source due to the nutritional and health benefits.

### **1.3.3. Health benefits**

The health benefits associated with chia plants have been widely reported (Mohd Ali et al. 2012; Ullah et al. 2016; Orona-Tamayo et al. 2017). According to Knez Hrnčič et al. (2019) chia seeds and their oils contain a large number of natural antioxidants, such as phytosterols and phenolic compounds. These natural antioxidants are playing a pivotal role in improving the quality of life in individuals that suffer from a wide variety of lifestyle diseases. Phytosterols are naturally occurring compounds present in plant cell membranes that resembles cholesterol (Shahzad et al. 2017). Dietary uptake of phytosterols, compete with cholesterol for absorption in the digestive system and consequently, blocks the absorption of cholesterol that in turn reduces the levels of blood cholesterol.

Phenolic compounds are the most abundant antioxidants found in the human diet. The main dietary sources of phenolic compounds are fruits and plant-derived beverages such as fruit juices, tea, coffee and red wine. Recent studies have demonstrated that the dietary intake of bioactive components such as phenolics in chia seeds are linked to the reduction of cardiovascular diseases (Poudyal et al. 2012) and have a protective effect against plasma oxidative stress (Marineli et al. 2015; Oliveira-Alves et al. 2017). A large array of phenolic acids have been identified in chia plants. These include caffeic acid and its precursor, *p*-



coumaric acid, which play a major role in the management and prevention of neurological disorders such as epilepsy (Coelho et al. 2015).

#### **1.4 Phenolic compounds**

Unlike primary metabolites such as starch or proteins, the abundance of phytochemicals in plants are quite low. Phytochemicals are essential for their pharmacological attributes and have always been part of the human diet (Padayachee and Baijnath 2020). Due to the perceived negative effects of phytochemicals for human nutrition, there has been an extensive drive to remove them from plant-based foods via plant breeding approaches and processing. However, recent research has shown that phytochemicals such as phenolic acids have positive effects for human health (Minatel et al. 2017). Phenolic compounds are the major source of natural antioxidants in plant food (Balasundram et al. 2006). As for vitamins and trace elements, there is a harmful, optimal, essential, or deficient dose, which has to be determined.

Plant phenolic compounds are an important class of secondary metabolites that are ubiquitous in nature and found in various plants species including fungi (Bravo 1998). They are grouped into three main categories including phenolics, flavonoids and tannins and are often referred to as polyphenols (Chung et al. 1998). However, the scope of this review will focus on phenolic acids, which are mostly referred to as monophenols due to the existence of only one phenol ring (Dixon 2004). The phenolic acids mostly found in the outer layers of most grains in both free and bound forms, are thought to inhibit the growth of various microorganisms (Dykes and Rooney 2006). On the other hand, phenolics have been exploited for several applications including bioremediation, plant growth promotion, and antioxidants as food additives (Bujor et al. 2015). Phenolics interact with the external environment stimulus in a complex signal transduction ranging from roots to leaves and are involve in the mobilization of nutrients



(Sharma et al. 2019). In humans, phenolic compounds have been linked to hyper protective effect against diabetes (Kim et al. 2012) and the lowering of cholesterol (Kim et al. 2015).

#### 1.4.1. Phenolic acid diversification and biosynthesis

To date, more than 8,000 phenolic acids have been identified in various plant species (Pandey and Rizvi 2009). Plant phenolic acids are derived from the concerted action of the pentose phosphate and shikimate pathways, where substrates generated from the catabolism of glucose-6-phosphate are converted to erythrose-4-phosphate leading to the synthesis of tyrosine and phenylalanine. The biosynthetic pathway of the aromatic amino acids tyrosine and phenylalanine are shown in Figure 1.2. The aromatic amino acid, phenylalanine is mostly responsible for the biosynthesis of hydroxycinnamic acids (Krause et al. 2003).

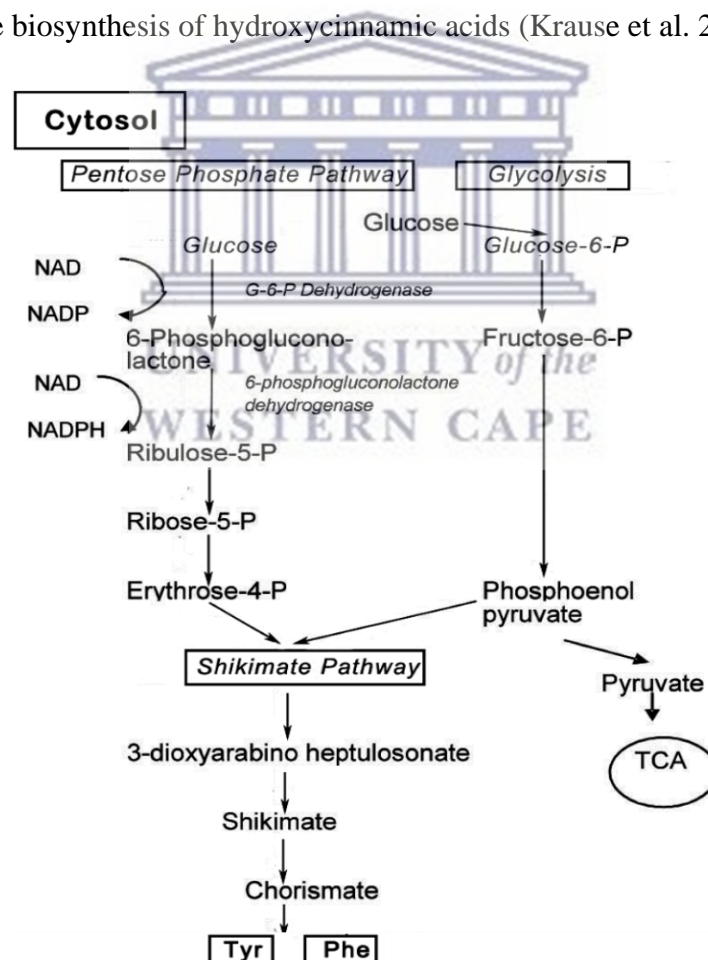


**Figure 1.2.** Synthesis of aromatic amino acids via the pentose phosphate pathway (PPP). Oxidative PPP provides a precursor erythrose-4-phosphate for the shikimate pathway. The shikimate pathway converts sugar phosphates into aromatic amino acids such as phenylalanine (Phe) and tyrosine (Tyr). Figure adapted from Lin et al. (2016).

Phenylalanine is an important amino acid in this pathway since this amino acid first produces cinnamic acid, a precursor for the majority of the hydroxybenzoic acids not produced by tyrosine. Generally, there are two classes of phenolic acids found in plants, which contain the hydroxybenzoic acid (C6-C1) and hydroxycinnamic acid (C6-C3) skeleton structures (Zhang and Stephanopoulos 2013). The hydroxybenzoic acids include benzoic-, protocatechuic-, gallic-, and vanillic acids, whereas the hydroxycinnamic acid includes *p*-coumaric-, caffeic-, sinapic-, and ferulic acids. Figure 1.3 shows the difference in chemical structures of hydroxybenzoic and hydroxycinnamic acids.

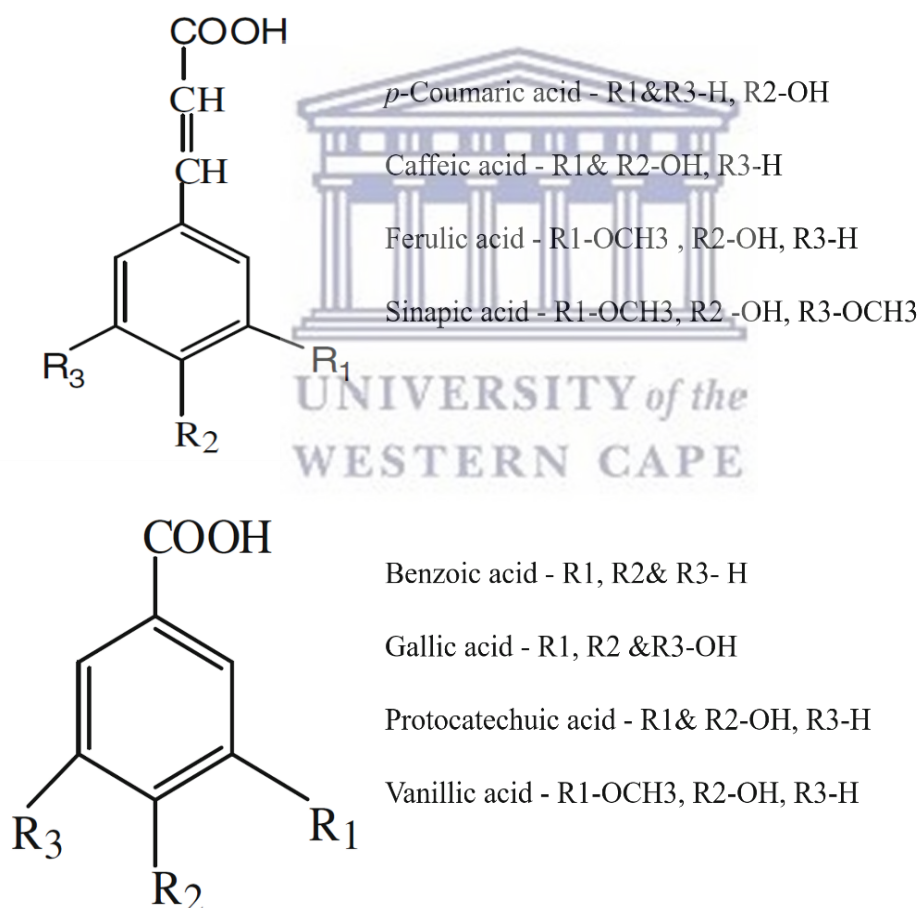


**Figure 1.3.** The chemical structural difference between the benzoic and hydroxycinnamic phenolic compound. Figure adapted from Sindhu et al. (2015).

#### **1.4.2. Phenolic acids as plant signalling molecules**

Phenolic acids act as key signalling molecules for induced resistance that is regulated by a network of interconnecting signal transduction pathways (Nkomo et al. 2019). They play a critical role during the initiation of establishment of arbuscular mycorrhizal and legumerhizobia symbioses, and can also have a role in plant defence. In legumes, phenolic acids are rapidly released from emerging roots during seed germination and seedling growth. A study by Mandal et al. (2009) showed that endogenous phenolic acids present in root nodules of *Vigna mungo* stimulate the efficiency of IAA production by its symbionts (*Rhizobium* sp.) and regulate nodule morphogenesis. Interestingly, the dual nature of phenolic acids has been demonstrated, where it has been shown to stimulate synthesis of plant hormones such as ABA (Hollapa and Blum 1991), whereas in other instances it has been shown to suppress or degrade IAA via the stimulation of IAA oxidase by dihydroflavonone naringenin (Stenlid, 1970).

Allelochemicals have been reported to mediate the synthesis or degradation of some plant hormones, such as the activation of ABA synthesis by ferulic acid (Hollapa and Blum, 1991), the degradation of IAA via the stimulation of IAA oxidase by dihydroflavonone naring.

#### **1.4.3. Phenolic acids and plant stress responses**

Plant phenolics or polyphenols are the most widely occurring groups of secondary metabolites with substantial physiological and morphological importance in plants. These phenolics play important roles in plant development, particularly in lignin and pigment biosynthesis. They also play a key role as defense compounds against abiotic stresses, such as drought, salinity stress, low temperatures, UV-B radiations, heavy metals and nutrient deficiency (Lattanzio 2013). It is thus very difficult to overestimate the functions of phenolic compounds in plant physiology and interactions with abiotic environments.

Drought is the major abiotic stress that affects plant growth and development and causes losses in agricultural production. A few lines of research have shown a marked increase in phenolics content under drought stress conditions (Naikoo et al. 2019). A study by Nakabayashi et al. (2014) reported that the accumulation in flavonoid is important to improve drought tolerance in wild-type and *Arabidopsis thaliana* mutants. This observation was supported by a previous study by Kirakosyan et al. (2003) who reported that an increase in flavonol levels in *Crataegus laevigata* and *Crataegus monogyna* in response to drought stress. In addition, Akula and Ravishankar (2011) reported that the defence mechanism against drought stress is triggered by bioactivity of leaf phenolic molecules.

The role of phenolics in plant responses to salinity stress have been well documented (Klein et al. 2013; Klein et al. 2015; Linić et al. 2019). Salt stress significantly alter various physiological and metabolic processes, thus leading to harmful effects in plants (Parida and Das 2005). Phenolic compounds such as phenolic acids and flavonoids, play an important role in reducing the detrimental effects caused by salinity (Hichem et al. 2009). The proven antioxidant activity of phenolics allows them to act as ROS scavenging agents. As a result, their synthesis is generally triggered in response to biotic/abiotic stresses and especially under salt stress conditions (Souza and Devaraj 2010). A study by Klein et al. (2015) showed that exogenous caffeic acid mitigated the negative effects caused by salinity in soybean plants. A similar response was observed for rice plants where exogenous gallic acid restricted salt-induced oxidative damage by improving the ROS-scavenging antioxidative system (Ozfidan-Konakci et al. 2015). Apart from their role in reducing the detrimental effects of salinity and drought stress, phenolic compounds exhibit wide range of physiological properties such as antiallergic, antiatherogenic, anti-inflammatory, antimicrobial, antithrombotic (Balasundram et al. 2006).

## 1.5. *p*-Coumaric acid in plants

*p*-Coumaric acid is a natural metabolite that is present in many edible plants (Boo 2019). Its antioxidant activities in reducing oxidative stress in various experimental models have been demonstrated. In plants, the biosynthesis of *p*-coumaric acid involves two biochemical processes (Figure 1.4). In the first biochemical process, phenylalanine ammonia-lyase (PAL) catalyzes the conversion of phenylalanine to trans-cinnamic acid, which is then hydroxylated at the para position under the action of trans-cinnamic acid 4-hydroxylase (C4H) (Krause et al. 2003; Li et al. 2019). However, some PAL enzymes can accept tyrosine as an alternative substrate (PAL/TAL) and directly form *p*-coumaric acid from tyrosine without the intermediary of trans-cinnamic acid (Li et al. 2019). As part of the phenylpropanoid pathway, *p*-coumaric acid is also a precursor of other phenolic acids such as caffeic-, ferulic- and sinapic acids (Figure 1.5).



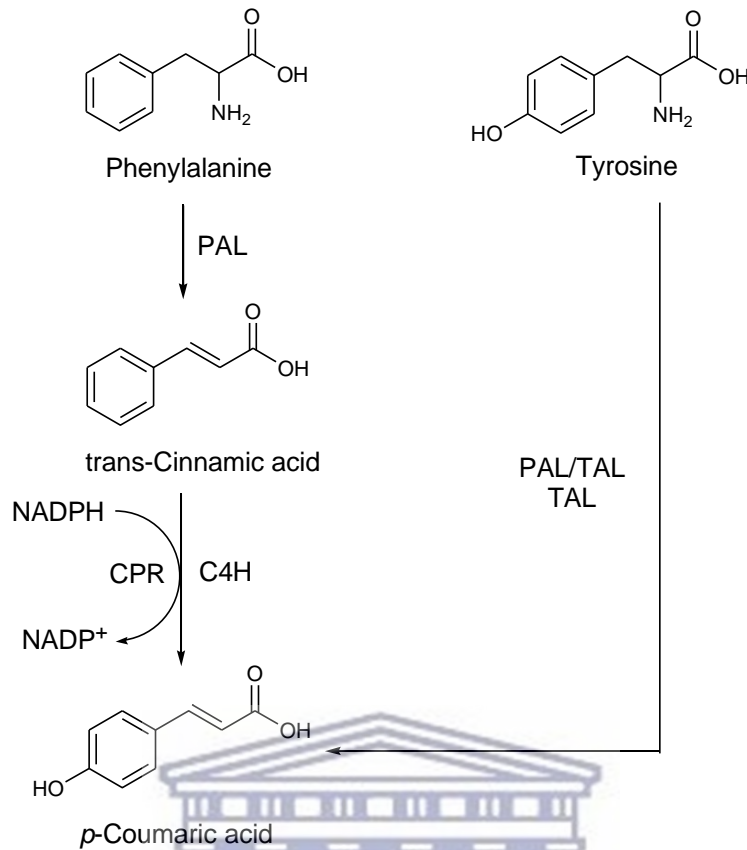


**Figure 1.4.** Biosynthetic pathways of *p*-coumaric acid. The phenylalanine route (PAL-C<sub>4</sub>H) describes the synthesis of *p*-coumaric acid in whereas the tyrosine route (PAL/TAL and TAL) describe its synthesis in microbes. The figure was adapted from Li et al. (2018).

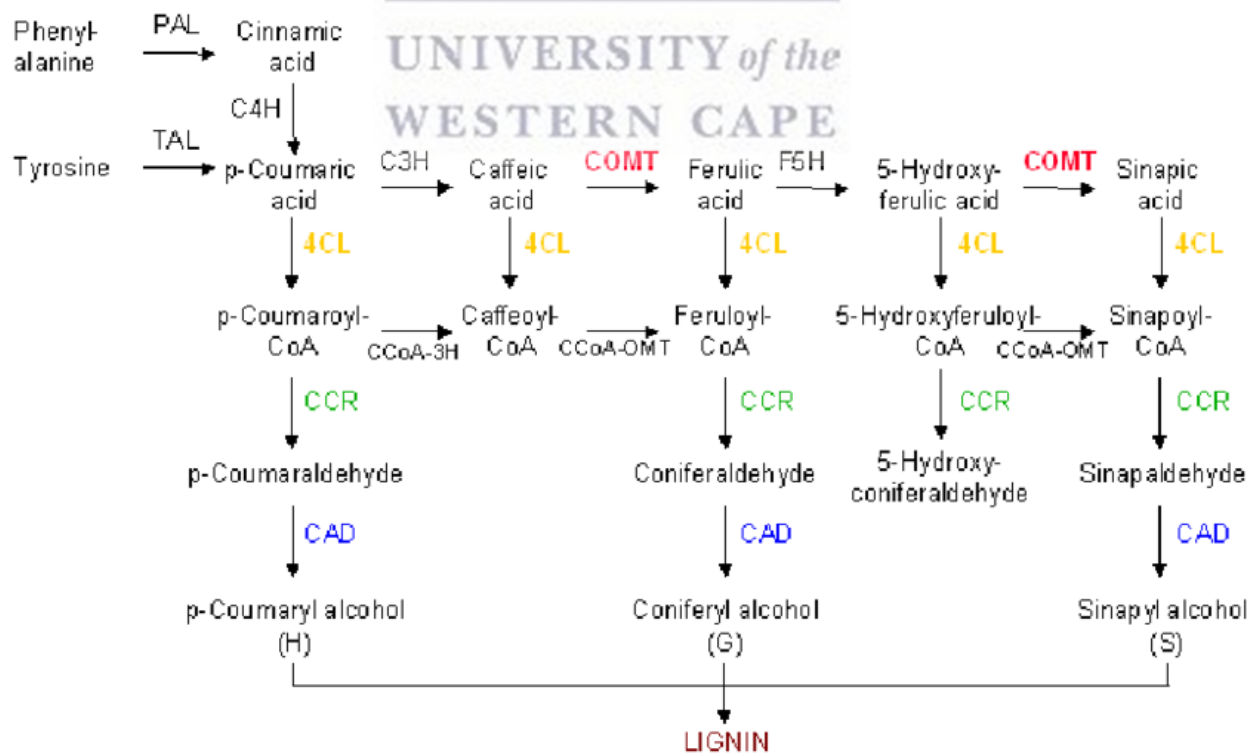


**Figure 1.5.** Biosynthesis of hydroxycinnamic acids and their derivatives involved in lignin production in plants. The biosynthetic enzymes resulting in the biosynthesis of lignin precursors (monolignols) and



lignins are: phenylalanine ammonia-lyase (PAL); tyrosine ammonia-lyase (TAL); cinnamate 4-hydroxylase (C4H); 4-hydroxycinnamate 3-hydroxylase (C3H); caffeic acid 3-O-methyltransferase (COMT); ferulate 5-hydroxylase (F5H); 4-coumarate (4CL): CoA ligase; coumaroyl-coenzyme A 3-hydroxylase (CCoA 3H); caffeoyl-coenzyme A O-methyltransferase (CCoA OMT); cinnamoyl-CoA reductase (CCR); and cinnamyl alcohol dehydrogenase (CAD) (Figure was adapted from Krause et al. 2003).

### **1.5.1. *p*-Coumaric acid as an antioxidant**

Antioxidant activity is defined as the capability of any compound to inhibit oxidative degradation such as lipid peroxidation (Boz 2015). Coumaric acids are derivatives of cinnamic acid mono-hydroxylated at the phenyl group, and *p*-coumaric acid is the most abundant isoform. The levels of *p*-coumaric acid found in fruits, vegetables, and cereals are quite significant. It has been reported that *p*-coumaric acid is a relatively potent antioxidant and scavenger of reactive oxygen species (ROS) and free radicals (Gani et al. 2012; Yoon et al. 2013). Its antioxidant activity has been demonstrated in various experimental models (Boo 2019). *p*-Coumaric acid have been shown to possess radical-scavenging activity and protect oxidation of low-density lipoprotein cholesterol in rats (Shahidi and Chandrasekara 2010). A few lines of research have shown that *p*-coumaric acid has chemoprotectant and antioxidant properties (Mussatto et al. 2007). A study by Ferguson et al. (2005) showed that *p*-coumaric acid have a protective effect against colon cancer on mammalian cells. It is reported that *p*-coumaric acid has a protective effect against heart diseases as it reduces lipid peroxidation, cholesterol oxidation and low-density lipoprotein resistance (Garrait et al. 2006; Zilic et al. 2011).

### **1.5.2 *p*-Coumaric acid in plant growth and development**

The effect of phenolic compounds on plant growth and development have been widely investigated (Reigosa et al. 1999; Klein et al. 2013; Klein et al. 2015, Nkomo et al. 2019). Phenolic compounds such as *p*-coumaric acid, gallic acid and caffeic acid have shown allelopathy effects in different plant species. *p*-coumaric acid is widely distributed in the natural plant communities is known as potent allelopathic agents (Baleroni et al. 2000). It is well



known to interfere with several physiological processes associated with seed germination as well as plant growth and development (Einhellig and Rasmussen 1979; Yang et al. 2004; Zanardo et al. 2009). Several studies have focused on the inhibitory effect of *p*-coumaric acid (*p*-CA), on germination and root growth (Baleroni et al. 2000; Ng et al. 2003; Zhou and Wu 2012). However, other investigations reported the growth stimulating activity of *p*-CA (Khairy and Roh 2016; Kaur et al. 2017; Nkomo et al. 2019). A recent study by Nkomo et al. (2019) showed that exogenous *p*-coumaric acid at low concentration improves the growth of chia seedlings. While, other studies demonstrated that exogenous application of *p*-CA reverses the effect of salt stress, which was exhibited by the improvement of plant growth biomass (Khairy and Roh 2016; Kaur et al. 2017). Thus, the impact of *p*-CA on plant growth seems to be specific to species, application method, and concentration (Baleroni et al. 2000; Ng et al. 2003; Zhou and Wu 2012; Khairy and Roh 2016; Kaur et al. 2017; Nkomo et al. 2019).

## **1.6. Integrating multi-omics approaches for improving stress tolerance**

The “multi-omics” technologies includes genomics, transcriptomics, proteomics, phenomics and ionomics in delineating the complex molecular machinery and providing independent information about the genes, genomes, RNAomes, proteomes and metabolomes (phenols and ions/elements). Integrating these omics technologies have been proven successful in exploring the plant molecular mechanism involving growth and development, with their responses to environmental stresses (Muthamilarasan et al. 2019). In the following section, we discuss the role of proteomics and metabolomics specifically ionomics under environmental stresses.

### **1.6.1. Proteomics**

While genomic analysis has enhanced our understanding of transcriptomic changes in plants' in response to environmental stresses, these transcriptomic changes are not always reflected at

protein level due to post translation modification (Gygi et al. 1999). Hence, proteomics was established to deal with large-scale expression of protein changes in any organ, tissue or cell under various stress factors (Blackstock and Weir 1999; Pandey and Mann 2000). To evaluate protein changes SDS-PAGE has been cited as one of the most useful analytical tool (Marchesi 2008). In this method proteins are separated based on their molecular weight (MW), due to the distance migrated on the polyacrylamide gel. To successfully resolve proteins in a polyacrylamide gel, native proteins have to be denatured by heating the sample with anionic detergent SDS to unfold the proteins into linearized polypeptide chain giving them a negative charge. The uniform negative charge ensures the migration of proteins towards the anode under the influence of an electric field (Figure 1.6), and the separation is achieved solely on the basis of protein molecular weight.

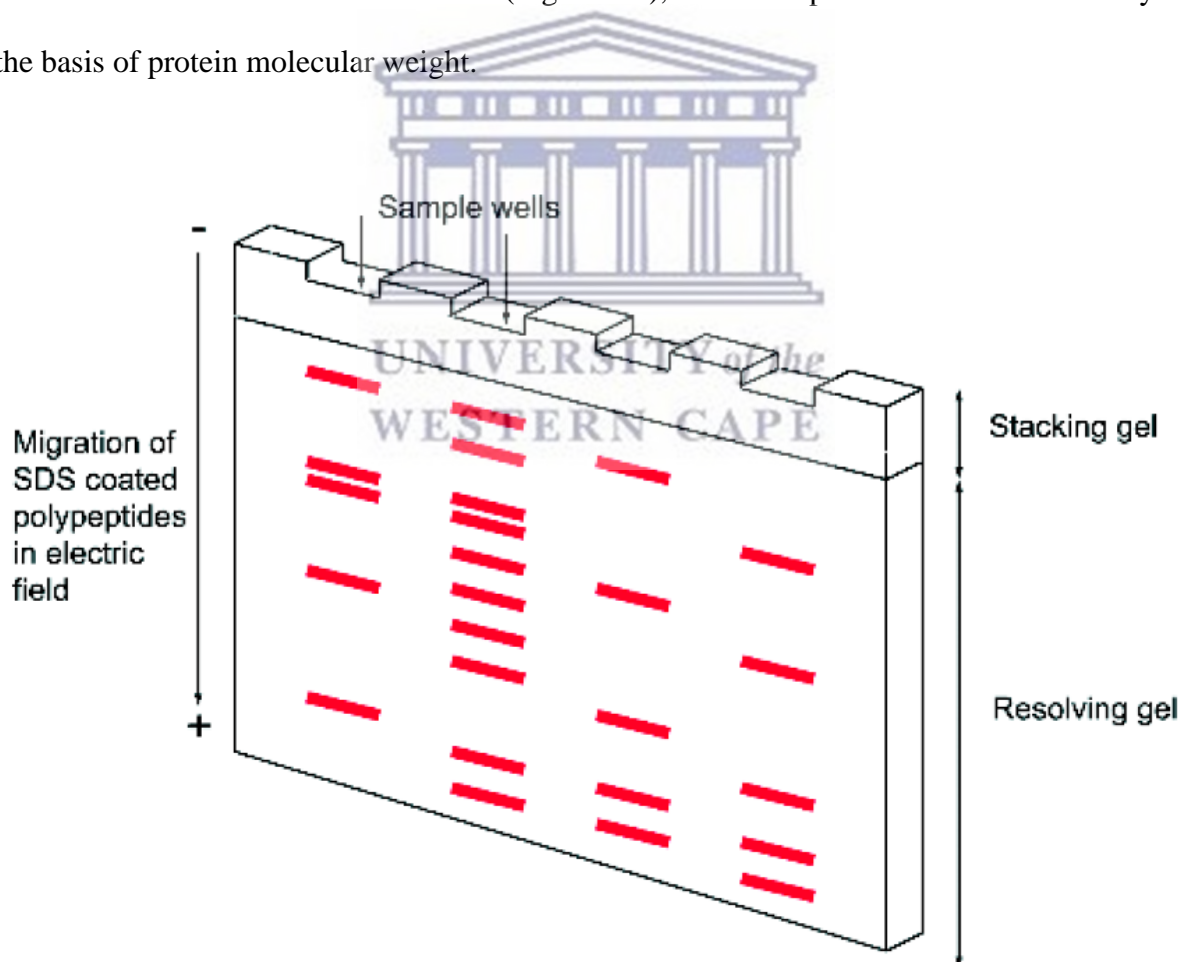


**Figure 1.6.** An illustration of the conventional polyacrylamide gel. A top ‘stacking’ gel containing a lower concentration of acrylamide facilitates entry of SDS-coated polypeptides into the ‘resolving’ gel where the bands separate according to molecular mass. Separation is shown by the different migration of bands (shown in red) within the gel.

An extension of the basic SDS–PAGE technique is Western blotting, which can be utilises by capillary action or by electroelution (Roy and Kumar 2014). This method allows the identification of an antigenic polypeptide within a mixture of size-separated components by its reaction with a specific antibody. While, after separation the SDS-PAGE gel can be visualised using different protein staining methods. The criteria used for selecting which staining method to use, depends on the ease of use, reliability, sensitivity and compatibility of staining method for further proteomic analysis using mass spectrometry and database searches (Ngara et al. 2012). However, gel-based proteomics have shown some limitations with extreme *pI*'s or molecular weights of lower abundance proteins, and hydrophobic membrane proteins (Ngara et al. 2012). Most researchers commonly preferred a gel-free method (multi-dimensional protein identification-MudPIT), which consist of an in-solution digestion instead of in-gel digestion. While most investigators will first run the SDS-PAGE for the initial start to view the quality of the protein, meaning both methods seem to complement each other.

### **1.6.2. Metabolomics/Ionomics**

The field of proteomics is increasingly gaining momentum in plant sciences with several studies having been made and reported on agriculturally important crops (Ngara et al. 2012). Although there have been major proteomic advances using several other mass spectrometry methods, much of the knowledge gained on plant developmental processes and stress response mechanisms has been gained from work using metabolomics (i.e., metabolites <1,200 Da) and ionomics (minerals 62–64) techniques (Salt 2004, Salt et al. 2008, Baxter et al. 2007). Both metabolomics and ionomics are frequently used to characterize the perturbations in metabolic pathways induced by exogenous factors (Zhang et al. 2012). In the present era of proteomics, ionomics is one of the subsets of the metabolomics study that gives high throughput results involving low cost, thus provides an easy means of analysis (Baxter 2010). Previous research

highlights the utility of gas-liquid chromatography-mass spectrometry (GC-MS) and proton-nuclear magnetic resonance ( $^1\text{H-NMR}$ ) as high-throughput methods to profile variation on ionomics study (Salt 2004). However, with the advent of inductively coupled plasma (ICP) technology, gave an ability to analyse all the significant element with specific accuracy. This also help in the better understanding of the relationship between the ions and identification of the genes involve in their regulation by combining “omics” techniques to produce micro-nutrient rich food. Many of the ions are toxic for the plant as well as the human beings and the herbivores. Hence, by the knowledge of the genes that regulate the accumulation of the ions, we can manipulate the ionic profile of the plant system (Satismruti et al. 2013).

### **1.7. In summary**

In this review, we have presented evidence indicating that, phenolic compounds may be directly involved in the scavenging of ROS, whereas the increase in antioxidant enzyme might be a secondary response to protect plants from oxidative damage. There is some suggestions that, phenolic acids may be directly involved in regulation of antioxidant enzymes which are responsible for scavenging free radicals (Klein et al. 2013). Although, pseudocereal crops such as chia are deemed to be high in phenolic compounds, the relationship between these phenolic compounds and salt stress, as well as their combined effect on pseudocereals, has not been extensively reported (Jones et al. 2017). This provides a knowledge gap to which our future studies can focus towards. During salt stress, exogenous application of *p*-coumaric acid and its derivatives (caffeic-, ferulic- and sinapic acids) increased salt tolerance in two contrasting wheat cultivar seedlings (Kaur et al. 2017). Although, much still remains to be learned about pseudocereals, Jones and co-workers showed a similar phenomenon to what was observed in wheat cultivars when studying the effect of exogenous caffeic acid on chia plants grown under salt stress. Jones et al. (2017) further determined a proteome dataset, which has been beneficial

for retrieving information of particular proteins involved in gene regulation and signalling under phenolic acid biosynthesis and salt stress conditions. In the context of the ongoing studies of phenolics in conferring plant stress tolerance under abiotic stress condition, the use of a phenolic acid inhibitor is required during these abiotic stresses experiments, so as to be certain that the results we see is of the direct influence of phenolic acids and not, other unrelated events occurring within the plant.



## CHAPTER 2

### METHODS AND MATERIALS

#### 2.1. List of chemicals and suppliers

**Table 2.1.** List of chemicals and suppliers

Chemical / Reagent	Supplier
2-Deoxy-D- Ribose	Sigma-Aldrich
2,4- Dinitrochlorobenzene	Sigma-Aldrich
2-(N-Morpholino)ethanesulfonic acid (MES) hydrate	Sigma Aldrich
2- Thiobarbituric acid	Sigma-Aldrich
3-[(3-Cholamidopropyl)dimethylammonio]1-Propanesulfonate CHAPS	Sigma Aldrich
5,5-Dithiobis(2-nitrobenzoic acid) (DTNB)	Sigma Aldrich
Acetone	Merck Millipore
Acrylamide/Bis (40 %)	BIO – RAD
Acetonitrile (ACN)	Merck Millipore
Agarose D – 1 LE	White Scientific
Ammonium acetate (C <sub>2</sub> H <sub>3</sub> O <sub>2</sub> NH <sub>4</sub> )	Sigma Aldrich
Ammonium Bicarbonate (AmBic)	Merck Millipore
Ammonium nitrate (NH <sub>4</sub> NO <sub>3</sub> )	Sigma Aldrich
Ammonium Persulfate (APS)	BIO – RAD
Ascorbic acid / Ascorbate	Sigma Aldrich
Bio – Lyte 3/10 Ampholyte (100 X)	BIO – RAD
Bovine Serum Albumin (BSA) Fraction V	Roche
Bradford Reagent (1X)	BIO – RAD

Bromophenol blue	Sigma Aldrich
$\beta$ -nicotinamide adenine dinucleotide (NADH)	Sigma Aldrich
$\beta$ -mercaptoethanol	Amresco
Coomassie® brilliant blue (CBB) R-250	BIO – RAD
Diaminobenzene	Sigma-Aldrich
Dithiothreitol (DTT) Cleland's reagent	Fermentas
Electrode wicks (gel-side down)	BIO – RAD
Ethanol 99.9%	Kimix
Ethylenediaminetetraacetic acid (EDTA)	Sigma Aldrich
Ethylenediaminetetraacetic acid ferric sodium salt	Sigma Aldrich
Evans Blue	Sigma Aldrich
Glacial acetic acid	Merck Millipore
Glycerol	Merck Millipore
Glycine	BIO – RAD
Hydrochloric acid (HCl)	Merck Millipore
Hydrogen peroxide (H <sub>2</sub> O <sub>2</sub> )	Merck Millipore
Iodoacetamide (IOA)	BIO – RAD
L- Ascorbic acid	Sigma-Aldrich
Methanol 99.9%	Merck Millipore
Methionine	Sigma Aldrich
Mineral oil (PlusOne DryStrip Cover Fluid)	GE Healthcare
Nitrotetrazolium blue chloride powder (NBT)	Sigma Aldrich
PageRuler™ pre-stained protein ladder	Fermentas
<i>p</i> -Coumaric acid	Sigma-Aldrich
Phenazine methosulfate (PMF)	Sigma Aldrich



UNIVERSITY OF  
WESTERN CAPE



Phenylmethylsulfonyl fluoride (PMSF)	Amresco
Phosphoric acid	Sigma-Aldrich
Piperonylic acid	Sigma-Aldrich
Polyvinylpyrrolidone (PVP) MW: 40 000	Sigma Aldrich
Potassium cyanide (KCN)	Sigma Aldrich
Potassium hydroxide pellets	Merck Millipore
Potassium iodide (KI)	Sigma Aldrich
Potassium phosphate monobasic (KH <sub>2</sub> PO <sub>4</sub> )	Sigma Aldrich
Potassium phosphate dibasic (K <sub>2</sub> HPO <sub>4</sub> )	Sigma Aldrich
Promix Organic	Cypress House
	Trading
Propan-2-ol (isopropanol)	Merck Millipore
Riboflavin	Sigma Aldrich
Sodium chloride (NaCl)	Merck Millipore
Sodium dodecyl sulfate (SDS)	BIO – RAD
Sodium hydroxide (NaOH)	Merck Millipore
Sucrose	Merck Millipore
N,N,N',N'-Tetramethylethylenediamine (TEMED)	BIO – RAD
Nitrosol ® Solution	
Thiobarbituric acid (TBA)	Sigma Aldrich
Thiourea	Sigma Aldrich
Trichloroacetic acid (TCA)	Merck Millipore
Trifluoroacetic acid (TFA)	Merck Millipore
Tris(hydroxymethyl)-aminethane	BIO – RAD
Trypsin	Promega



UNIVERSITY OF THE  
WESTERN CAPE

Tween 80	Sigma- Aldrich
Urea	Sigma Aldrich
Nitric acid (65 %)	Sigma- Aldrich

---

## 2.2. Stock solutions and buffers

**Table 2.2** List of buffers and stock solutions prepared for this study

<b>Buffer/Stock solution</b>	<b>Composition</b>
Acetone (80 %)	80 % (v/v) acetone in distilled water.
APS (10 %)	10 % (w/v) APS in distilled water. The solution was freshly prepared before use.
BSA stock solution I (5 mg/ml)	5 mg/ml BSA in PVP extraction buffer
BSA stock solution II (5 mg/ml)	5 mg/ml BSA in IEF buffer
Binding buffer	100 mM sodium acetate, 30% acetonitrile, pH 4.5
CAT assay buffer	50 mM K <sub>2</sub> HPO <sub>4</sub> buffer (pH 7.0) and 0.5 mM EDTA
CBB stock solution (1.25 %)	1.25 % (w/v) CBB R-250 in d.H <sub>2</sub> O.
CBB staining solution I	50 ml of 1.25 % (w/v) CBB stock solution, 10 % (v/v) glacial acetic acid and 25 % (v/v) propan-2-ol in d.H <sub>2</sub> O.
CBB staining solution II	6.25 ml of 1.25 % (w/v) CBB stock solution, 10 % (v/v) glacial acetic acid and 10 % (v/v) propan-2-ol in d.H <sub>2</sub> O.

CBB staining solution III	6.25 ml of 1.25 % (w/v) CBB stock solution and 10 % (v/v) glacial acetic acid in d.H <sub>2</sub> O.
Destaining solution	10 % (v/v) acetic acid and 1 % (v/v) glycerol in d.H <sub>2</sub> O.
Ethanol (70 %)	70% (v/v) ethanol in d.H <sub>2</sub> O.
Equilibration buffer	6 M urea; 2 % (w/v) SDS, 50 mM Tris – HCl, pH 8.8 and 20 % (v/v) glycerol in d.H <sub>2</sub> O.
Evans blue stock solution (0.5 %)	0.5% (w/v) Evans blue in d.H <sub>2</sub> O.
HCl (1 M) for pH	1 M HCl in d.H <sub>2</sub> O.
IEF buffer	7 M Urea; 2 M thiourea; 4 % (w/v) CHAPS; 20 mM DTT; 1 % (w/v) bromophenol blue in d.H <sub>2</sub> O.
KH <sub>2</sub> PO <sub>4</sub> (1M) stock solution	1 M KH <sub>2</sub> PO <sub>4</sub> in d.H <sub>2</sub> O.
K <sub>2</sub> HPO <sub>4</sub> (1M) stock solution	1 M K <sub>2</sub> HPO <sub>4</sub> in d.H <sub>2</sub> O.
KI (0.5 M) stock solution	0.5 M KI in d.H <sub>2</sub> O.
KOH (5 M) for nutrient solution pH	5 M KOH in d.H <sub>2</sub> O.
Native gel running buffer stock solution (5 X)	25 mM Tris-base; 192 mM glycine in d.H <sub>2</sub> O.
Native PAGE loading dye (6 X)	375 mM Tris-HCl at pH 6.8; 50 % (v/v) glycerol; 0.02 % (w/v) bromophenol blue in d.H <sub>2</sub> O.
<i>p</i> -Coumaric acid (5 mM) stock solution	5 mM <i>p</i> -coumaric acid dissolved in 0.001 M NaOH and made up with d.H <sub>2</sub> O.
Piperonylic acid (5 mM) stock solution	5 mM Piperonylic acid dissolved in 0.001 M NaOH and made up with d.H <sub>2</sub> O.

PVP extraction buffer	40 mM K <sub>2</sub> HPO <sub>4</sub> at pH 7.4; 1 mM EDTA; 5 % PVP MW = 40 000; 5 % glycerol in d.H <sub>2</sub> O.
SDS buffer	0.1 M Tris-HCl, pH 8.0; 2 % (w/v) SDS; 5 % (v/v) β-mercaptoethanol; 30 % (w/v) sucrose and 1 mM PMSF in d.H <sub>2</sub> O.
SDS gel loading dye	100 mM Tris-HCl at pH 6.8; 4% (w/v) SDS; 0.2% (w/v) bromophenol blue; 20% (v/v) glycerol; 200 mM DTT in d.H <sub>2</sub> O.
SDS running buffer stock solution (5 X)	25 mM Tris-base; 192 mM glycine; 0.1 % (w/v) SDS in d.H <sub>2</sub> O.
SDS (10 %) stock solution	10 % (w/v) SDS in d.H <sub>2</sub> O.
SOD assay buffer	50 mM KPO <sub>4</sub> at pH 7.4; 13 mM methionine; 75 μM NBT; 0.1 mM EDTA; 2 μM riboflavin in d.H <sub>2</sub> O.
Solution A	100 mM Tris, 1 % TritonX-100 and 4 M guanidine hydrochloride
TCA (6 %) extraction buffer	6 % (w/v) TCA in d.H <sub>2</sub> O.
TCA/Acetone (10 %)	10% (w/v) TCA in acetone.
TCA (20 %) / TBA (0.5 %)	0.5 % (w/v) TBA in 20 % (v/v) TCA stock solution
Tris-HCl (0.1 M), pH 7.9	0.1 M Tris in d.H <sub>2</sub> O adjusted to pH 7.9 with concentrated HCl.
Tris-HCl (0.5 M), pH 6.8	0.5 M Tris in d.H <sub>2</sub> O adjusted to pH 6.8 with concentrated HCl.
Tris-HCl (1.5 M), pH 8.8	1.5 M Tris in d.H <sub>2</sub> O adjusted to pH 8.8 with concentrated HCl.
Washing buffer	100 mM sodium acetate, 15 % acetonitrile, pH 4.5

### 2.3. Evaluation of seed germination

Chia (*Salvia hispanica* L) seeds (50 seeds per treatment) purchased from Faithful to Nature, Cape Town, South Africa were germinated on half strength Murashige and Skoog basal media supplemented with different concentrations of *p*-CA (100  $\mu$ M, 250  $\mu$ M, 500  $\mu$ M and 1000  $\mu$ M) or without *p*-CA (control group) in the dark for a period of five days. Seed germination percentage for each treatment (in triplicate) was scored after five days using the following formula:

$$\text{Seed germination \%} = \frac{\text{number of seeds germinated}}{\text{number of seeds per treatment}} \times 100$$

### 2.4. Plant growth and treatment

For plant growth experiments, germinated chia seeds were transferred to 19/20 cm plastic pots containing moist promix growth medium (Stodels Garden Centre, Brackenfell, South Africa) and allowed to grow on a 27/19 °C day/night temperature cycle under a 16/8 hour dark cycle at a photosynthetic photon flux density of 300  $\mu$ mol photons.m<sup>-2</sup>.s<sup>-1</sup> during the day phase until the end of the experiment. Seedlings were grown in a completely randomized block design to eliminate the effect of variations in environmental conditions at different positions in the growth room.

Plants at the same developmental stage and of similar height were selected for all experiments. Control plants were supplemented with 50 ml of Nitrosol<sup>(R)</sup> solution diluted in water (1:300). For treatment with *p*-CA, PA, salt stress or a combination of *p*-CA and salt stress, plants were supplemented with Nitrosol<sup>(R)</sup> containing 100  $\mu$ M *p*-CA, 100  $\mu$ M PA, 100 mM NaCl and a combination of 100  $\mu$ M *p*-CA and 100 mM NaCl at 2-day intervals for a period of 14 day.

## 2.5. Measurement of plant growth

Chia seedlings were carefully removed from the growth medium to avoid any damage. Subsequently, the roots were separated from the shoots to prevent erroneous data interpretation caused by possible root damage. The shoots from each treatment were scored for length (SL), fresh weight (FW) and dry weight (DW). The DW was determined by drying the seedlings in an oven at 55 °C for 48 hours as described by Gokul et al. (2016). Leaf area measurements from representative plants from each treatment were recorded using ImageJ software (Gao et al. 2011).

## 2.6. Measurement of shoot chlorophyll content

Total chlorophyll content in the shoots of chia plants was estimated using a method previously described by Nxele et al. (2017). Freshly harvested shoots (100 mg) were mixed with 5 ml of dimethylsulfoxide (DMSO) and incubated at 65 °C for 3 h. The absorbance of an aliquot of the leaf-DMSO extract (200 µl) was recorded at 645 nm and 663 nm, with DMSO used as a blank.

## 2.7. Measurement of *p*-coumaric acid content

The levels of *p*-CA in the shoots of chia seedlings were quantified using reversed-phase high performance liquid chromatography (RP-HPLC). *p*-CA was successfully separated on Alltima™ C18 column (250 mm × 4.6 mm, 5 µm) at 30°C, using a mixture of acetonitrile: 0.1% (V/V) acetic acid solution (25:75, V: V) as mobile phase and detection at 308 nm. The flow rate was 1.0 mL min<sup>-1</sup>, and the injection volume was 20 µl.

## 2.8. Protein extraction for biochemical analysis

Shoots from all treatments were harvested and ground into a fine powder using liquid nitrogen. Shoot material (0.1 g) from each treatment was homogenized in 1 ml of 6 % (w/v) trichloroacetic acid (TCA) for analysis of H<sub>2</sub>O<sub>2</sub> content and lipid peroxidation or in 1 ml of homogenizing PVP extraction buffer (see section 2.2) for the measurement and detection of

superoxide dismutase (SOD), ascorbate peroxidase (APX) catalase (CAT) and guaiacol peroxidase (POD) enzymatic activities. Protein concentrations were determined using the RC DC Protein Assay Kit 11 (Bio-Rad Laboratories).

## **2.9. Measurement of superoxide content**

Superoxide content ( $O_2^-$ ) in the shoots of chia seedlings was quantified using a method previously described by Gokul et al. (2016). Superoxide concentrations were determined by submerging intact seedling shoots in a solution containing; 10 mM KCN (to inhibit Cu/Zn SODs), 10 mM  $H_2O_2$  (to inhibit Mn and Cu/Zn SODs), 2% (m/v) SDS (to inhibit Mn and Fe SODs), 80  $\mu$ M nitro blue tetrazolium chloride (NBT) (sigma; powder, for molecular biology) and 50 mM potassium phosphate (pH 7.0). The seedling shoots were incubated for 20 min within the solution after which the seedlings were homogenized (in solution), centrifuged (10,000g for 5 min) and the supernatant was spectrophotometrically analysed at 600 nm. The superoxide concentration was calculated using the NBT extinction coefficient of 12.8 mM  $cm^{-1}$ .

## **2.10. Measurement of hydrogen peroxide content**

Hydrogen peroxide content was determined based on a method previously described by Velikova et al. (2000). The reaction mixture contained 75  $\mu$ l of the TCA extract, 5 mM  $K_2HPO_4$ , pH 5.0 and 0.5 M KI. Samples were incubated at 25 °C for 20 min and absorbance readings of the samples were recorded at 390 nm. Hydrogen peroxide content was calculated using a standard curve based on the absorbance ( $A_{390\text{ nm}}$ ) of  $H_2O_2$  standards.

## **2.11. Determination of malondialdehyde (MDA) content**

The extent of lipid peroxidation (malondialdehyde; MDA) in the shoots of chia seedlings were quantified as described by Egbichi et al. (2013). Chia shoots (100 mg) was ground into a fine powder in liquid nitrogen. The tissue was homogenized in 400  $\mu$ l of cold 5% (w/v)



trichloroacetic acid (TCA). The homogenate was centrifuged at 12,000 ×g for 30 min at 4 °C. Aliquots (100 µl) of the supernatant were mixed with 400 µl of 0.5% TBA (prepared in 20% TCA). The mixture was incubated at 95 °C for 30 min and the reaction was stopped by placing the mixture on ice for 5 min. The mixture was further centrifuged at 12,000 ×g for 5 min at 4 °C. The absorbance of the supernatant was measured at 532 nm and 600 nm. After subtracting the non-specific absorbance (A<sub>600 nm</sub>), the MDA concentration was determined by its extinction coefficient of 155 mM<sup>-1</sup> cm<sup>-1</sup> and expressed as nmol g<sup>-1</sup> of fresh weight.

### **2.12. Measurement and detection of SOD activity**

Total SOD activity was measured as described by Beyer and Fridovich (1987) with slight modifications. The sample reaction mixture consisted of 10 µl PVP protein extract and 190 µl SOD assay buffer (see section 2.2) in a final volume of 200 µl. The reaction was initiated when the sample mixture was exposed to light for 15 mins or until a colour change was observed. The absorbance was measured at 560 nm and SOD activity calculated based on the amount of enzyme that was required to reduce 50 % of NBT to blue formazan.

For detection of individual SOD isoforms in the shoots of chia seedlings a method previously used by Klein et al. (2013) was used. Protein extracts from various treatments (containing 100 µg protein per sample) were separated on a 10% native polyacrylamide gel at 4 °C. SOD activity was detected by photochemical staining with riboflavin and nitrotetrazolium blue chloride (NBT). SOD isoforms were identified by incubating gels in 6 mM H<sub>2</sub>O<sub>2</sub> to inhibit Cu/ZnSOD and FeSOD, or in 5 mM KCN to inhibit only Cu/ZnSOD, with MnSOD activity assigned on the basis of its resistance to both H<sub>2</sub>O<sub>2</sub> and KCN.

### **2.13. Measurement of total APX activity**

APX activity in the shoots of chia seedlings was measured using a modified method previously described by Asada (1992). Each reaction contained 10 µl PVP protein extract and 180 µl of

APX assay buffer (50 mM K<sub>2</sub>HPO<sub>4</sub> at pH 7.0; 0.2 mM EDTA; buffer 0.25 mM ascorbic acid in d.H<sub>2</sub>O) in a final volume of 190 µl. The reaction was initiated with the addition of 10 µl H<sub>2</sub>O<sub>2</sub> (90 µM), and the absorbance measured at 290 nm. APX activity was calculated using the extinction coefficient of 2.8 mM<sup>-1</sup> cm<sup>-1</sup>.

#### **2.14. Measurement of total CAT activity**

Catalase (CAT) activity was determined using a modified method described by Aebi (1984) based on the decomposition of H<sub>2</sub>O<sub>2</sub>. Crude protein extract (50 µg) was combined with CAT assay buffer (see section 2.2) and the reaction initiated with 30 mM H<sub>2</sub>O<sub>2</sub>. The absorbance was recorded at 240 nm and CAT activity calculated using the extinction coefficient of 43.6 M<sup>-1</sup> cm<sup>-1</sup>.

#### **2.15. Measurement of total POD activity**

Guaicol peroxidase (POD) activity in the shoots of chia plants was estimated using a modified method previously described by Pitel and Cheliak (1985). The reaction mixture consisted of 100 mM Na-acetate (pH 5.3), 37 mM guaicol, 10.3 mM H<sub>2</sub>O<sub>2</sub> and 100 µl of PVP protein extract in a final volume of 3 ml. The reaction mixture was incubated at 30°C for 15 mins and absorbances was recorded at 436 nm. POD activity was calculated using the extinction coefficient of 26.6mM<sup>-1</sup> cm<sup>-1</sup>.

#### **2.16. Determination of proline content**

Total free proline content in the shoots of chia plants was estimated using a modified method described by Nxele et al. (2017). Fresh shoot material from each treatment (0.1 g) were homogenized in 500 µl of 3 % (w/v) sulphosalicylic acid using a mortar and pestle. About 200 µl of each homogenate was mixed with 200 µl of glacial acetic acid to which 200 µl of ninhydrin was added. The reaction mixture was boiled in a water bath at 100 °C for 30 mins and immediately cooled in an ice bath. After cooling, 400 µl of toluene was added to the

reaction mixture. After thorough mixing, the chromophore containing toluene was separated and absorbance of red colour developed was read at 520 nm against toluene blank using the FLUOstar Omega UV-visible spectrophotometer (BMG LabTech GmbH, Ortenberg, Germany).

## **2.17. Determination of glycine betaine**

Glycine betaine content in the shoots of chia seedlings was estimated using a method previously described by Ullah et al. (2016) with slight modifications. Shoot material (0.25 g) from each treatment were ground to a fine powder in liquid nitrogen. The tissue was incubated in tubes containing 20 ml of de-ionized water for 24 hours at 25 °C. The samples were filtered and mixed with 2 N H<sub>2</sub>SO<sub>4</sub>. An aliquot (250 µl) was transferred into a test tube and cooled in ice water for 1 hour. Cold potassium iodide-iodine reagent (100 µl) was added, vortexed, and then centrifuged at 10,000 × g for 30 mins at 4 °C. The sample was incubated for 24 hours at 4 °C. The formed periodite crystals were dissolved in 14 ml of 1,2-dichloroethane with gentle agitation at room temperature for 48 hours. The absorbance was recorded at 365 nm using a FLUOstar Omega UV-visible spectrophotometer (BMG LabTech GmbH, Ortenberg, Germany).

## **2.18. Profiling the shoot proteome of chia seedlings**

### **2.18.1. Sample preparation for proteomic analysis**

Total soluble proteins from the shoots of chia seedlings were extracted (in triplicate) using a modified method previously described by Ngara (2009). Shoot material (0.2 g) from each treatment were homogenized in 10 % (w/v) TCA/Acetone and centrifuged at 13,000 × g for 6 mins. The supernatant was discarded and the resultant pellets washed with 80 % (v/v) methanol containing 0.1 M ammonium acetate. This was followed by another wash step with 80 % (v/v) acetone. The pellets were allowed air dry at room temperature for an hour and re-suspended in

a 1:1 ratio phenol and SDS buffer (see section 2.2). The samples suspension was incubated on ice for 6 mins and centrifuged at 13, 000 x g for 6 mins. The upper phenol phase was transferred to a sterile 2 ml Eppendorf tube and filled with the 80 % (v/v) methanol containing 0.1 M ammonium acetate to allow for protein precipitation overnight at -20 °C. The precipitates were centrifuged at 13, 000 x g for 6 mins and the supernatant discarded. The pellets were washed with 100 % (v/v) methanol followed by an additional wash with 80 % (v/v) acetone. The pellets were allowed to air dry at room temperature for an hour and re-suspended in IEF buffer (see section 2.2) for 1D PAGE analysis. Pellets not re-suspended in IEF buffer were stored at -20 °C.. Protein concentrations for all samples were determined using the RC DC Protein Assay Kit 11 (Bio-Rad Laboratories).

### **2.18.2. One dimensional polyacrylamide gel electrophoresis (1D PAGE)**

A fraction of each sample (10 µg of each protein) was denatured and size fractionated on a 12% SDS PAGE gel for 90 mins at 120 V. After gel electrophoresis, the SDS-PAGE gel was stained with Coomassie Brilliant Blue G-250 for 30 mins and transferred to a de-staining solution (see section 2.2) for 2 hours. The resolved protein bands were visualized using the ENDURO™ GDS Gel Documentation System (Labnet International, Edison, NJ).

### **2.18.3. Protein pellet solubilization**

Protein pellets not used for 1D SDS PAGE was solubilised in a solution A (see section 2.2) followed by three, one-minute sonication cycles. After first sonication, solution A was removed (transferred to a sterile 2 ml tube) and replaced with 1 % formic acid (FA) followed by three, one-minute sonication cycles. After the second sonication step, the FA was removed and combined with solution A to perform a methanol-chloroform liquid-liquid analysis. The solution A and FA mixture was combined with 4 volumes of methanol. To this mixture, 1

volume of chloroform was added and mixed thoroughly. Phase separation was induced by the addition of three volumes water prior to centrifugation at 13,000 x g for 5 mins. The upper phase was discarded and four volumes of methanol added. The reaction mixture was again centrifuged 13,000 x g for 5 mins and the methanol-chloroform phase removed. The protein pellet was air-dried at room temperature and suspended in 50 mM Tris buffer containing 2 % SDS and 4 M urea.

#### **2.18.4. On-bead digest**

Solubilised protein samples were re-suspended in 50 mM triethyl ammonium bicarbonate (TEAB) and reduced with 5 mM triscarboxyethyl phosphine (TCEP) and 50 mM TEAB for 1 hour at 60°C. Cystein residues were thiomethylated with 20 mM *S*-Methyl methanethiosulfonate in 50 mM TEAB for 30 mins at room temperature. After thiomethylation the samples were diluted two-fold with binding buffer (see section 2.2). The protein solution was added to MagResyn HILIC magnetic particles prepared according to manufacturer's instructions and incubated overnight at 4 °C. After binding, the supernatant was removed and the magnetic particles washed twice with washing buffer (see section 2.2). After the wash steps, the magnetic particles were suspended in 50 mM TEAB containing trypsin (New England Biosystems) to a final ratio of 1:10 and incubated for 6 hours at 37 °C. After incubation, peptides were extracted once with 50 µl water and once with 50 % acetonitrile. The samples were dried down and re-suspended in 30 µl solution of 2 % acetonitrile:water and 0.1 % FA. Residual digest reagents were removed using an in-house manufactured C<sub>18</sub> stage tip (Empore Octadecyl C<sub>18</sub> extraction discs; Supelco). The samples were loaded onto the stage tip after activating the C<sub>18</sub> membrane with 30 µl methanol and equilibrating it with 30 µl of 2 % acetonitrile:water and 0.05 % Trifluoroacetic acid (TFA). The bound sample was washed with 30 µl of 2 % acetonitrile:water and 0.1 % TFA before elution with 30 µl 50 % acetonitrile:

water and 0.05 % TFA. The eluate was dried and peptides dissolved in 2 % acetonitrile: water and 0.1 % FA for LC-MS analysis.

### **2.18.5. Peptide fractionation and detection using LC-MS/MS**

A high-pressure liquid chromatography system running at nano-flow rates was used for peptide fractionation prior to mass spectrometry analysis. The method for LC-MS/MS analysis was adapted from Yasmeeen et al. (2016). Chromatography was performed using a Thermo Scientific Ultimate 3000 RSLC equipped with a 2 cm x 100  $\mu$ m C18 trap column and a 35 cm x 75  $\mu$ m C18 analytical column (Luna C18, 5  $\mu$ m; Phenomenex). The solvent system employed was loading: 2 % ACN : water; 0.1% FA; Solvent A: 2 % ACN : water; 0.1 % FA and Solvent B: 100% ACN : water. Samples were loaded onto the trap column using loading solvent at a flow rate of 15  $\mu$ l/min from a temperature controlled autosampler set at 7 °C. The flow rate was set to 500 nl/min and a gradient generated as follows: 2-10 % solvent B over 5 min; 5 %-25 % solvent B from 5 to 50 min using Chromeleon non-linear gradient 6, 25 %-45 % from 50 to 65 min. Chromatography was performed at 50 °C and the outflow delivered to the mass spectrometer through a stainless-steel nano-bore emitter.

Detection was performed using a Thermo Scientific Fusion mass spectrometer equipped with a Nanospray Flex ionization source. The sample was introduced through a stainless-steel emitter. Data were collected in a positive mode with spray voltage set to 2 kV and ion transfer capillary set to 275 °C. Spectra were internally calibrated using polysiloxane ions at  $m/z = 445.12003$  and  $371.10024$ . MS1 scans were performed using the orbitrap detector set at 120,000 resolution over the scan range 350-1650 with AGC target at  $3 \times 10^5$  and maximum injection time of 40 ms. Data were acquired in profile mode. MS2 acquisitions were performed using monoisotopic precursor selection for ion with charges +2-+6 with error tolerance set to  $\pm 0.02$  ppm. Precursor ions were excluded from fragmentation once for a period of 30 s. Precursor ions were selected for fragmentation in higher energy dissociation (HCD) mode using the



quadrupole mass analyzer with HCD energy set to 32.5 %. Fragment ions were detected in the orbitrap mass analyzer set to 15, 000 resolution. The AGC target was set to 1E4 and the maximum injection time to 45 mins. The data were acquired in centroid mode.

#### **2.18.6. Protein validation and data analysis**

The raw files generated by the MS were imported into Proteome Discoverer v1.4 software (Thermo Scientific, USA) and processed using Sequest algorithm. Database interrogation was performed against a concatenated database created using the Uniprot human database with semi-tryptic cleavage allowing for 2 missed cleavages. Precursor mass tolerance was set to 10 ppm and fragment mass tolerance set to 0.02 Da. Deamidation (NQ) and oxidation (M) was allowed as dynamic modifications and carbamidomethylation of C as static modification. Peptide validation was performed using the peptide validator node set to search against a decoy database with strict FDR 1% and delta Cn of 0.1. The result files were imported into Scaffold 4.8.8 and identified peptides validated using the X!Tandem search algorithm included in Scaffold. Peptide and protein validation were done using the Peptide and Protein Prophet algorithms. Protein quantitation was performed using Fischer's Exact Test on the paired data with the Benjamini-Hochberg correction applied. Protein identifications were accepted if they could be established at greater than 95% probability and contained at least two unique identified peptides.

#### **2.19. Statistical analysis**

All experiments described were performed six times independently. For measurement of plant growth parameters (shoot height, shoot fresh weight, shoot dry weight) and superoxide content, 30 individual chia seedlings per treatment were analyzed. For all other experiments, 50 chia seedling shoots were homogenized per treatment. For statistical analysis, the one-way analysis of variance (ANOVA) test was used for all data, and the means (for six independent



experiments) were compared according to the Tukey–Kramer test at 5 % level of significance, using GraphPad Prism 5.03 software.



## CHAPTER 3

### EXOGENOUS *p*-COUMARIC ACID IMPROVES CHIA SEEDLING SHOOT GROWTH

#### 3.1. Abstract

*p*-Coumaric acid (*p*-CA) belongs to a family of natural esters of hydroxycinnamic acid compounds that have been shown to modulate plant growth metabolism. In this study, we investigated the effect of exogenous *p*-CA on plant growth, ROS-induced oxidative damage, photosynthetic metabolism, osmolyte content and changes in superoxide dismutase (SOD) enzymatic activity. Exogenous *p*-CA improved *Salvia hispanica* (chia) growth by significantly enhancing shoot length, fresh and dry weights coupled with augmented levels of total chlorophyll and carotenoid contents. Furthermore, *p*-CA also triggered an induction in proline, glycine betaine (GB) and superoxide ( $O_2^-$ ) levels while no changes were observed for hydrogen peroxide ( $H_2O_2$ ) and downstream malondialdehyde (MDA) content. Also, no change in SOD activity was observed in the *p*-CA treatment relative to the control. Therefore, the results suggest that exogenous *p*-CA improves chia seedling growth possibly via activation of a ROS-signalling pathway involving  $O_2^-$  under the control of proline accumulation.

#### 3.2. Introduction

Phenolic acids are divided into two groups based on their chemical structure, namely hydroxybenzoic and hydroxycinnamic (Shahidi and Yeo 2018). Hydroxycinnamic acids (includes *p*-coumaric-, caffeic-, ferulic-, and sinapic acid) derived from the phenylalanine pathway, have gained recent attention due to their revealed properties, such as antimicrobial, antitumor, anti-inflammatory, antioxidant and other health benefits like antidiabetic activity (Heleno et al. 2015; Kwak et al. 2015; Yang et al. 2013). In plants, these hydroxycinnamic acids have been referred to as allelochemicals and are commonly found in soils at

concentrations ranging from 0.01 to 0.1 mM and have been shown to affect plant growth at concentrations of up to 10 mM (Macias 1995; Bubna et al. 2011). Of these hydroxycinnamic acids, *p*-CA resides at a metabolically important position, linked to the synthesis of other hydroxycinnamic acids such as caffeic-, ferulic- and sinapic acid. A few lines of research have shown that *p*-CA reduced the rate of seed germination, root length and biomass in different plant species (Patterson 1981; Janovicek et al. 1997; Reigosa et al. 1999; Baleroni et al. 2000; Politycka and Mielcarz 2007). This led to a general perception that exogenously applied *p*-CA restricts plant growth and development in various plant species (Patterson 1981; Janovicek et al. 1997; Reigosa et al. 1999; Baleroni et al. 2000; Politycka and Mielcarz 2007; Zanardo et al. 2009; Orcaray et al. 2011). Jones et al. (2017) showed that exogenous application of caffeic acid (a derivative of *p*-CA) improved the growth of chia plants through differential regulation of photosynthetic metabolism and antioxidant enzyme activities under salt stress conditions. This result is in contradiction to what was reported for legume plants (Batish et al. 2008; Klein et al. 2015). To our knowledge, to date, no study has investigated the effect of exogenous application of *p*-CA on the physio-biochemical responses of pseudocereal plants.

Chia is an oilseed pseudocereal plant known for its nutritional and health promoting properties. The seed is a natural source of omega-3 fatty acids ( $\alpha$ -linolenic acid), soluble and insoluble fibers, and proteins in addition to other important nutritional components, such as vitamins, minerals, and natural antioxidants (Bushway et al. 1981; Ayerza and Coates 2005). Furthermore, it has been shown that chia plants (seeds and leaves) contain various bioactive components such as tocopherols and phenolic compounds, which reduces the risk of liver, cardiovascular and obesity-related diseases (Poudyal et al. 2012; da Silva Marineli et al. 2015; Capitani et al. 2012; da Silva Marineli et al. 2014; Porrás-Loaiza et al. 2014). In view of the nutritional and health-promoting properties of chia plants in recent years there has been considerable interest to explore the biological and technological potential of this plant. In this

study, we investigated the effect of exogenously applied *p*-CA on the growth, photosynthetic pigments, osmolyte content, ROS-induce oxidative damage and changes in SOD activity in chia seedlings.

### 3.3. Results

#### 3.3.1. *p*-CA alters chia germination percentage

Among the four concentrations used for germination tests, at a concentration of 1000  $\mu$ M a strongly inhibition on chia seed germination (100 % inhibition) was observed. Although, the rest of the concentration showed a 100 % germination rate which was relative to the control, at 500  $\mu$ M the germinated sprouts were smaller in size compared to the rest of the germinated treatment (Fig. 3.1)

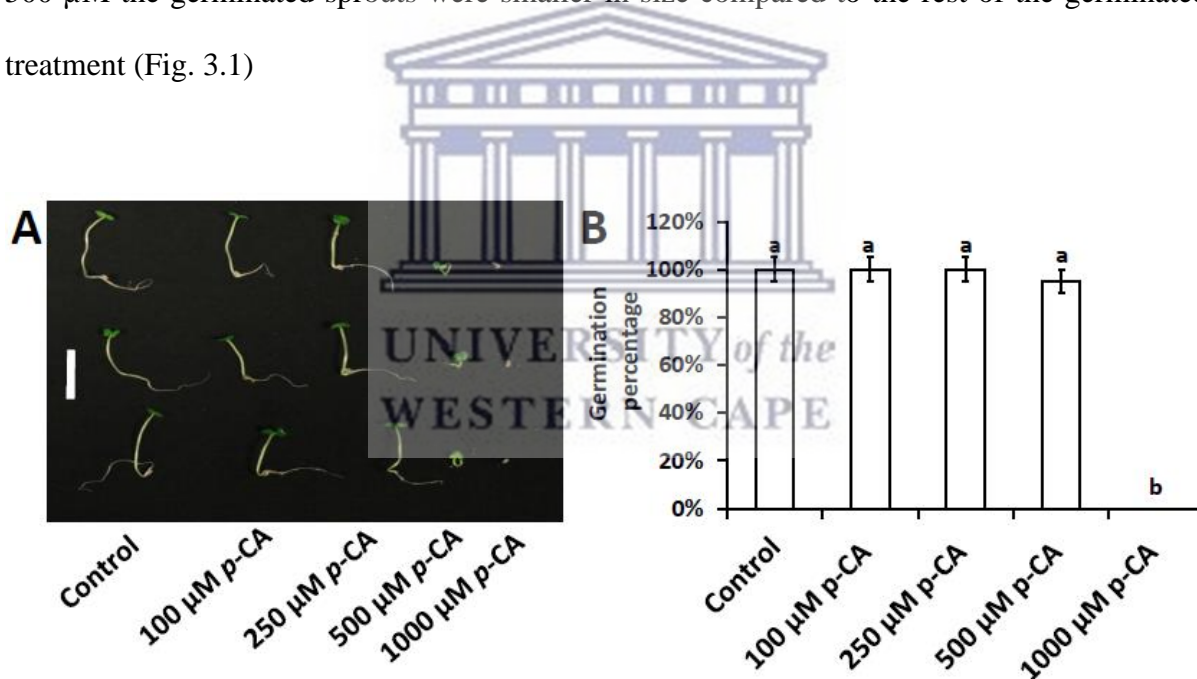


**Figure 3.1.** Concentration dependant germination of chia seedlings. The white bar = 2 cm (A) Data represent the means ( $\pm$ SE) of three independent experiments and different letters indicate the mean values that are significantly different at  $p \leq 0.05$  using the Tukey Kramer test.

#### 3.3.2. *p*-CA improves chia seedling growth

In this study, we investigated the effect of exogenous application of *p*-CA on plant growth and chlorophyll content. The results show that exogenous *p*-CA significantly increase shoot growth

of chia seedlings (Fig. 3.2), as observed for shoot height (SH), fresh weight (FW) and dry weight (DW). Exogenous *p*-CA improved SH by 37.2 % when compared to control plants (Figure 3.2B). A similar trend was observed for FW and DW. On average FW and DW were enhanced by 43.6 % and 54.1 % respectively under *p*-CA treatment relative to the control (Figure 3.2C and 3.2D).

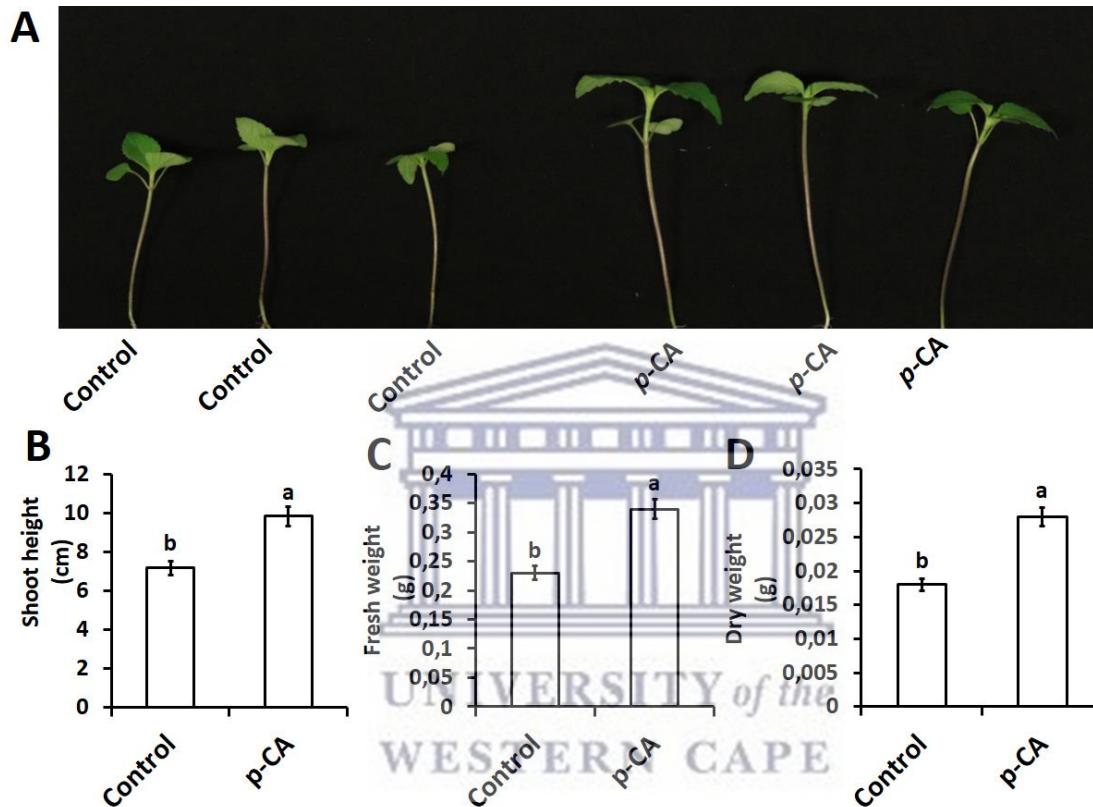


**Figure 3.2.** Representative chia seedling shoots under control and *p*-CA treatments (A). Shoot height (B), shoot fresh weight (C) and shoot dry weight (D) of chia seedlings treated with *p*-CA. Data represent the mean ( $\pm$ SE) from six independent experiments. Different letters represent statistical significance at  $p \leq 0.05$  (Tukey-Kramer test).

### 3.3.3. The effect of exogenous *p*-CA on chlorophyll metabolism and osmolyte content

Chlorophyll pigments are a good indicator of cellular physiological state of plant's photosynthesis apparatus and are highly correlated with an increase in plant growth. The data obtained from plant growth parameters, prompted further investigations to evaluate the effect of *p*-CA on chlorophyll pigment. Both chlorophyll *a* and chlorophyll *b* content, showed similar results, which significantly increased by 36.2 % and 38.5 % when compared to the control.

Parallel to chlorophyll a and chlorophyll b, there was a significant increase in total chlorophyll (37.6 %) and carotenoid (25.1 %) content in response to exogenous application of *p*-CA (Table 3.1). The *p*-CA treatment also caused a significant increase in osmolyte compounds (GB and proline), when compared to the control. Furthermore, there was a significant increase in both proline (170 %) and GB (22.4 %) content (Table 3.1) when compared to the control.

**Table 3.1.** Chlorophyll and osmolyte concentration in chia seedling shoots in response to *p*-coumaric acid. Data represent the means ( $\pm$  SE) of six independent experiments and different letters per row indicate the mean values that are significant different at  $p \leq 0.05$  using the Tukey-Kramer test.

Trait ( $\mu\text{g}\cdot\text{g}^{-1}\text{FW}$ )	Control	<i>p</i> -CA
Chlorophyll <i>a</i>	15.70 $\pm$ 0.83 <sup>b</sup>	21.30 $\pm$ 0.88 <sup>a</sup>
Chlorophyll <i>b</i>	24.80 $\pm$ 1.01 <sup>b</sup>	34.4 $\pm$ 0.50 <sup>a</sup>
Total Chlorophyll	40.50 $\pm$ 1.80 <sup>b</sup>	55.70 $\pm$ 1.38 <sup>a</sup>
Carotenoids	1009.70 $\pm$ 10.17 <sup>b</sup>	1263.3 $\pm$ 8.82 <sup>a</sup>
Glycine Betaine	6030 $\pm$ 233.03 <sup>b</sup>	7380 $\pm$ 60.02 <sup>a</sup>
Proline	1.21 $\pm$ 0.02 <sup>b</sup>	3.26 $\pm$ 0.04 <sup>a</sup>

### 3.3.4. Effects of *p*-CA on superoxide radical and superoxide dismutase

Exogenous application of *p*-CA significantly increased  $\text{O}_2^{\cdot-}$  content by 522 % relative to the control (Figure 3.3A). Since the  $\text{O}_2^{\cdot-}$  radical can be detoxified through the Halliwell-Asada pathway by SOD enzymes we evaluated the scavenging capacity of chia seedling by quantifying the total SOD activity together with detection of individual SOD isoforms. The results demonstrated no significant changes in total SOD activity in response to exogenous *p*-CA when compared to the control (Figure 3.3B).



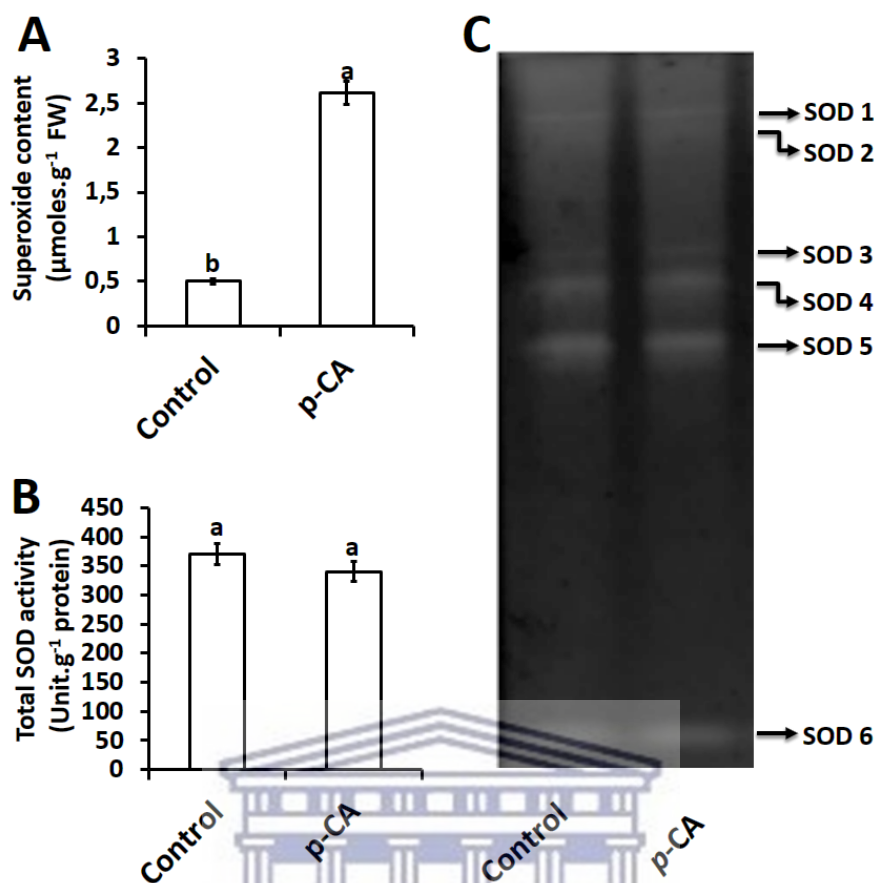


**Figure 3.3.** Superoxide content (A), total SOD activity (B) and the activity of individual SOD isoforms (C) in control and *p*-CA treated chia seedlings. Data represent the mean ( $\pm$  SE) from six independent experiments. Different letters represent statistical significance at  $p \leq 0,05$  (Tukey-Kramer test).

A total of six SOD isoforms were detected and named SOD1-6 (Figure 2C). Upon visual inspection together with densitometry analysis (data not shown) no significant difference was observed for all 6 isoforms in the *p*-CA treatment when compared to the control (Figure 3.3C).

### 3.3.5. Effects of exogenous application of *p*-CA on H<sub>2</sub>O<sub>2</sub> and its extent of lipid peroxidation

The effect of exogenous *p*-CA on H<sub>2</sub>O<sub>2</sub> content and MDA content (an indicator of lipid peroxidation) in the shoots of chia seedlings were investigated. Compared to the control, *p*-CA had no effect on H<sub>2</sub>O<sub>2</sub> content (Figure 3.4A). Based on the results presented here, no significant changes in the extent of lipid peroxidation was observed in shoots of chia seedlings treated with *p*-CA (Figure 3.4B).



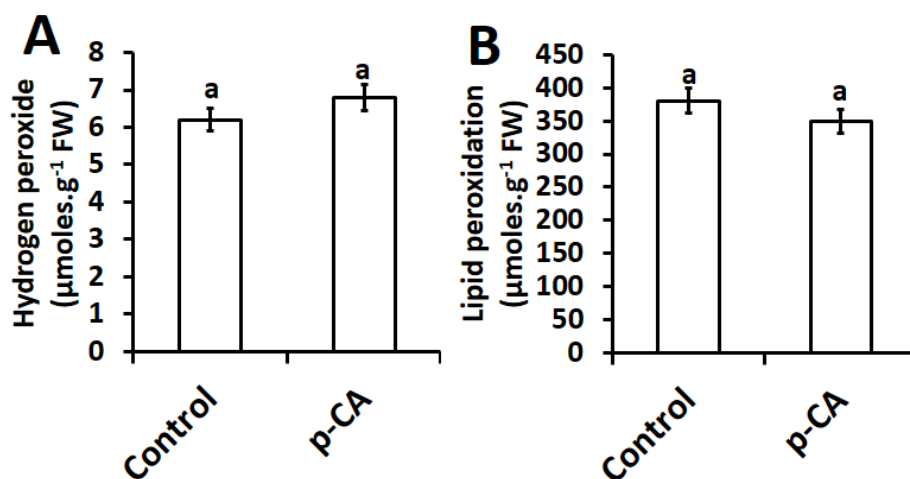


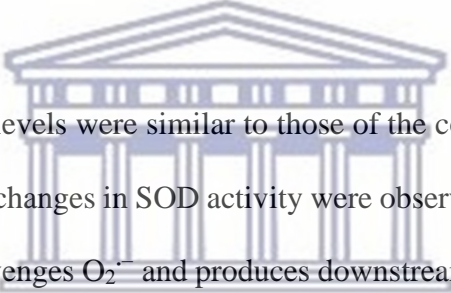
**Figure 3.4.** Hydrogen peroxide content (A) and lipid peroxidation (B) in chia seedling shoots under control and *p*-CA treatment. Data represent the mean ( $\pm$  SE) six independent experiments. Different letters represent statistical significance at  $P \leq 0.05$  (Tukey-Kramer test).

### 3.4. Discussion

In this study we have dissected the role of exogenous *p*-CA on chia plant growth and biochemistry. Exogenous application of *p*-CA has been studied previously in many plant species (Patterson 1981; Baleroni et al. 2000; Ng et al. 2003; Zanardo et al. 2009). Reigosa et al. (1999) performed a germination study on six weed species using different phenolic compounds including *p*-CA and observed that higher concentrations of *p*-CA inhibited germination while low concentrations had no effect on the rate of germination across all six of the weed species. These results are in agreement with our preliminary investigation conducted on chia seeds to test the rate of germination under different concentrations of *p*-CA (0 μM, 100 μM, 250 μM, 500 μM, and 1000 μM). We observed that the final germination percentage was similar across all treatments except for 1000 μM at which no germination occurred (Fig. 3.1 B). Our data also revealed that treatments from germination to sprouting showed no effect across all treatments with an exception for 500 μM and 1000 μM which minimised sprout growth (Fig. 3.1 A). Furthermore, we identified 100 μM as a suitable concentration for further studies on chia seedling growth, physiology and biochemistry. Previous work on *p*-CA supplementation demonstrated that treatment with 100 μM *p*-CA reduced cucumber leaves

(Gerig and Blum 1991). Similar relationships were also observed by many other authors using various concentrations (100  $\mu\text{M}$  - 1000  $\mu\text{M}$ ) of *p*-CA. In those studies, it was demonstrated that exogenous application of *p*-CA had inhibitory effects on root length, root fresh and dry weights of many tested plants species (Patterson 1981; Janovicek et al. 1997; Baleroni et al. 2000; Ng et al. 2003; Politycka and Mielcarz 2007; Zanardo et al. 2009). Contrastingly, an opposite phenomenon was observed in our study because we observed that treatment with 100  $\mu\text{M}$  *p*-CA promoted chia seedling growth and biomass (Fig. 3.2). In addition, we examined chlorophylls *a* and *b*, total chlorophyll and carotenoid contents in the shoots of chia seedlings treated with *p*-CA compared to untreated controls. We observed an increase in chlorophyll pigments (Table 3.1) in chia seedlings treated with *p*-CA, which suggests that exogenous *p*-CA positively regulates chlorophyll synthesis in chia plants. Therefore, we hypothesized that the increase in growth could be as a result of an increase in chlorophyll pigments. This hypothesis is supported by Yan et al. 2016 study, that observed a positive correlation between chlorophyll content and biomass. Contrasting results were observed by Einhellig and Rasmussen (1979) which treated soybean (*Glycine max*) seedlings with exogenous *p*-CA and observed a reduction in chlorophyll content. Einhellig and colleague (1979) suggested that the decrease in chlorophyll content in soybean might be as a result of other secondary responses, as the same phenomenon was not observed in sorghum seedlings. These secondary responses include ROS molecules such as  $\text{O}_2^{\cdot-}$ , which have been shown to interact directly with chlorophyll *a* ultimately leading to chlorophyll degradation (Merzlyak et al. 1991), however Yan et al. 2016 observed an increase in chlorophyll content and  $\text{O}_2^{\cdot-}$  content in response to exogenous salicylic acid and sodium nitroprusside (nitric oxide donor) in wheat. In contrast, exogenous caffeic acid decreased  $\text{O}_2^{\cdot-}$  content in soybean plants Klein et al. 2013, which led to unaltered levels of chlorophyll content Klein et al. 2015. These studies point to a complex interaction between  $\text{O}_2^{\cdot-}$  and chlorophyll in different plants, which has not been elucidated to

date. In our study, higher levels of  $O_2^{\cdot-}$  were detected under exogenous *p*-CA and the scavenging mechanism of  $O_2^{\cdot-}$  did not involve a direct role of SOD enzymes. We observed that total SOD activity and individual SOD isoforms were unaltered in *p*-CA treated chia seedlings, which suggests that other mechanisms of  $O_2^{\cdot-}$  scavenging were possibly triggered by exogenous *p*-CA in the chia seedlings. This phenomenon was also observed by Yan et al. 2016, where the increase in  $O_2^{\cdot-}$  did not result in an increase in SOD activity in response to exogenous sodium nitroprusside. Contrastingly, Klein et al. 2013 showed that exogenous caffeic acid decreased  $O_2^{\cdot-}$  content in soybean plants whereas a significant increase in SOD activity was observed. These studies show a complex interaction between  $O_2^{\cdot-}$  accumulation and scavenging via SOD, which is not well understood.



We also observed that  $H_2O_2$  levels were similar to those of the control seedlings. This finding supports our result where no changes in SOD activity were observed. According to the Asada–Halliwell pathway, SOD scavenges  $O_2^{\cdot-}$  and produces downstream  $H_2O_2$ , which has the ability to oxidize polyunsaturated fatty acids (PUFA) ultimately producing secondary products such as MDA, which is an indicator of lipid peroxidation (Smirnoff, 1993). Lipid peroxidation is a marker for testing membrane cellular damage following oxidative stress (Sheokand et al. 2009). In our study, lipid peroxidation was measured in terms of MDA content and we observed unaltered levels in *p*-CA treated seedlings when compared to the controls (Fig. 3.4B) which might be expected considering no changes in  $H_2O_2$  content was observed under *p*-CA supplementation. The protective effects of compatible osmolytes (GB and proline) in limiting membrane injury have been reported and studies have shown that proline can scavenge ROS molecules (Flowers and Yeo 1986; Hasegawa et al. 2000). Furthermore, compatible osmolytes can also act as osmoprotectants of cellular molecules under a wide range of abiotic stresses (García-Mata and Lamattina 2001; Yancey 2005; Sanchez 2012; Hossain et al. 2014). Matysik

and colleagues 2002, showed that proline can protect the photosystem PSII by scavenging  $O_2^-$  thus reducing lipid peroxidation in the thylakoid membranes. However, our study is in agreement with the results obtained by Jones et al. (2017), which showed that exogenous supplementation of hydroxycinnamic acids (caffeic acid) increased chia plant growth. We propose a mechanism by which exogenous application of *p*-CA improves the growth of chia shoots, possibly through the activation of  $O_2^-$  (Fig. 3.5). This is indicated by our experiments where both  $H_2O_2$  (Fig. 3.4A) and total SOD activity were not affected (Fig. 3.3B). In support of our results, there are several reports showing that, besides directly scavenging  $O_2^-$  (Mathew et al. 2015), *p*-CA can also increase proline accumulation, which has also been linked to  $O_2^-$  scavenging (Flowers and Yeo 1986; Hasegawa et al. 2000).

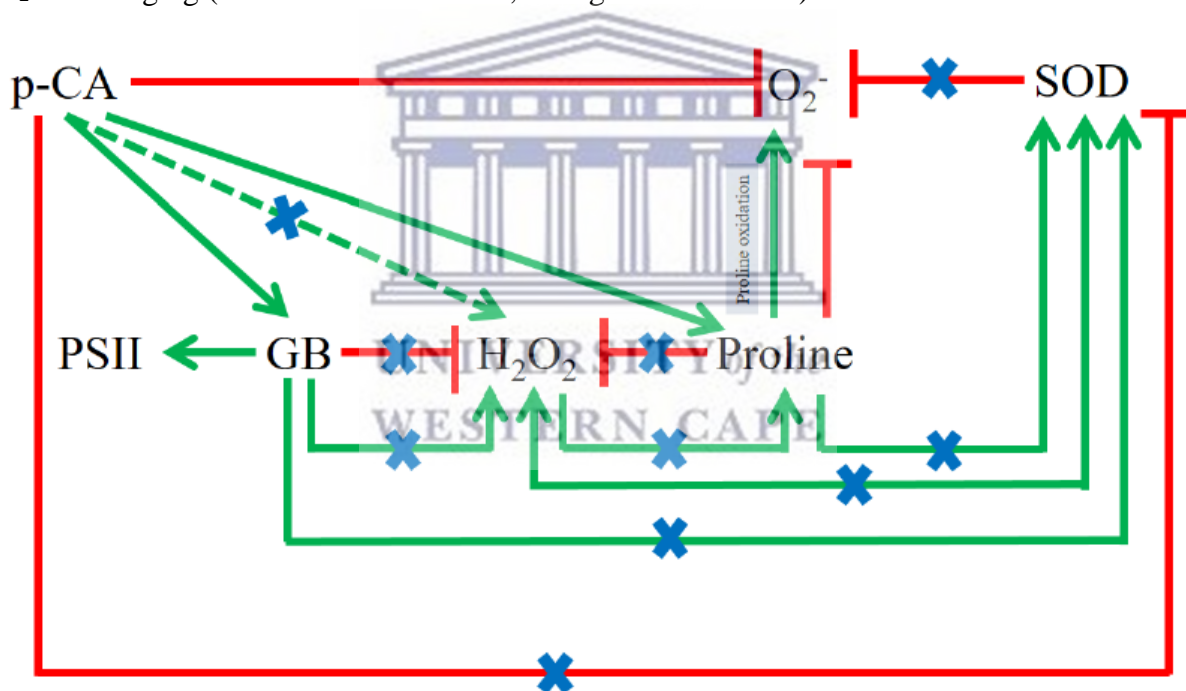


**Figure 3.5.** Schematic model of *p*-CA signalling in chia seedlings. Inhibition or scavenging (red lines). Activation or increase (green lines). Indirect activation or indirect increase (dashed green line). Did not occur in this study (blue crosses).

### 3.5. Conclusion

After summarizing studies on exogenous *p*-CA on plants in a hypothetical model (Fig. 3.5) and incorporating our findings of this study, we conclude that  $O_2^-$  plays a crucial role in the

downstream signalling mechanism of *p*-CA in chia seedlings. This hypothesis was also observed by Gokul et al. (2016) where increases in  $O_2^{\cdot-}$  led to improved growth of *Brassica napus* seedlings. However, in contrast to Gokul et al. (2016), our results showed that the regulation of  $O_2^{\cdot-}$  content in chia seedlings does not occur via SOD but rather through direct scavenging of  $O_2^{\cdot-}$  by *p*-CA (Shen et al. 2019; Kiliç et al. 2013). Furthermore, we hypothesize that the redox buffering capacity of proline (Hossain et al. 2014) (after direct increase by *p*-CA) specifically with regards to  $O_2^{\cdot-}$  plays a major role in synthesis and scavenging of the  $O_2^{\cdot-}$  in addition to the direct scavenging capacity of the *p*-CA. This carefully controls the  $O_2^{\cdot-}$  levels without triggering an increase in SOD activity. Furthermore, we observed no changes in  $H_2O_2$  content and we attribute this to the unchanged SOD activity. We also conclude that the increase in GB by exogenous *p*-CA application led to improved chlorophyll and photosynthetic pigments. This result is supported by findings from Rajendrakumar et al. (1997) which highlighted the role of GB in improving photosynthetic pigments. We hypothesize that *p*-CA improves chia seedling growth via GB and proline activation. Future work should investigate whether the GB pathway occur separately or independently from the proline pathway in chia seedlings treated with *p*-CA.

## CHAPTER 4

### INHIBITION OF *p*-COUMARIC ACID ALTERS CHIA SEEDLING GROWTH, MINERAL CONTENT AND ROS SCAVENGING CAPACITY

#### 4.1. Abstract

*p*-Coumaric acid, as a component of lignin, is ubiquitously present in plants albeit at low concentrations. The biosynthesis of *p*-coumaric acid in plants involves the conversion of phenylalanine to trans-cinnamic acid via phenylalanine ammonia-lyase (PAL), which is then hydroxylated at the para position under the action of trans-cinnamic acid 4-hydroxylase (C<sub>4</sub>H). Alternatively, some PAL enzymes accept tyrosine as an alternative substrate and convert tyrosine directly to *p*-coumaric acid without the intermediary of trans-cinnamic acid. In recent years, the contrasting role of *p*-CA in regulating plant growth and development has been well documented. To understand the contribution of C<sub>4</sub>H activity in *p*-coumaric acid-mediated plant growth coupled with the regulation of reactive oxygen species levels and osmolyte content, we investigated the effect of a trans-cinnamic acid 4-hydroxylase inhibitor (piperonylic acid) on plant growth, osmolyte content, ROS-induced oxidative damage, antioxidant capacity and mineral content in chia seedlings. Piperonylic acid restricted the accumulation of endogenous *p*-coumaric acid which compromised chia seedling development by reducing shoot length, fresh weight and leaf area measurements coupled with enhanced levels of ROS markers (as seen for superoxide and hydrogen peroxide contents). Furthermore, piperonylic acid also triggered an increase in lipid peroxidation and proline accumulation. The inhibition of C<sub>4</sub>H significantly increased the enzymatic activities of ROS scavenging enzymes such as superoxide dismutase, ascorbate peroxidase, catalase and guaiacol peroxidase. Apart from sodium, piperonylic acid significantly reduced the accumulation of the other macro nutrient elements. Given the increase We conclude that *p*-coumaric acid produced from C<sub>4</sub>H activity plays an



essential role in promoting chia seedling growth the findings based on physiological analysis, suggested inhibition of *p*-CA biosynthesis decrease seedling biomass and altered essential macro elements, which is believed to cause by the accumulation of ROS molecules (superoxide  $O_2^-$  and hydrogen peroxide  $H_2O_2$ ) resulting in damage in lipid membranes. Even though there was an increase in essential  $H_2O_2$  scavenging enzymes and proline content the increase was not sufficient enough to minimise the effect caused as a result of ROS-induced damage. Overall, these results further demonstrated phenolic compounds (such *p*-Coumaric acid) play an important role in plant growth and development. As the inhibition of  $C_4H$  enzyme, which is involved in the production of *p*-Coumaric acid, resulted in decrease in plants growth and development.

## 4.2 Introduction

*p*-Coumaric acid (*p*-CA) is one of the phenolic acids which is widely distributed in plants and possess a versatile role in modern medicine as an antioxidant (Castelluccio et al. 1995), as a potential cardioprotective (Castelluccio et al. 1995), anti-microbial (Cho et al. 1998), anti-mutagenic (Ferguson et al. 2003), anti-platelet (Luceri et al. 2007), and anti-inflammatory (Luceri et al. 2004) agent. In plants, *p*-CA has been shown to reduce the rate of germination, root length and biomass in different plant species (Patterson 1981; Janovicek *et al.* 1997; Reigosa et al. 1999; Baleroni et al. 2000; Ng et al. 2003; Politycka and Mielcarz 2007). This led to a general perception that exogenous application of *p*-CA acid inhibits plant growth and development as observed in leguminous plants (Zanardo et al. 2009). However, an opposite phenomenon was observed in a study conducted in our laboratory (Nkomo et al. 2019; see Chapter 3), which demonstrated that treatment with 100  $\mu$ M *p*-CA, promoted plant growth and biomass of chia seedling. Thus, we proposed that different species may react differently to exogenous application of *p*-CA. However, there seems to be a lack of published data regarding the effect of *p*-CA on pseudocereals.



Thus, to determine if the increase in plant growth observed in the study by Nkomo et al. (2019) and documented in Chapter 3, was due to exogenous application of *p*-CA, we investigated the impact of *p*-CA inhibition on chia plant growth. To test this hypothesis, we used piperonylic acid (PA); an efficient competitive inhibitor of the Cinnamate 4-hydroxylase (C<sub>4</sub>H) enzyme which is responsible for the biosynthesis of *p*-CA (Schalk et al. 1998). The C<sub>4</sub>H enzyme is found upstream in the phenylpropanoid pathway and it catalyses the hydroxylation of cinnamic acid to produce endogenous *p*-CA. In this chapter, we investigated the mechanism underlying the inhibition of endogenous *p*-CA by using PA as an efficient inhibitor of C<sub>4</sub>H enzyme. The primary aim was to study the physiological and molecular effects of PA on chia seedling growth. Furthermore, we will also examine the influence of PA on essential macro elements of chia seedlings using ICP-OES

### 4.3. Results

#### 4.3.1. Inhibition of *p*-CA restricts chia plant growth

Plants treated with PA experienced a loss in shoot height (16 %) and fresh weight (40 %) compared to control plants (Figure 4.1A-C). A similar trend was observed for the leaf area measurement in PA treatment compared to the control (Figure 4.1D). The leaf area of chia seedlings treated with PA was reduced by 46 % when compared to the control (Figure 4.1D). A direct relationship exists between C<sub>4</sub>H activity and *p*-CA production therefore quantifying the level of *p*-CA in the shoots of chia seedlings serves as a good indicator of C<sub>4</sub>H activity. The results showed that exogenous PA reduced C<sub>4</sub>H activity (as seen for *p*-CA content levels) in the shoots of chia seedlings by 98 %, when compared to the control (Figure 4.1E).

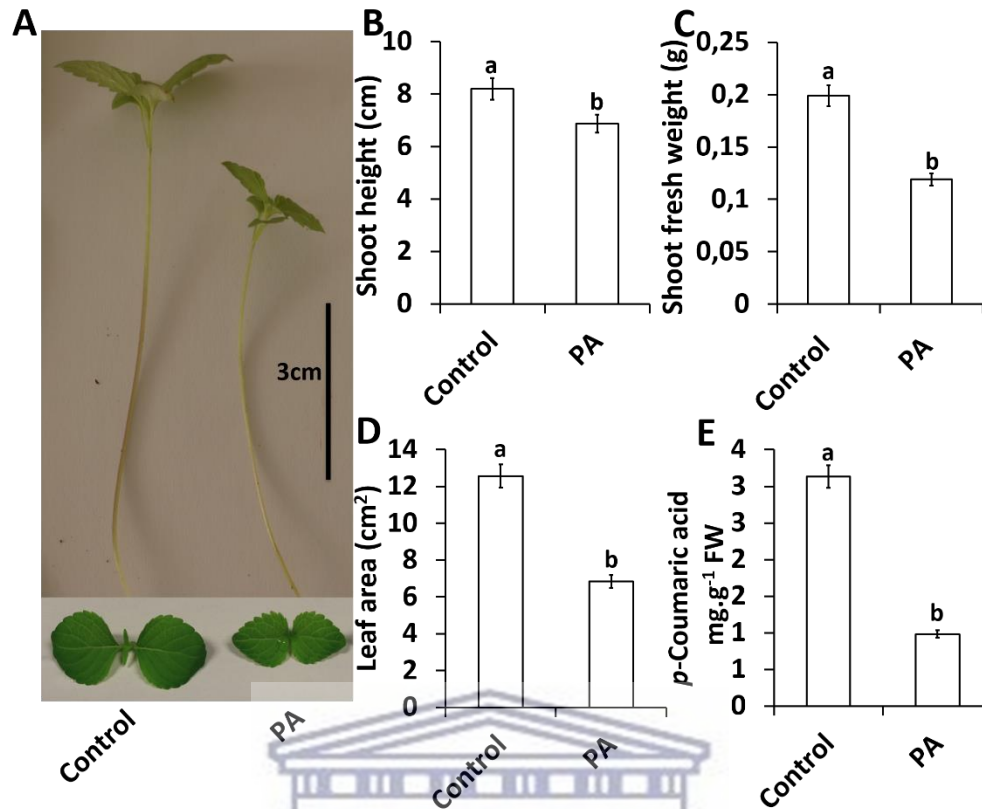


**Figure 4.1.** Exogenous PA restricts chia seedlings growth and *p*-CA content. Plant growth parameters include individual representatives of each treatment (A) shoot height (B), fresh weight (C), leaf area (D) and measurement of *p*-CA (E). Data represent the mean ( $\pm$ SE) from six independent experiments. Different letters above the error bars indicate means that are statistically significantly different at 5% level of significance.

UNIVERSITY of the  
WESTERN CAPE

#### 4.3.2. PA increases ROS accumulation and the extent of lipid peroxidation

The impact of *p*-CA inhibition (as a consequence of PA treatment) on ROS marker accumulation and ROS-induced oxidative damage was measured. Exogenous application of PA significantly increased superoxide content by 1755% in the shoots of chia seedlings when compared to the control seedlings (Figure 4.2A). A similar trend was observed for hydrogen peroxide content although not to the same extent as was observed for superoxide content. Chia seedlings treated with PA increased hydrogen peroxide content in the shoots with 77% when compared to the control (Figure 4.2B). The increase in ROS biomarkers resulted in a significant increase in oxidative damage manifested as enhanced levels of malondialdehyde (MDA). The malondialdehyde content in PA treated plants was increased by 164% when compared to that of the control plants (Figure 4.2C).

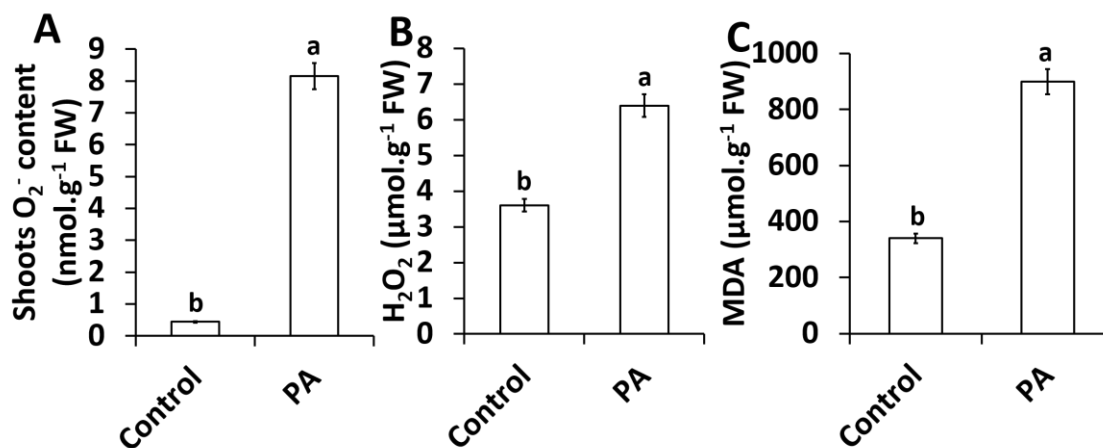


**Figure 4.2.** The influence of PA on superoxide content (A) hydrogen peroxide content (B) and malondialdehyde content (C). The O<sub>2</sub><sup>-</sup> content was measured using freshly harvested shoot material from chia seedlings. Data represent the mean (± SE) of six independent experiments. Means with different letters are significantly different from each other ( $p \leq 0.05$ ).

#### 4.3.3. Exogenous PA augments proline and total SOD in the shoots of chia seedlings

It is well known that the accumulation of ROS molecules triggers a cascade of events that ultimately leads to degradation of lipids membrane (known as lipid peroxidation). Osmolytes such as proline plays a highly beneficial role in plants exposed to various stress conditions. Besides acting as an excellent osmolyte, it helps plants minimise ROS-induced oxidative damage by means of direct ROS-scavenging. Here, we illustrate a direct relationship between ROS accumulation (Figure 4.2A-B) and increased proline content in chia seedlings treated with PA (Figure 4.3A). A significant increase in proline content (1444%) was observed in the shoots of chia seedlings in response to exogenous PA when compared to the control plants (Figure 4.3A). In light of the augmented levels of superoxide observed in chia shoots treated with PA (Figure 4.2A), changes in total SOD activity (superoxide scavenging antioxidant enzyme) in the same tissue was measured. The result showed that when exogenous PA was augmented, that also increased total SOD activity (121%) to levels significantly higher than those for the control plants (Figure 4.3B).

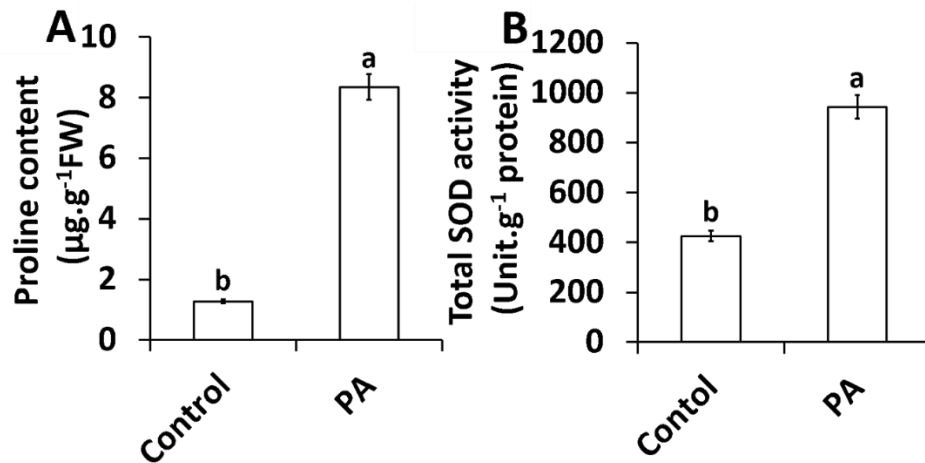


**Figure 4.3.** PA increased proline content (A) and total SOD activity (B) in chia seedlings shoots. Data represent the mean ( $\pm$  SE) of six independent experiments. Different letters represent statistical significance at  $p \leq 0.05$ .

#### 4.3.4. PA alters changes in hydrogen peroxide scavenging antioxidant enzyme activities

Alteration of the activity of antioxidant enzymes in response to ROS-induced oxidative damage is well-documented in a variety of plant species and there is evidence (albeit minimal) that such responses are modulated by phenolic acids such as *p*-CA. However, reports on the modulation of these antioxidant responses when *p*-CA is inhibited remain elusive. In light of the increase in hydrogen peroxide content (Figure 4.2B) we investigated the effect of PA (*p*-CA inhibitor) on the enzymatic activities of some H<sub>2</sub>O<sub>2</sub>-scavenging enzymes including ascorbate peroxidase (APX), catalase (CAT) and guaiacol peroxidase (POD). The results showed that exogenous PA increased the total enzymatic activities of all three antioxidants relative to their respective controls (Figure 4.4). APX activity in the shoots was increased by 22% in response to treatment with PA when compared to the untreated control (Figure 4.4 A). Similar trends were observed for enzymatic activities of CAT and POD in response to PA although their increase in activity was significantly higher than was observed for APX when compared to their respective controls. The enzymatic activity of CAT in the shoots of chia seedlings was increased by 124% in response to PA when compared to the untreated controls (Figure 4.4B). POD activity in the

shoots of chia seedlings was augmented by 80% in response to treatment with PA relative to the control (Figure 4.4C).

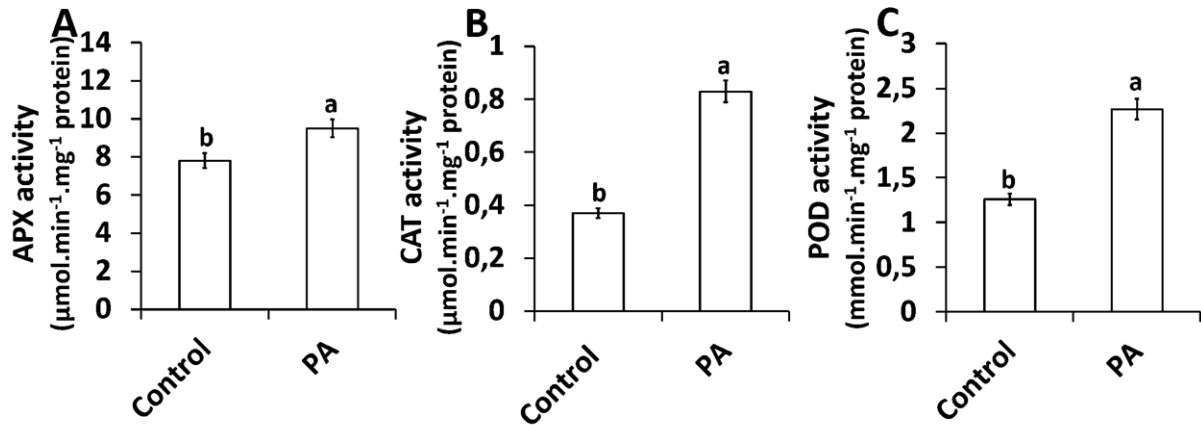


**Figure 4.4.** Changes in shoot APX (A), CAT (B) and POD (C) activities in response to exogenous PA. Data represent the mean ( $\pm$  SE) of six independent experiments. Different letters represent statistical significance at  $p \leq 0.05$ .

#### 4.3.5. A survey of essential macro-elements in response to exogenous PA

Changes in mineral content was monitored in the shoots of chia seedling after treatment with PA. The mineral contents of five essential macro-elements measured in chia seedlings are shown in Table 4.1, and the values are expressed as mg/g fresh weight of plant material. The macro-elements analysed included sodium (Na), magnesium (Mg), phosphorus (P), potassium (K) and calcium (Ca). For the mineral content analysis, we expressed our results relative to the controls (red arrow indicates a decrease with the blue arrow indicating an increase) to express the abundance of essential macro-elements. The macro element Na was increased by 19 % in response to PA when compared to the control (Table 4.1). Interestingly, the rest of the essential macro elements showed a significant reduction in content in response to PA when compared to the control. Potassium (K) content was reduced by 64 % in the PA treatment relative to the control. Both phosphorus (P) and magnesium (Mg) contents was reduced by 56 % when compared to their respective control. Finally, calcium (Ca) content was decreased by 53 %, when compared to the control.

**Table 4.1.** Content of essential macro elements in the shoots of chia seedlings. Macro elements data expressed in mg.g<sup>-1</sup> FW, presented by the means ± SE (n = 3). The blue arrow represents an increase in macro elements, while the red arrow represents a decrease when comparing the *p*-CA treatment to the control.

Minerals	Mineral relative content (mg.g <sup>-1</sup> FW)		Class
	Control	PA	
Na	0.057±0.004	0.068±0.005 ↑	Essential Macro-elements
K	4.513±0.0068	1.609±0.048 ↓	
P	0.329± 0.002	0.146±0.005 ↓	
Mg	0.387±0.006	0.169±0.006 ↓	
Ca	0.497±0.002	0.231±0.006 ↓	

#### 4.4. Discussion

The present study demonstrated that inhibition of endogenous *p*-CA (using PA) significantly affected chia seedling growth. Furthermore, there was a reduction in levels of essential macro elements, which was accompanied by significant biochemical alteration in ROS-signalling homeostasis. A recent study done in our laboratory showed that exogenous application of *p*-CA enhanced chia seedling growth (Nkomo et al. 2019; see Chapter 3). To our knowledge, this was the first study that showed a positive effect of exogenous *p*-CA on plant growth. In the present study, we attempt to establish a link or prove the role of *p*-CA as a plant growth-signalling molecule by restricting the enzymatic activity of the enzyme (C<sub>4</sub>H) responsible for its biosynthesis. This was achieved through the use of a selective inhibitor, piperonylic acid (PA), which is known to inhibit the production of endogenous *p*-CA by blocking the trans-cinnamate 4-hydroxylase (C<sub>4</sub>H) enzyme (Schalk et al. 1998).

##### 4.4.1. Inhibition of *p*-CA impairs growth and development in chia seedlings

The underlying idea behind this study, was to demonstrate that if *p*-CA improved plant growth (as seen in Chapter 3; Nkomo et al. 2019), then inhibition of endogenous *p*-CA could perturb



the growth and development of chia seedlings. We first analysed the efficiency of C<sub>4</sub>H enzyme in producing endogenous *p*-CA, and noted that PA reduced *p*-CA content in the shoots of chia seedlings to a level that is two times less than observed in the control seedlings (Fig. 4.1E). This is in line with the work performed by Schalk and co-workers which showed PA to be an efficient inhibitor (showed a 58 % irreversible inhibition) of C<sub>4</sub>H compared to other tested inhibitors (Schalk et al. 1998). In addition to the reduction in *p*-CA content we observed a significant reduction in plant growth as shown through the reduction of shoot length and fresh weight in response to exogenous PA, when compared to the control (Figure 4.1A-C). The decrease in *p*-CA accumulation together with a reduction in plant growth and biomass for chia seedlings suggested that there could be a direct link between *p*-CA biosynthesis and plant growth. However, we could not find substantial literature which focused on plant growth effects, as there is fewer plant research performed using this specific elicitor (PA) and those that we found only focus on its effect on C<sub>4</sub>H biosynthesis of lignin content (Zanardo et al. 2009). To our knowledge, this study is a first of its kind that investigated the impact of PA on above ground growth as the only other study we could find, explored the impact of PA on *Arabidopsis* root growth under UV-light stress Wong et al. (2005).

#### **4.4.2. PA augments ROS content and reduces membrane stability**

Inhibition of plant growth is caused by a plethora of biological processes, with ROS-induced damage as the most dominant in literature. While, evidence about modulation of ROS-induced oxidative stress using phenolic acids are slowly emerging (Klein et al. 2015; Jones et al. 2017), little information is known about the mechanisms by which these phenolic acids regulate ROS molecules. Here, we analysed the effect of PA on ROS accumulation and the extent of lipid peroxidation (measured as MDA) in the shoots of chia seedlings. The role of PA on ROS accumulation in plants remain very limited, and the only report found in literature shows that



PA reduced ROS accumulation (Lee et al. 2018). This is in contradiction to the observation made in this study where we showed that PA at a final concentration of 100  $\mu$ M increased ROS accumulation (as seen for superoxide and hydrogen peroxide levels) in the shoots of chia seedlings (Figure 4.2A-B). However, it is noteworthy that the work done by Lee et al. (2018) was on keratinocyte growth and not plant seedlings as reported in this study. The increase in ROS observed in response to exogenous PA resulted in an even higher increase in malondialdehyde content (manifested as increased lipid peroxidation). The observed increase in ROS molecules (Figure 4.2A-B) could be directly linked to the increase in MDA (Figure 4.2C), as most plant studies seem to point out that there is a direct correlation between the build-up of ROS molecules and damage to membrane lipids (Keyster et al. 2012; Keyster et al. 2013).

#### **4.4.3. PA augments proline accumulation**

Plants exhibit a variety of adaptive strategies to alleviate the adverse effects of ROS accumulation. One of these strategies involves the accumulation of compatible solutes, such as proline, which plays an essential role in osmotic adjustment and stabilization of enzymes, involve in ROS scavenging (Mittler 2002; Yancey 2005; Slama et al. 2015). This in turn helps re-establishing a cellular redox balance through suppression of ROS production. Considerable interest has been developed on the influence of proline on scavenging ROS molecules in plants. Using chia seedling, Nkomo et al. (2019) was able to demonstrate that proline accumulation was essential and had an ability to scavenge  $O_2^-$  radical. However, in our current study, the higher level of proline in PA treatment couldn't lead to the reduction or scavenging of  $O_2^-$  radical. As, we observed high levels of  $H_2O_2$ , which is mostly produced from the direct dismutation of  $O_2^-$  by an enzyme called superoxide dismutase. Therefore, it could be argued that under PA treatment, proline accumulation was unable to act as a ROS scavenger. This

could be possible explained by the dual role of proline, meaning the higher level of proline content may be part of a stress signal influencing adaptive responses.

#### **4.4.4. PA augments antioxidant enzymes**

In plants SOD is the main key enzyme that plays a role in O<sub>2</sub>- detoxification and producing H<sub>2</sub>O<sub>2</sub> as a by-product in plants (Foyer and Noctor 2005). Therefore, in our study, we observed an enhanced conversion of O<sub>2</sub>- to H<sub>2</sub>O<sub>2</sub> due to the increase in SOD enzymatic activity in response to inhibition of endogenous *p*-CA on our PA treatment (Figure 4.3 B). This implies that there would be accumulation of H<sub>2</sub>O<sub>2</sub> in the plant tissue, which is seen in the results presented here (Figure 4.2 B). Hence, in our study, we further measured H<sub>2</sub>O<sub>2</sub> scavenging antioxidant enzymes after observing that the increase in SOD activity led to an increase in chia shoots H<sub>2</sub>O<sub>2</sub> content, following PA treatment. It is now widely accepted that the degree of oxidative cellular damage in plants is controlled by the capacity of H<sub>2</sub>O<sub>2</sub> scavenging enzymes such as APX, CAT and POD (Figure 4.4). Ascorbate peroxidase (APX) is valued for its ability to be functional within the chloroplast, mitochondria, peroxisomes as well as in the cytosol (Mittler et al. 2004). According to Pandey et al. (2015), ascorbate peroxidase (APX) is labelled as the key enzyme within the ascorbate – glutathione (Halliwell – Asada) pathway by functioning to reducing H<sub>2</sub>O<sub>2</sub> to H<sub>2</sub>O and O<sub>2</sub>, using ascorbate (AsA) as an electron donor. The total APX activity increased when endogenous *p*-CA was inhibited using elicitor PA (Figure 4.5 A), similar results were also observed with another peroxidase (POD) that utilises guaiacol instead of ascorbate (Figure 4.5 C). Gill and Tuteja 2010, claimed that one molecule of CAT can convert 6 million H<sub>2</sub>O<sub>2</sub> molecules and this is without the use of any substrate. This could possibly explain why, we observed a slight increase in H<sub>2</sub>O<sub>2</sub> content considering that O<sub>2</sub>- levels were almost nineteen times higher under PA-treatment when compared to the control.

Based on the research and literature conducted in this study, Nkomo et al. (2019) and Jones et al. (2017), were the only studies we could find focusing on the involvement of phenolic acids and its role in antioxidant protection of chia plants. While no data exist of the role of antioxidant on the inhibition of endogenous phenolic acids. So, this study, is important due to the fact that it forms a base line study to which future studies can refer. Hence, we can only suggest that the increased lipid peroxidation, signified by increased MDA levels, in response inhibition of endogenous *p*-CA was caused as a consequence of the increased ROS production seen in the shoots of chia seedlings treated with PA. We, therefore had to speculate that the increase of the H<sub>2</sub>O<sub>2</sub> scavenging enzymes was not low enough to cause an appreciable decrease in H<sub>2</sub>O<sub>2</sub>, which lead to an increase in lipid peroxidation.

#### **4.4.5. PA augments essential mineral content**

To date no positive correlation link or negative correlated linked study has been performed on any essential macro elements under PA treatment. Essential macro elements and osmolytes play a significant role in the plant's biochemistry, contributes to physiological defence against oxidative and free-radical-mediated reactions in the plant systems. The relationship between certain types of phenolic acids and essential macro elements or antioxidants is an ongoing topic. However, to our knowledge; no previous studies are available regarding the evaluation of the status of Na, K, P, Mg and Ca in the evaluation of these macro-elements, under phenolic acids inhibition. Our result found significantly lower level of K, P, Mg and Ca in seedlings supplemented with PA when compared to control (Table 4.1). Thus, significant depletion of these essential macro elements as reported in the current study may trigger the reduction in plant growth. Moreover, the results from our study seems to lay a proper foundation for future research focusing on the alteration of these essential macro elements and phenolic acids.

## 4.5. Conclusions

The results presented in this study show that PA inhibited growth and development in chia seedlings. With this experimental model, we have confirmed that *p*-CA plays an active influential role in promoting growth. As, demonstrated in the previous study by Nkomo et al. (2019), exogenous application of *p*-CA at a concentration of 100  $\mu$ M showed a promoting effect on the growth and development of chia seedlings. In conclusion, this study demonstrated that the inhibition of endogenous *p*-CA using PA had antagonistic effect on the plants physiological processes. An increase in ROS was also observed in response to PA, resulting in an increase in lipid peroxidation. This increase in lipid peroxidation was most likely attributed by the effect of PA on the antioxidant capacities within chia seedling and thus the seedlings were unable to induce its antioxidant system adequately. This study in correlation with our previous study (Nkomo et al. 2019), seems to demonstrate that *p*-CA, is crucial for the regulation of the plant antioxidant system which in turn maintains redox homeostasis within plants. Although an existing body of evidence is available on the effect of other phenolic compounds supporting Nkomo et al. (2019) results (Linic et al. 2019; Silva et al. 2018; Wang et al. 2019), the seems to be a lack of data or literature on the effect of phenolic acid inhibition (using PA) on proline accumulation and its role as a ROS scavenger. Another important factor that was not explored within our previous study is the role of essential macro-elements.

Current study seems to suggest that the reduction in essential elements such as K, P, Ca and Mg could have also contributed to the reduction in chia seedling growth. This is due to the fact that these essential elements are known to play an important role in plant growth promotion and development. In future studies, proteomics could be an option for identification, characterization and profiling of proteins, that are unique to the changes in exogenous *p*-CA applications and endogenous *p*-CA inhibition imposed by PA. This would ultimately give us a

better understanding as to how *p*-CA promotes plants growth and its role in mediating changes in the production and metabolism of reactive oxygen species.



## CHAPTER 5

### ***p*-COUMARIC ACID AND SALT STRESS DIFFERENTIAL ALTERS THE IONOMIC AND PROTEOMIC PROFILES OF CHIA SHOOTS**

#### **5.1. Abstract**

The aim of this study is to determine the physiological, ionomics and proteomics effect of *p*-CA on chia seedlings under salt stress. To that end, chia seedlings were supplemented with Nitrosol(R) containing: 100  $\mu$ M *p*-CA, 100 mM NaCl and their combined (100 mM NaCl + 100  $\mu$ M *p*-CA) solutions, at 2-day intervals for a period of 14 day with (control) containing Nitrosol ® only. Salt stress decreased the growth parameters and the majority of the essential macro-elements (K, P, Ca and Mg), except that of sodium (Na). While, simultaneous application of *p*-CA with salt stress treatment (*p*-CA + NaCl) alleviated the effect of salt stress on chia shoots seedlings and this was notably by the increase in chia biomass.

While, simultaneous application of *p*-CA with salt stress showed a significant increase in the essential microelements, Mg and Ca. In the proteomic analyses, a total 907 proteins were identified across all treatments. These proteins were localised to various cellular compartments including the chloroplast and ribosomes. Interestingly, 14% of identified proteins were not localised to any cellular compartment due to the lack of genomic and proteomics data for chia and/or related species. However, this study was focused on the proteins involving *p*-CA induced plant growth in both the presents and absence of salt stress. Based on the functional characterisation of the identified protein isoform, these proteins seem to play a significant role in various biological processes including photosynthesis, metabolism, signal transduction and stress responses. While the proteins which are involved in conferring *p*-CA induced salt stress tolerant (identified 26 protein), of which the majority were uncharacterized proteins.



Hence, we suggest that future studies should focus on the functional characterization of this uncharacterised proteins. While, exploring the possible link between these uncharacterised proteins and essential macro-elements (Mg and Ca), which were demonstrated to be higher in NaCl + *p*-CA treatment. As, it was suggested that both Mg and Ca, could be involve in promoting growth under salt stress.

## 5.2. Introduction

Salt stress is primarily caused by improper agricultural practices, which have been estimated to affect 20 % of total cultivated land and 33 % of irrigated agricultural lands worldwide (Jamil et al. 2011). Generally, plants grown in salt stress environment mainly come across major drawbacks, which may occur when there is irregular irrigation, inadequate drainage, wrong fertilizer application and the use of sea water in mining (George et al. 1997; Wang et al. 2003). In plants, the most common effect of salt stress includes slow growth or inhibition, which mostly arises from disturbance of nutritional macro elements (Marschner 1995; Grossman and Takahashi 2001). In fact, long term exposure to salt stress, is also associated with reduction in biomass and crop yield that results in agricultural damage causing millions of dollars (Mahajan and Tuteja 2005).

Several strategies have been developed in order to alleviate the effect caused by salt on plant growth and development, which includes plant genetic engineering (Wang et al. 2003), and recently the use of phenolic compounds to promote growth (Nkomo et al. 2019). While, the role of phenolic compounds in plant growth promotion and nutrient management is not well known or established. There is a slow emerging trend on the use of phenolic compounds in overcoming salt stress (Klein et al. 2015; Jones et al. 2017; Khairy and Roh 2016; Kaur et al. 2017). *p*-Coumaric acid (*p*-CA) is one of the phenolic compounds that have received much attention in the literature, with fewer studies suggesting that utilization of *p*-CA can become a promising alternative to alleviate salt stress (Khairy and Roh 2016; Kaur et al. 2017). While,



decrease in cell membrane permeability, reactive oxygen species-, compared to an increase in antioxidant enzyme and osmoprotectant were proposed by these authors to explain the positive effect of *p*-CA on the elongation of plant growth under salt stress. However, apart from these studies which have reported on the physiological and biochemical changes, there seems to be lack of molecular data on nutritional elements and protein abundance. Thus, studies involving ion/mineral uptake or protein abundance may help in addressing how phenolic compounds are able to confer tolerance against salt stress. This is due to the fact that ionomics studies on salt stress, mostly shows a great correlation between salt stress tolerance and mineral uptake. Hence in the current research our aim will be to study the influence of *p*-CA on macro elements presents in chia seedling exposed to salt stress, and further perform a large-scale proteomics analysis to help identify and characterized proteins associated *p*-CA induced salt stress tolerant, as no proteome information is available on the non-specific or direct effect of *p*-CA on salt stress.

### 5. 3. Results

#### 5.3.1. *p*-CA improves chia seedling growth under salt stress

The result shows that *p*-CA and salt stress (imposed by application of 100 mM NaCl) differentially alters shoot growth of chia seedlings (Figure 5.1). Exogenous application of *p*-CA enhanced the shoot length by 26 % when compared to the control (Figure 5.1A). Salt stress negatively influenced shoot growth as seen for the reduction of 14 % relative to the control (Figure 5.1B). *p*-CA showed a reversal of the negative effects caused by salt stress. Shoot fresh weight was increased by 59 % in response to *p*-CA, whereas a significant reduction of 19 % was observed in the salt stress treatment when compared to the control (Figure 5.1B). However, salt stress plants supplemented with *p*-CA showed a marked increase in shoot length relative salt treatment and the control plants (Figure 5.1B). A similar trend was observed for the shoot dry weights (Figure 5.1C). Exogenous *p*-CA enhanced shoot dry weight by 28 % compared to

the control whereas a significant reduction of 17 % was observed in the salt stress treatment. However, application of *p*-CA to salt stressed plants reversed the reduction in dry weights (to the level of the control) that resulted from the salt stress treatment.

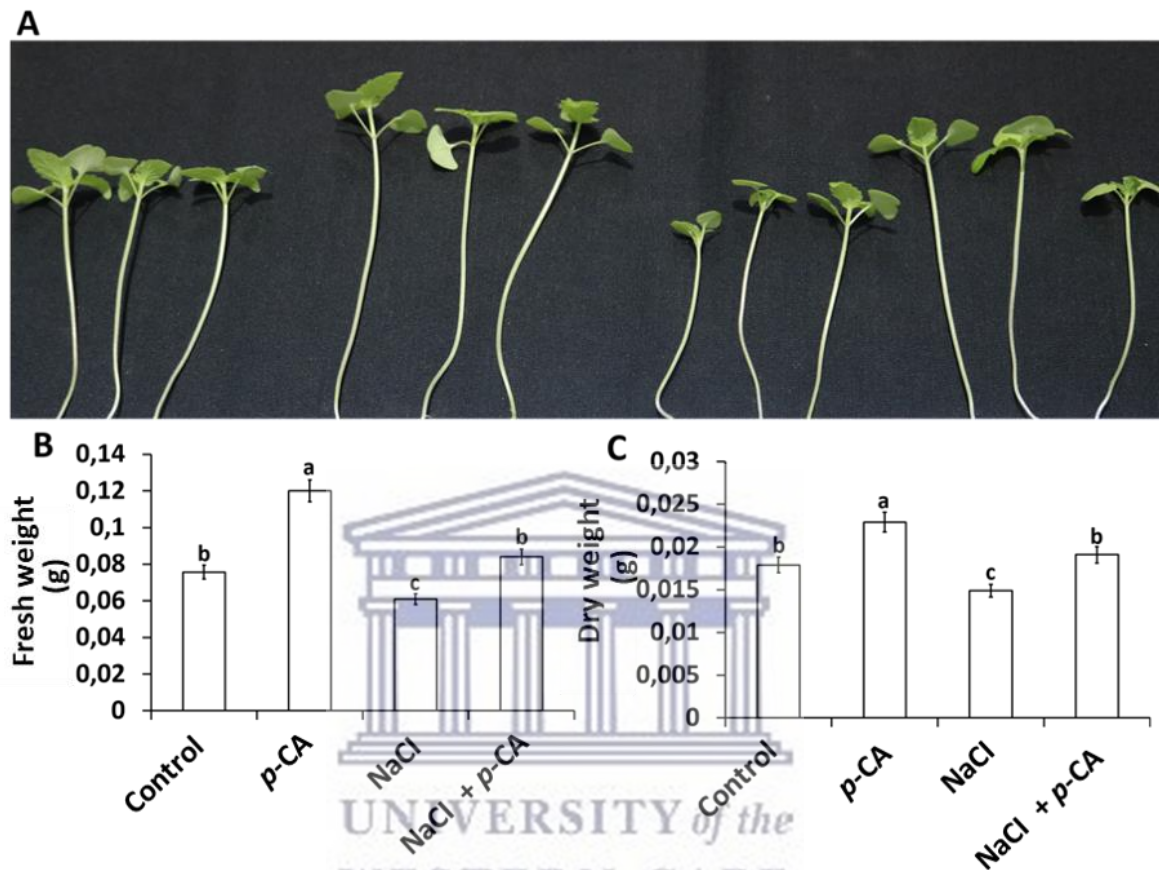


**Figure 5.1.** The effect of *p*-CA and salt stress (NaCl) on chia seedling growth and biomass. Changes in (A) shoot length of chia seedlings (left to right; Control, *p*-CA, NaCl and NaCl + *p*-CA) and (B) fresh weights and (C) dry weights was measured in response to the different treatments. Data represent the mean ( $\pm$ SE) from six independent experiments. Different letters represent statistical significance at  $P \leq 0.05$  (Tukey-Kramer test).

### 5.3.2. Effects *p*-CA and salt stress on mineral content

The Na, K, P, Mg and Ca content were measured in the shoots of chia seedlings in response to *p*-CA, salt stress and a combination of *p*-CA and salt stress (Table 5.1).

#### *a. Na content*

The shoot Na content of chia seedlings were significantly enhanced in all the treatments with the highest increased observed in the combined treatment (*p*-CA + NaCl) when compared to

the control. *p*-CA increased Na content by 322 %, whereas salt stress increased Na content by 512 %. However, the highest increase in Na content (1175 %) was observed in the salt stressed treatment supplemented with *p*-CA. The increase in Na content in all treatments were quantified relative to the untreated control (Table 5.1)

#### ***b. K content***

The results showed that *p*-CA did not alter K content when compare to the control. However, a significant reduction in K content was observed in response to salt stress (NaCl). Salt stress reduced K content in the shoots of chia seedlings by 66 % when compared to the control. The decrease in K content in the combined treatment was not as pronounced as observed in the salt stress treatment. Salt stressed chia seedlings supplemented with *p*-CA reduced K content by 11 % relative to the control.

#### ***c. P content***

The P content in the shoots of chia seedlings was differentially altered by the different treatments. A slight but significant increase (14 %) in P content was observed in response to *p*-CA. However, chia seedlings treated with salt stress and a combination of salt stress and *p*-CA showed a significant reduction in K content with the more significant reduction observed in the salt stress treatment (75%). In the combined treatment (*p*-CA + NaCl) K content was reduced by 35 % relative to the untreated control.

#### ***d. Mg content***

Similar to what was observed for Na and P, exogenous *p*-CA increased Mg content to a level significantly higher (13 %) than observed for the untreated control. In response to salt stress, Mg content was reduced by 57 % when compared to the untreated control. Contrary to what was observed in the salt stress treatment, a significant increase (22 %) in Mg content was observed in the salt stress treatment supplemented with exogenous *p*-CA. This increase in Mg

content was significantly higher than was observed in both the *p*-CA treatment and untreated control.

**Table 5.1.** The differences in mineral contents (mg.g<sup>-1</sup> FW) in response to *p*-CA, salt stress and a combination of *p*-CA and salt stress. The data that represents the mean ± SE in same column with dissimilar letters are significant at  $p \leq 0.05$ . The blue arrow shows an increase in mineral content, while the red arrow represents a decrease and the star sign shows that no significant difference was observed when compared to the control.

Minerals	Mineral relative content (mg.g <sup>-1</sup> FW)				Class
	Control	<i>p</i> -CA	NaCl	NaCl + <i>p</i> -CA	
Na	0.057±0.004	0.241±0.194 ↑	0.349±0.015 ↑	0.727±0.067 ↑	Essential Macro elements
K	4.513±0.068	4.326±0.270*	1.552±0.062 ↓	4.007±0.707 ↓	
P	0.329± 0.002	0.376±0.064 ↑	0.081±0.004 ↓	0.214± 0.012 ↓	
Mg	0.387±0.006	0.439±0.035 ↑	0.168±0.007 ↓	0.471±0.031 ↑	
Ca	0.497±0.002	0.751±0.200 ↑	0.250±0.008 ↓	0.773±0.039 ↑	

### 5.3.3. Separation and visualization of chia shoot proteome

A fraction (10 µg) of each treatment was size fractionated on a 1D SDS polyacrylamide gel prior to identification of differential proteins using liquid chromatography mass spectrometry (LC MS). The results show that separated proteins are of high quality with no visible streaking or protein degradation. Separated proteins from all treatments covered a molecular weight range between 10 to 200 kDa. Distinct banding patterns with different intensities (abundance) were observed in all treatments when compared to the untreated control (See black arrows; Figure 5.2). The results showed that *p*-CA and salt stress (imposed by 100 mM NaCl) significantly reduced protein abundance (as seen for band intensities) in relation to the untreated control.

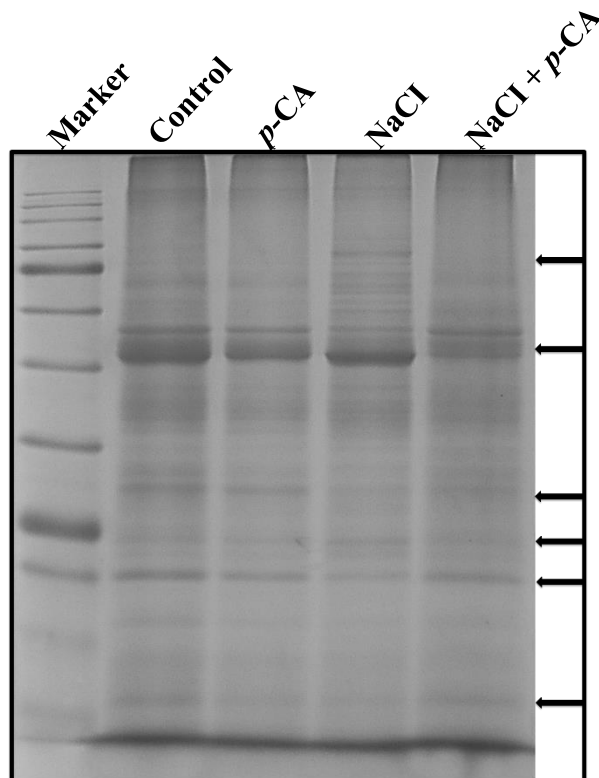


**Figure 5.2.** One – dimensional shoots proteome profile of chia in response to *p*-CA and salt stress. Protein extracts (10 µg) from different treatments were size fractionated on a 12 % denaturing 1D SDS polyacrylamide gel. Black arrows indicate differences that were visually observed.

However, the combined treatment of *p*-CA and salt stress showed a similar profile to that of the untreated control. Based on the visual confirmation about the quality and integrity of isolated proteins, protein pellets from each sample was digested in a trypsin compatible buffer system (as described in section 2.14.1). The protein content/concentration of each samples was determined using the direct detect system (Table 5.2).

**Table 5.2.** Shoot protein concentrations of chia seedlings in response to different treatments

Samples/Treatments	Protein concentrations (mg/ml)
Control	1.5
<i>p</i> -CA	1.19
NaCl	1.00
<i>p</i> -CA + NaCl	1.03

### 5.3.4 Identification and subcellular localisation of shoot proteins using LC MS analysis

As a critical component of bio-analysis, a system suitability test was performed to ensure that the LC/MS/MS system is operating in a manner that leads to the production of accurate and reproducible data. For this test, a blank (A) and suitability sample (B; consisting of all four protein mixtures) were analysed and the results were captured as peaks on a total ion chromatogram (TIC) (Figure 5.3). The results of the blank show that no major contamination was detected (Figure 5.3A). A similar response was observed when the suitability mixture sample as analysed on the mass spectrometer (Figure 5.3B).

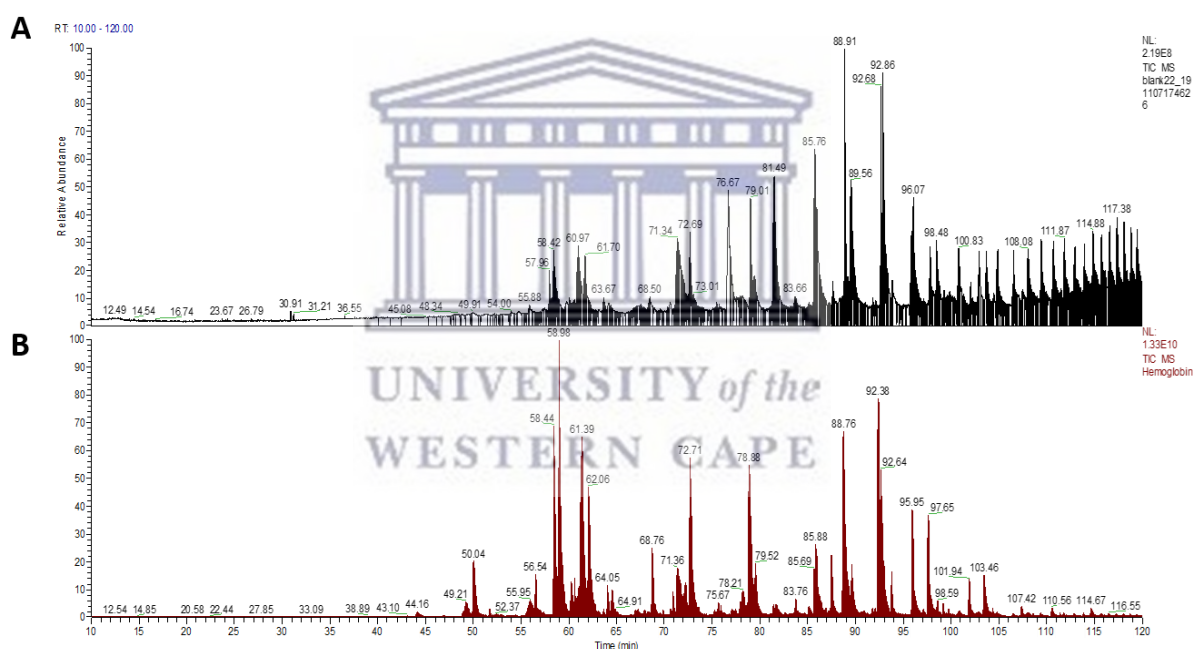


**Figure 5.3.** Total ion chromatograms of the system blank (A) and suitability mixture (B) injection.

Based on the data generated for the blank and the system suitability sample all individual treatment samples were analysed using LC MS and captured as individual TICs (Figure 5.4). The peaks detected for the control and *p*-CA treated samples on a total ion chromatogram (TIC) show uniformity and no contamination (Figure 5.4A-B). All salt stressed samples showed low



peak detection due to low protein content/concentration when compared to the untreated control and the *p*-CA treated samples (Figure 5.4 C-D).

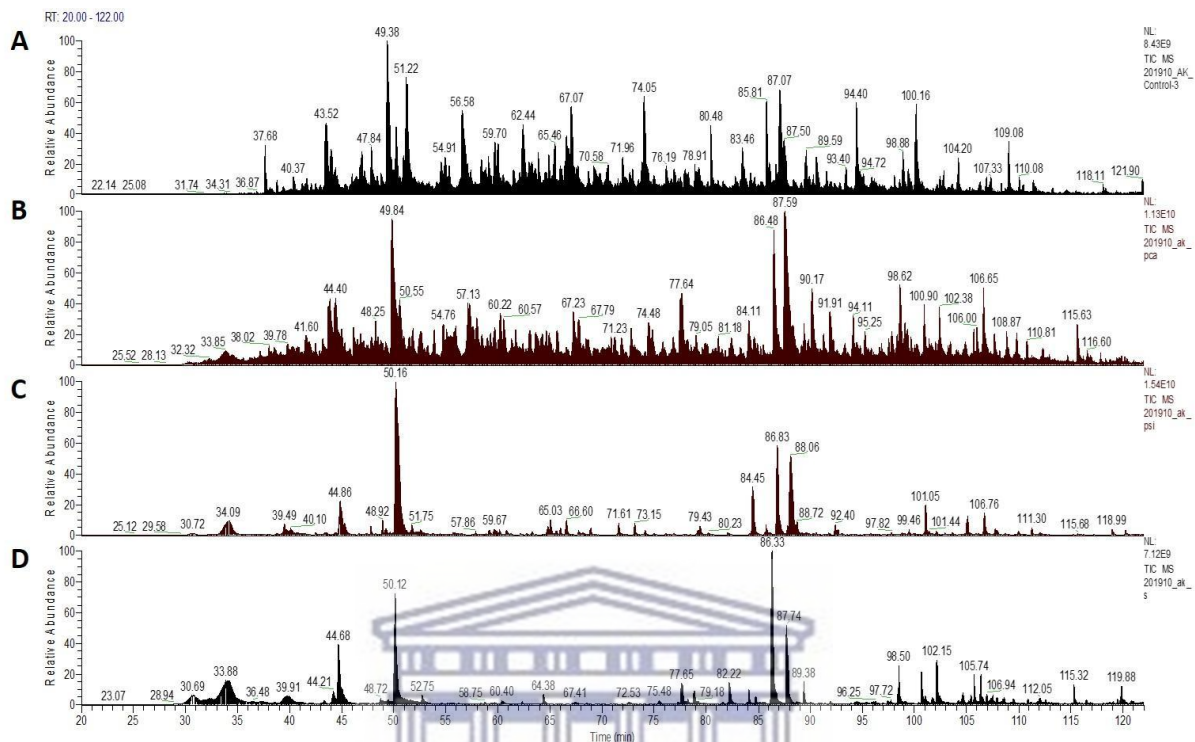


**Figure 5.4.** The total ion chromatography LC MS analysis of chia seedlings treated with *p*-CA and NaCl-induced salt stress. A) Control, B) *p*-CA, C) NaCl and D) NaCl + *p*-CA.

The total ion chromatography for all samples was interrogated against the Uniprot *Lamaiceae* database where 3158 proteins in 1074 clusters was identified with a FDR of 0.9%. However, to ensure quality and correct identification of proteins, a threshold criterion was set for the identified proteins. To be considered as a positive identification, protein exclusive unique peptide count should be  $\geq 2$ ; protein identification probability should be  $\geq 95\%$  or 0.95 and the percentage sequence coverage should be greater than zero. Using these parameters a total 907 proteins were identified across all treatments (including 437 in control, 364 in *p*-CA-treatment, 47 in NaCl-treatment and 59 combined treatment (NaCl + *p*-CA) as shown in Figure 5.5A (Table S1 and S2).

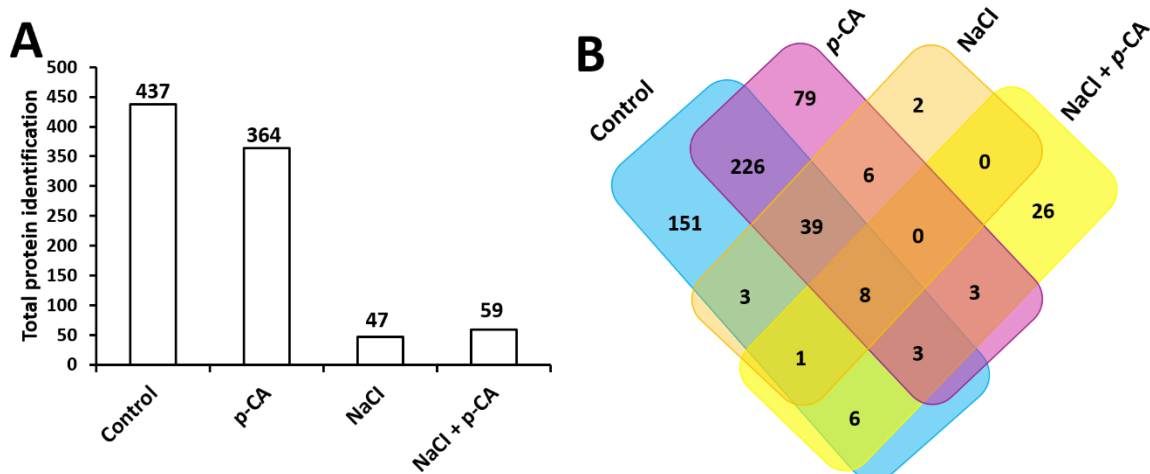


**Figure 5.5.** Detection of *p*-CA responsive protein on chia seedlings exposed to salt stress. A) Total number of proteins identified in the different treatments. B) Venn diagram illustrating the common and unique proteins identified in all treatments.

Protein accessions identified in this study (Supplementary data; Table S1 and S2) were analysed using the FunRich Multi analysis software package (version 3.1.3), to identify common and unique proteins in each of the different treatments (Figure 5.5B). The results showed that 258 of 907 proteins identified in this study was unique across all treatments (151 – control; 79 – *p*-CA; 2 – NaCl; 26 – NaCl + *p*-CA). On the other hand, eight proteins were conserved in all treatments. For the comparison of proteins identified in the control and *p*-CA treatments, 160 proteins were unique to the control and 88 to the *p*-CA treatment. A total of 276 proteins were shared between the two treatments. When comparing the proteins identified in the NaCl treatment relative to the control, 385 proteins were unique to the control treatment with only eight proteins unique to the NaCl treatment. A total of 51 proteins were shared between the control and NaCl treatment. For the comparison of proteins identified in the control and combination treatment (NaCl + *p*-CA), 418 proteins were unique to the control and 29 to the combination treatment. In this comparison, 18 proteins were shared between the control and the combination treatment (Figure 5.5B).

All proteins identified with LC MS analysis was localised to various subcellular locations using homology searches against the Universal Protein Sequence database (<http://www.uniprot.org>) embedded in the FunRich Multi analysis software package (version 3.1.3). The majority of the proteins identified were localised to the chloroplast (68 %) and ribosomes (13 %). Interestingly, the subcellular location of about 14 % of the identified proteins remained unknown. The rest of the proteins were found in the plastid (3 %), mitochondria (1 %) and cell wall (1 %) (Figure 5.6). Proteins localised in the cytoplasm were only detected in the *p*-CA treatment (Figure 5.6; Figure S1). After an in-depth subcellular localization of proteins identified in each treatment, we observed that the limited number of proteins localised in the cytoplasm were only detected in *p*-CA treatment (Figure S1B).

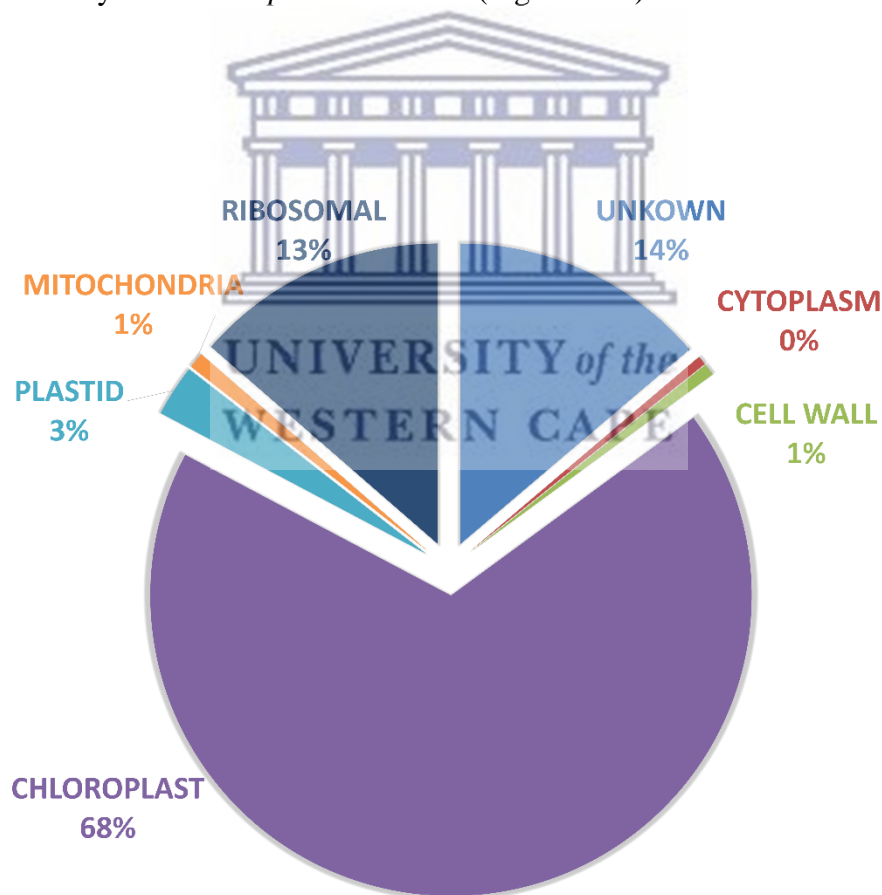


**Figure 5.6.** Subcellular localisation of positively identified proteins expressed in chia shoots.

### 5.3.5 Functional characterisation of *p*-CA induced protein isoforms

Relative to the control, 79 unique proteins were identified in the *p*-CA treatment (Figure 5.5B). Of the 79 unique proteins, 51 showed similar protein isoforms either encoded by different gene copies or corresponded to different forms of the same gene product. (Figure 5.7A; Table S1). The majority of the identified protein isoforms in the *p*-CA treatment were localised to the chloroplast (74 %). However, about 10 % of these proteins isoform could not be functional categorised to a specific subcellular location.

Furthermore, all proteins identified in the *p*-CA treatment was also categorised according to their biological processes (Figure 5.7C). The data showed that 68 % of the proteins play a role in photosynthesis whereas 16 % have been linked to various metabolic processes. The other categories including transport, stress response, and signal transduction make up 14 % whereas the biological function of 8 % of the identified proteins remain unknown (Figure 5.7C).

Subcellular localization helps in determining key functional characteristic of proteins, it is also critical to understand if any of the observed proteins have a tendency to physically interact or associated with any other proteins using domain fusion, phylogenetic profiling and neighbourhood methods. Using the Interaction tool in the Fun Rich software package we identified three of the isoforms that interacted with other genes outside of our database. These isoforms include *atpB*, *psbD*, *rbcl*. *atpB* showed interaction with 3 other genes (*atpa*, *ATPC1*, *ABA4* and *UBQ3*), *psbD* showed interaction with *DEGP1* and *rbcl* showed interaction with *ABA4*. *H2B* showed no interaction with any other proteins (Figure 5.7D).

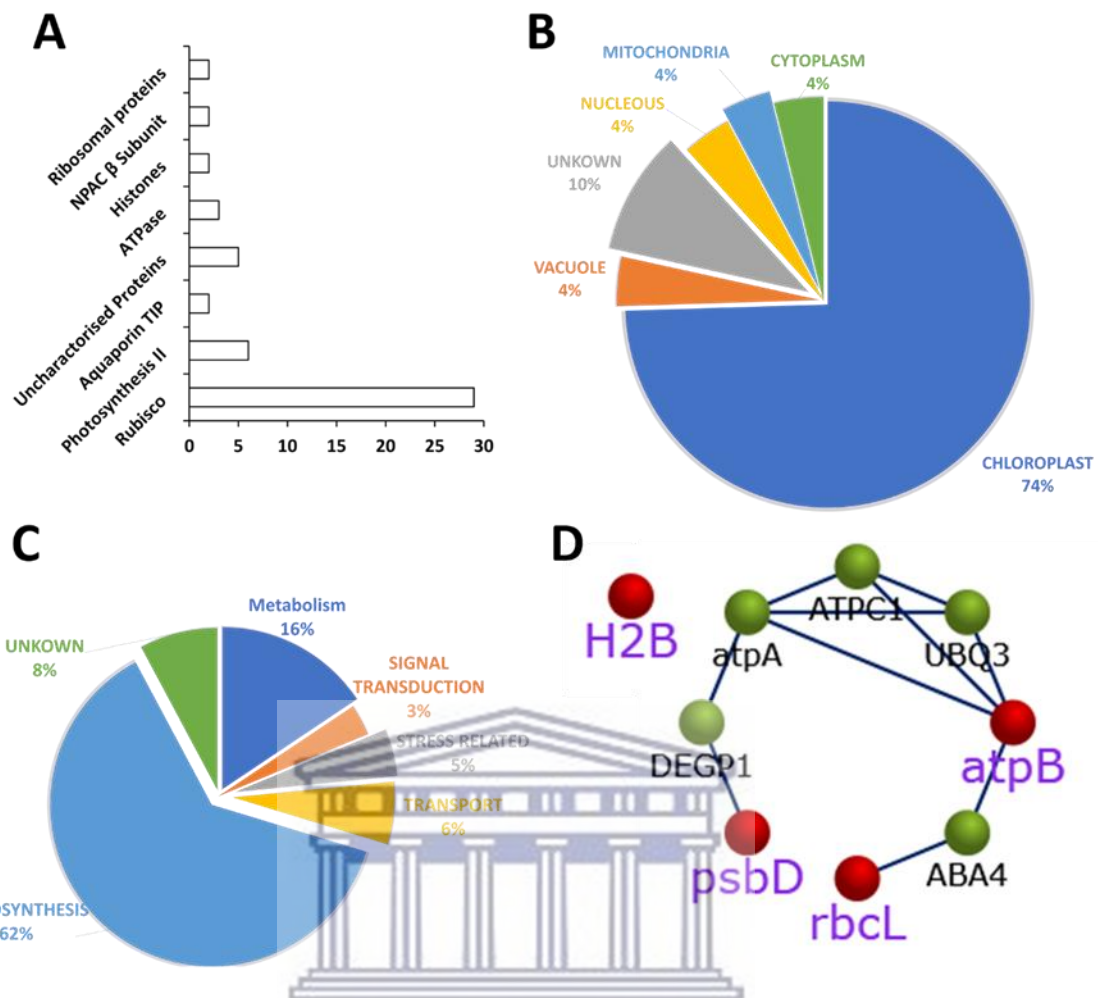


**Figure 5.7.** Identification and gene ontology classification of unique isoform proteins based on subcellular component. A) Protein isoforms identified in the *p*-CA treatment. B) Subcellular localisation of identified protein isoforms. C) Biological processes of proteins isoforms in *p*-CA treatment. D) Interaction network of unique protein isoforms in *p*-CA treatment. Red nodes represent identified protein isoforms. Blue line colour indicates protein interaction. Green nodes represent protein interaction from my inquiry database.

### 5.3.6 Functional characterisation of *p*-CA induced protein isoforms under salt stress

Based on the 26 positively identified unique proteins (Figure 5.4 B) in the combined treatment (NaCl + *p*-CA), two clusters of protein isoforms (Histones and Uncharacterised proteins) were detected, which comprised approximately 39 % of the total unique proteins identified (Table 5.3). To add some context, it is noteworthy that, only two unique proteins (TIC214 and uncharacterised protein) were identified in the NaCl treatment relative to the control (Figure 5.5B; Table S1) and these proteins did not form part of any clusters. The subcellular localisation

of the majority protein isoforms (70%) identified in the combined treatment remain unknown, where the remaining 30 % of the proteins isoforms were localised to the nucleus (Table 5.3). These protein isoforms play a vital role in various signalling transduction pathways. Contrary to what was observed for the proteins in the *p*-CA treatment, no interaction of proteins in the combined treatment was observed.

**Table 5.3.** Representative of unique protein isoforms identified in the combined treatment

Best Match Protein	Cellular compartment	Biological process	Reference organism	Exp. MW	Accession
Histone acetyltransferase	Nucleus	Signal transduction	<i>Salvia splendens</i>	207,212	A0A4D8ZFW5
Histone acetyltransferase	Nucleus	Signal transduction	<i>Salvia splendens</i>	200,709	A0A4D8XW78
Histone H2B	Nucleus	Signal transduction	<i>Salvia splendens</i>	50,396	A0A4D8YI34
Uncharacterized protein	Unknown	Unknown	<i>Salvia splendens</i>	90,152	A0A4D8ZMB7
Uncharacterized protein	Unknown	Unknown	<i>Salvia splendens</i>	301,483	A0A4D8Y3H3
Uncharacterized protein	Unknown	Unknown	<i>Salvia splendens</i>	389,757	A04D8XUM7
Uncharacterized protein	Unknown	Unknown	<i>Salvia splendens</i>	133,868	A0A4D8XZS0
Uncharacterized protein	Unknown	Unknown	<i>Salvia splendens</i>	194,680	A0A4D9AQ17
Uncharacterized protein	Unknown	Unknown	<i>Salvia splendens</i>	163,630	A0A4D8ZNY9
Uncharacterized protein	Unknown	Unknown	<i>Salvia splendens</i>	312,376	A0A4D8XX72

## 5.4. Discussion

### 5.4.1 *p*-CA improves chia seedling shoot biomass under salt stress

The obtained results illustrated that salt stress reduced the growth characters of chia seedlings when compared with control plants. Our results are in harmony with those obtained by Jones



et al. (2017). However, exogenously applied *p*-CA effectively resulted in enhancing the plant growth characters (Figure 5.1). In this experiment, shoot length, fresh and dry weights were significantly reduced due to salt stress while the exogenous application of *p*-CA significantly improved these parameters (Figure 5.1). These results may be attributed to the *p*-CA role in improving plant biomass and chlorophyll content in Chia seedlings (Nkomo et al. 2019; see Chapter 3). While, simultaneous addition of exogenous *p*-CA and salt stress was shown to reverse the effect caused by salt stress. This, similar phenomenon was also observed in other studies which demonstrated that exogenous application of *p*-CA reverses the effect of salt stress, exhibited by the improvement of plant growth biomass (Khairy and Roh 2016; Kaur et al. 2017). Beside the physiological effect, these studies most focused on the biochemical changes (antioxidant enzymes ROS metabolism) associated with *p*-CA induced salt stress. These results all seem to indicate that *p*-CA has a robust ability to minimise the effect of salt stress. However, the model of action of *p*-CA-induced salt stress tolerant remains elusive. This study will further, determine the role of *p*-CA under NaCl treatment and possible involvement of protein and to maintain a positive balance of essential macro elements in response to salt stress.

#### **5.4.2. Exogenous *p*-CA alters Mg and Ca elements under salt stress conditions**

The greater effect of salt stress on plants is known to be associated with larger increasing the content of sodium (Na) content (Yamaguchi and Blumwald 2005; FAO 2009). The excessive accumulation of intracellular sodium (Na) is known to lead to ion imbalance and toxicity with the plants (Zhu 2001; Zhu 2002; Zhu 2003). As was expected, under salt stress there was an increase in Na, which ultimately reduced the content of all the other essential macro elements which were tested in the study (Table 5.1). Other previous studies have also reported a similar phenomenon which was observed in our study (Table 5.1), which demonstrated that under salt stress there was a reduction in essential macro-elements such as K (Chen et al. 2005; Shabala

et al. 2010), P (Martinez et al. 1996; Loupassaki et al. 2002; Kopittke 2012), Mg (Loupassaki et al. 2002; Tavakkoli et al. 2011) and Ca (Davenport et al. 1997; Kopittke 2012). However, considering, our previous results that demonstrated that inhibition of endogenous *p*-CA altered a reduction in all the essential macro elements which had a major impact on growth (Chapter 4). In this study, we observed an opposite phenomenon when treating chia seedlings with exogenous *p*-CA, part of this could further explain why we observed an increase in plant growth under *p*-CA treatment (Nkomo et al. 2019). While, under salt plus *p*-CA treatment we observed an increase in Mg and Ca, while we had also observed the reversal on the effect of salt stress on plant biomass (Fig. 5.1). A previous study by Tester and Davenport 2003, reported that the reduction in shoot growth under salt stress could be attributed to the excessive accumulation of Na, although we observed the highest increase of Na in our NaCl + *p*-CA treatment, we also observed an increase in growth suggesting that Mg and Ca might be playing an essential role in conferring tolerance.

#### **5.4.3. Towards the proteomic mapping of *p*-CA induced salt stress tolerant**

Here we describe the influence of exogenous *p*-CA and salt stress on chia seedlings, in a role towards building a proteomic map of chia seedlings. We were able to identify proteins which were conserved amongst the treatments, to which some of them were photosynthesis related proteins (Supplementary Data; Table S1). In the presence of *p*-CA, not only did we notice an increase in plant growth but the protein concentration and the spectrum count also increased. In the proteomic analyses, total 907 proteins were identified across all treatments. However, this study was focused on the protein isoforms involved in conferring *p*-CA induced salt stress tolerance to which we later identified 105 proteins, belonging to *p*-CA and the combination of NaCl + *p*-CA of which the majority were uncharacterized proteins.

#### 5.4.4. Protein isoforms identified in chia seedlings

Given the existence of multiple proteins isoforms in the *p*-CA treatment (Figure 5.7 A), it is possible that chia seedling proteins could have undergone post – translational modifications (PTM) (Pejaver et al. 2014). As, of the 79 unique protein that were identified under *p*-CA treatment (Figure 5.5 B), 51 of the proteins were identified as multiple proteins isoforms, that could have been produced as a result of combination of PTM, translation, transcription or protein turn over (Abdallah et al. 2012). Different protein isoforms identified in our study were shown to be derived from different genes of a multigene family where each isoform is encoded by its own gene (Supplementary data Table S1) or random chemical modifications of proteins, such as carbamylation. Most of the *p*-CA treated proteins appear to be involved in photosynthesis, metabolism, transport, stress signaling and signal transduction (Figure 5.7 C), while fewer proteins remained unidentified/unknown. A brief description of major protein isoforms identified in *p*-CA and combination of NaCl and *p*-CA was given below according to their biological processes.

##### *a. Proteins isoforms associated with photosynthesis*

Photosynthetic proteins such as photosystem II oxygen-evolving enhancer protein, photosystem II D2 protein, and ribulose-bisphosphate carboxylase (RuBisCO) are abundantly available as expected in green tissue. Lee et al. (2015), indicated that the photosystem II oxygen-evolving enhancer protein and RuBisCO are the key proteins in photosynthesis. Their absence in plants is mostly related to the reduction in photosynthetic pigment and ultimately inhibition of plant growth. This category constitutes 62 % of the positively identified proteins isoforms within this study (Figure 5.7C) under *p*-CA treatment.

Protein localization is a good complementation technique to biological process, due to the fact that it can precisely define the functional and mechanism of action of identified proteins and their interaction (Kumar et al. 2002). RuBisCO is one of the key photosynthetic protein

isoforms found within the chloroplast (Figure 5.7B), which takes part in the CO<sub>2</sub> fixation and photorespiration. These protein isoforms constituted a large pool of nitrogen (~30 %), which can be remobilized under stressful conditions (Hirel and Gallais 2006). Abundance of these protein isoforms could be another alternative answer, to why we observed an increase in chia seedling growth under *p*-CA treatment (Figure 5.1).

#### ***b. Proteins Associated with Transport***

In *p*-CA treatment, only six percent of the total unique proteins were involved in transport, while under NaCl treatment we could only identify one unique protein TIC 214 and one other protein which was uncharacterized. The limitation of perform such an important proteomic study is the lack of sequenced data on pseudocereals. This was mainly because the majority of the proteins which were unique in obtaining *p*-CA-induced salt tolerant were mostly uncharacterized (Table 5.2). While the majority of the *p*-CA induced transporter protein ATP synthase, which are known to serve as a general energy currency of the cell (Junge et al. 1997) through the conversion be involve in transportation of protons across the chloroplast thylakoid membrane ADP to ATP in the presence of a proton gradient across the thylakoid membrane (von Ballmoos and Dimroth 2007). The presence of these protein isoforms in *p*-CA treated seedlings is consistent with the presence of active cellular processes throughout chia seedling growth and development (Figure 5.1).

#### ***c. Proteins isoforms associated with stress response and signal transduction***

Aquaporins (TIP) have important roles in various physiological processes in plants, including growth, development and adaptation to stress. TIP plays a crucial role in many cellular processes including signal transduction, TIP selectively conduct water molecules in and out of the cell, while preventing the passage of ions and other solutes. TIP's are also essential for the

water transport system in plants (Kruse et al. 2006) and tolerance to drought and salt stresses (Xu et al. 2014).

#### *d. Other functional proteins*

Due to the limited information about chia in the public domain, we have identified five *p*-CA responsive protein isoforms that were uncharacterised (Figure 5.7 A) and seven NaCl + *p*-CA induced proteins isoforms, which were previously identified in *Salvia splendens* (Table 5.3; Supplementary data S1). Further research needs to be done, in order to understand the biological functions of these candidates in *p*-CA induced salt stress tolerance.

## **5.5. Conclusion**

In conclusion, this work further illustrates the complexity of the mechanisms underlying salinity tolerance in plants using *p*-CA and has added two additional mechanisms that involves ionomics and proteomics in chia seedlings that were not previously explored. Based on physiological and ionomics data, we found that there was a strong correlation between the elements (Mg and Ca) and plant growth. This may be suggesting that chia seedling growth and adaptation to salt stress may be through ionic homeostasis of Mg and Ca, rather than Na. This is due to the fact that, though we observed higher levels of Na in the combined (NaCl + *p*-CA) treatment than salt stress treatment, the combined treatment seemed to reversed the physiological growth effect caused by salt stress (Figure 5.1; Table 5.1). Hence, we suggested that both Mg and Ca maybe the major contributing essential macro elements in the growth of chia seedlings, as their levels increased to much higher levels in the combined treatment. Using 1D SDS-PAGE the electrophoresis samples profile where able to reviled that all protein fraction where of good quality, but could not provide definitive information on the protein involved (Figure 5.2). Hence, following 1D SDS-PAGE it becomes insightful to provide some direct identification and mapping of this protein fraction using non-gel-based proteomics. The

results were successful in identifying 258 unique proteins across all treatments, to which 26 unique proteins are thought to play a crucial role in *p*-CA induced salt stress tolerant. The vast majority of these proteins were classified as uncharacterised proteins, meaning that future studies would have to further functional characterization of these proteins to help in understanding the mechanism of salt stress tolerant induced by *p*-CA. Furthermore, due to limitations in project resource and cost of proteomic equipment's, it was not possible to submit the proteomics samples in triplicate. However, for future research it would be worthwhile to attempt to identify the expression of the proteins that we mapped in this study.





## CHAPTER 6

### CONCLUDING REMARKS AND FUTURE OUTLOOK

This study explores the roles of exogenously applied *p*-CA, on the antioxidant system in pseudocereals (exemplified by chia) together with their influence on macronutrient, proteomic analysis and osmoprotectants. In this thesis, we firstly demonstrated the role of exogenous *p*-CA in promoting plant growth. It was further suggested that the increase in plant growth could be via the activation of reactive oxygen species-signalling pathway involving  $O_2^{\cdot-}$  under the control of proline accumulation (Chapter 3). It is important to note that this was the first study to demonstrate a positive role of *p*-CA in enhancing plant growth.

Hence, to ascertain if the observed results of increase in plant growth in Chapter 3 were due to exogenous application of *p*-CA, we hypothesized that inhibiting endogenous *p*-CA would reduce chia plant growth. To test this hypothesis, we used piperonylic acid (PA) due to the fact that an independent study by Schalk et al. (1998) showed PA an efficient competitive inhibitor of Cinnamate 4-hydroxylase ( $C_4H$ ) enzyme. The  $C_4H$  enzyme is found upstream in the phenylpropanoid pathway and it catalyses the hydroxylation of cinnamic acid to produce endogenous *p*-coumaric acid. The findings based on physiological analysis, suggested that inhibition of *p*-CA biosynthesis decrease seedling biomass and might be due to alteration in ROS molecules. The results further showed that although antioxidant enzymes were augmented in response to PA, this *up*-regulation was not sufficient to scavenge total ROS caused by the inhibition of  $C_4H$  enzyme. The accumulation of ROS molecules (superoxide  $O_2^{\cdot-}$  and hydrogen peroxide  $H_2O_2$ ) resulting in damage in lipid membranes that resulted in leaching out of essential macro elements, and this might explain why we observed a reduction in essential macro elements in the PA treatment (Chapter 4). However, the results have further demonstrated that *p*-CA play an important role in plant growth and development.

This study further analysed the role of exogenously applied *p*-CA in response to salt stress (Chapter 5) by monitoring changes in protein abundance. Although the role of *p*-CA in response to salt stress have been extensively studied (Kim et al. 2014; Khairy et al. 2016; Kaur et al. 2017) and shown to mitigate the effect of salt stress. These studies mostly focused on the physiological and biochemical homeostasis of ROS molecules and antioxidant enzymes. The role of *p*-CA in mediating plant tolerance to salt stress cannot be limited only to modification of the plant antioxidant system, but can be extended to analysing ionomics (mineral content) and proteome mapping (identification protein). This is due to a fact that salt stress is known to affect the mineral uptake on plant and thus impeding growth. While salt tolerance is known to be associated with plethora of genes, thus a proteomic study would provide a meaningful contribution towards dissecting molecular pathways on the role of *p*-CA in mitigating salt stress effect on plants.

Hence, chapter 5 extends the scope of these studies (Kim et al. 2014; Khairy et al. 2016; Kaur et al. 2017), by investigating the influential role of *p*-CA on essential macro element accumulation and protein abundance in the seedlings of chia plants under salt stress. Although the influence of salt stress on plant proteomes are well documented, this study is the first to describe the effect of *p*-CA on plants proteomes and how *p*-CA regulates changes in plants under salt stress. We identify 26 unique proteins, which are thought to play a role in *p*-CA induced salt stress tolerance. The majority of the unique proteins identified in the *p*-CA + salt treatment, were classified as uncharacterized, and it would be of great importance for future studies to try and further characterized these proteins, which might give insight into the mechanism of *p*-CA induced salt stress tolerance in plants.

## CHAPTER 7

### REFERENCES

1. Abdallah, C.; Dumas-Gaudot, E.; Renaut, J.; Sergeant, K. Gel-based and gel-free quantitative proteomics approaches at a glance. *Int. J. Plant Genom.* **2012**, 1-17.
2. Aebi H. Catalase in vitro. *Methods Enzymol.* **1984**, 105, 121–126.
3. Akula, R.; Ravishankar, G.A. Influence of abiotic stress signals on secondary metabolites in plants. *Plant Signal. Behav.* **2011**, 6(11), 1720-1731.
4. Asada, K. Ascorbate peroxidase - a hydrogen peroxide scavenging enzyme in plants. *Physiol. Plant.* **1992**, 85, 235-241.
5. Ayerza, R. Crop year effects on seed yields, growing cycle length, and chemical composition of chia (*Salvia hispanica* L) growing in Ecuador and Bolivia. *Emir J Food Agric.* **2016**, 28, 196-200.
6. Ayerza, R.; Coates, W. Ground chia seed and chia oil effects on plasma lipids and fatty acids in the rat. *Nutr. J.* **2005**, 25, 995-1003.
7. Ayerza, R.; Coates, W. Some quality components of four chia (*Salvia hispanica* L.) genotypes grown under tropical coastal desert ecosystem conditions. *Asian J Plant Sci.* **2009**, 8, 301-307.
8. Balasundram, N.; Sundram, K.; Samman, S. Phenolic compounds in plants and agricultural by-products: Antioxidant activity, occurrence, and potential uses. *Food Chem.* **2006**, 99(1), 191-203.
9. Baleroni, C.R.S.; Ferrarese, M.L.; Braccini, A.L.; Scapim, C.A.; Ferrarese-Filho, O. Effects of ferulic and *p*-coumaric acids on canola (*Brassica napus* L. cv. *Hyola 401*) seed germination. *Seed. Sci. Technol.* **2000**, 28, 201-207.

10. Baleroni, C.R.S.; Ferrarese, M.L.; Braccini, A.L.; Scapim, C.A.; Ferrarese-Filho, O. Effects of ferulic and *p*-coumaric acids on canola (*Brassica napus* L. cv. *Hyola* 401) seed germination. *Seed. Sci. Technol.* **2000**, 28, 201-207.
11. Batish, D.R.; Singh, H.P.; Kaur, S.; Kohli, R.K.; Yadav, S.S. Caffeic acid affects early growth, and morphogenetic response of hypocotyl cuttings of mung bean (*Phaseolus aureus*). *J. Plant. Physiol.* **2008**, 165, 297-305.
12. Baxter, I. Ionomics: the functional genomics of elements. *Brief. Funct. Genomics.* **2010**, 9, 149–156.
13. Baxter, I.; Ouzzani, M.; Orcun, S.; Kennedy, B.; Jandhyala, S.S.; Salt, D.E. “Purdue Ionomics Information Management System (PiiMS): An Integrated Functional Genomics Platform,” *Plant Physiol.* **2007**, 143, 600-611.
14. Berners-Lee, M.; Kennelly, C.; Watson, R.; Hewitt, C.N. Current global food production is sufficient to meet human nutritional needs in 2050 provided there is radical societal adaptation. *Elem Sci Anth.* **2018**. <https://doi.org/10.1525/elementa.310>.
15. Beyer, W.F.; Fridovich, Y. Assaying for superoxide dismutase activity: some large consequences of minor changes in conditions. *Anal. Biochem.* **1987**, 161, 559- 566.
16. Blackstock, W. P.; Weir, M. P. Proteomics: quantitative and physical mapping of cellular proteins. *Trends Biotechnol.* **1999**, 17, 121-127.
17. Boo, Y.C. *p*-Coumaric acid as an active ingredient in cosmetics: A review focusing on its antimelanogenic effects. *Antioxidants.* **2019**, 8(8), 275.
18. Boz, H. Phenolic amides (avenanthramides) in oats – a review. *Cz J Food Sci.* **2015**, 33: 1-7.
19. Bravo, L. 1998. Polyphenols: chemistry, dietary sources, metabolism, and nutritional significance. *Nutr. Rev.* **1998**, 56(11), 317-333.

20. Bubna, G.A.; Lima, R.B.; Zanardo, D.Y.L.; Dos Santos, W.D.; Ferrarese, M.L.L.; Ferrarese-Filho, O. Exogenous caffeic acid inhibits the growth and enhances the lignification of the roots of soybean (*Glycine max*). *J. Plant. Physiol.* **2011**, 168, 1627-1633.
21. Bujor, O.C.; Talmaciu, I.A.; Volf, I.; Popa, V.I. Biorefining to recover aromatic compounds with biological properties. *TAPPI J.* **2015**, 14(3), 187-193.
22. Bushway, A.A.; Belyea, P.R.; Bushway, R.J. Chia seed as a source of oil, polysaccharide, and protein. *J. Food Sci.* **1981**, 46, 1349-1350.
23. Busilacchi, H.; Quiroga, M.; Bueno, M.; Di Sapia, O.; Flores, V.; Severin, C. Evaluaci'ón de *Salvia hispanica* L. cultivada em el sur de santa fe (Republica Argentina). *Cultivos Tropicales.* **2013**, 34(4), 55–59.
24. Capitani, M.I.; Spotorno, V.; Nolasco, S.M.; Tomás, M.C. Physicochemical and functional characterization of by-products from chia (*Salvia hispanica* L.) seeds of Argentina. *LWT – Food. Sci. Technol.* **2012**, 45, 94-102.
25. Caruso G.; Cavaliere C.; Foglia P.; Gubbiotti R.; Samperi R.; Laganà A. Analysis of drought responsive proteins in wheat (*Triticum durum*) by 2D-PAGE and MALDI-TOF mass spectrometry. *Plant Sci.* **2009**, 177, 570–576.
26. Castelluccio, C.; Paganga, G.; Melikian, N.; Bolwell, G.P.; Pridham, J.; Sampson, J.; Rice-Evans C. Antioxidant potential of intermediates in phenylpropanoid metabolism in higher plants. *FEBS Lett.* **1995**, 368, 188–192.
27. Chandrasekara, A.; Shahidi, F. Content of insoluble bound phenolics in millets and their contribution to antioxidant capacity. *J. Agric. Food Chem.* **2010**, 58(11), 6706-6714.
28. Chen, Z.H.; Newman, I.; Zhou, M.X.; Mendham, N.; Zhang, G.P.; Shabala, S. Screening plants for salt tolerance by measuring K<sup>+</sup> flux: a case study for barley. *Plant Cell Environ.* **2005**, 28, 1230–1246.

29. Cho, J. Y.; Moon, J. H.; Seong, K. Y.; Park, K. H. Antimicrobial activity of 4-hydroxybenzoic acid and trans 4-hydroxycinnamic acid isolated and identified from rice hull. *Biosci. Biotechnol. Biochem.* **1998**, 62, 2273–2276.
30. Chung, K.T.; Wong, T.Y.; Wei, C.I.; Huang, Y.W.; Lin, Y. Tannins and human health: a review. *Crit. Rev. Food Sci. Nutr.* **1998**, 38(6), 421-464.
31. Coelho, V.R.; Vieira, C.G.; de Souza, L.P.; Moysés, F.; Basso, C.; Papke, D.K.M.; Pires, T.R.; Siqueira, I.R.; Picada, J.N.; Pereira, P. Antiepileptogenic, antioxidant and genotoxic evaluation of rosmarinic acid and its metabolite caffeic acid in mice. *Life Sci.* **2015**, 122, 65-71.
32. Comino, I.; de Lourdes Moreno, M.; Real, A.; Rodríguez-Herrera, A.; Barro, F.; Sousa, C. The gluten-free diet: testing alternative cereals tolerated by celiac patients. *Nutrients.* **2013**, 5(10), 4250-4268.
33. D'Souza, M.R.; Devaraj, V.R.; Biochemical responses of Hyacinth bean (*Lablab purpureus*) to salinity stress. *Acta Physiologiae Plantarum.* **2010**, 32(2), 341-353.
34. da Silva Marineli, R.; Moraes, E.A.; Lenquiste, S.A.; Godoy, A.T.; Eberlin, M.N, Maróstica, Jr M.R. Chemical characterization and antioxidant potential of Chilean chia seeds and oil (*Salvia hispanica* L.). *LWT – Food. Sci. Techno.* **2014**, 59, 1304-1310.
35. da Silva Marineli, R.; Moura, C.S.; Moraes, E.A.; Lenquiste, S.A.; Lollo, P.C.B.; Morato, P.N.; Maróstica, Jr M.R. Chia (*Salvia hispanica* L.) enhances HSP, PGC-1 $\alpha$  expressions and improves glucose tolerance in diet-induced obese rats. *Nutr. J.* **2015**, 31, 740-748.
36. Das, A. Advances in Chia Seed Research. *Adv. Biotechnol. Microbiol.* **2018**, 5:5–7. doi: 10.19080/AIBM.2017.05.555662.
37. Davenport, R.J.; Reid, R.J.; Smith, F.A. Sodium–calcium interactions in two wheat species differing in salinity tolerance. *Physiol. Plant.* **1997**, 99, 323–327.



38. De Villiers, M.C.; Nell, J.P.; Barnard, R.O.; Henning, A. Salt-affected soils: South Africa. *ARC-Institute for Soil, Climate and Water*. **2003**, ISCW Project GW/56/003/20. DOI: 10.13140/2.1.2529.8722
39. Dixon, J.; Friedberg, I.; Bottini, N.; Friedberg, I.; Godzik, A.; Mustelin, T.; Osterman, A.; Sasin, J.; Hunter, T; Alonso, A. 2004. Protein Tyrosine Phosphatases in the Human Genome. *Cell*. **2004**, 117(6), 699-711.
40. Dykes, L.; Rooney, L.W. Sorghum and millet phenols and antioxidants. *J. Cereal Sci.* **2006**, 44(3), 236-251.
41. Egbichi, I.; Keyster, M.; Jacobs, A.; Klein, A.; Ludidi, N. Modulation of antioxidant enzyme activities and metabolites ratios by nitric oxide in short-term salt stressed soybean root nodules. *S. Afr. J. Bot.* **2013**, 88, 326-333.
42. Einhellig, F.A.; Rasmussen, J.A. Effects of three phenolic acids on chlorophyll content and growth of soybean and grain sorghum seedlings. *J. Chem. Ecol.* **1979**, 5, 815-823.
43. FAO. **2009**. FAO land and plant nutrition management service. <http://www.fao.org/ag/agl/agll/spush>.
44. Ferguson, L.R.; Fong, I.L.; Pearson, A.E.; Ralph, J.; Harris, P.J. Bacterial antimutagenesis by hydroxycinnamic acids from plant cell walls. *Mutat. Res.* **2003**, 52, 49–58.
45. Ferguson, L.R.; Zhu, S.T.; Harris, P.J. Antioxidant and antigenotoxic effects of plant cell wall hydroxycinnamic acids in cultured HT-29 cells. *Mol. Nutr. Food Res.* **2005**, 49, 585– 593.
46. Flowers, T.J.; Yeo, A.R. Ion relations of plants under drought and salinity. *Aust. J. Plant. Physiol.* **1986**, 13, 75-91.

47. Gani, A.; Wani, S.M.; Masoodi, F.A.; Hameed, G. Whole-grain cereal bioactive compounds and their health benefits: a review. *J Food Process Technol.* **2012**, 3(3), 146-56.
48. Gao, J.C.; Guo, G.J.; Guo, Y.M.; Wang X.X.; Du, Y.C. Measuring plant leaf area by scanner and ImageJ software. *China Vegetables.* **2011**, 1(2), 73–77.
49. García-Mata, C.; Lamattina, L. Nitric oxide induces stomatal closure and enhances the adaptive plant responses against drought stress. *Plant Physiol.* **2001**, 126, 1196-1204.
50. Garrait, G.; Jarrige, J.F.; Blanquet, S.; Beyssac, E.; Cardot, J.M.; Alric, M. Gastrointestinal absorption and urinary excretion of trans-cinnamic and *p*-coumaric acids in rats. *Journal of agricultural and food chemistry.* **2006**, 54(8), 2944-2950.
51. George, R.; Mcfarlane, D.; Nulsen, B. Salinity threatens the viability of agriculture and ecosystems in western Australia. *Hydrogeol. J.* **1997**, 5, 6-21.
52. Gill, S.S.; Tuteja, N. Reactive oxygen species and antioxidant machinery in abiotic stress tolerance in crop plants. *J. Agric. Food Chem.* **2010**, 48, 909-930.
53. Gokul, A.; Roode, E.; Klein, A.; Keyster, M. Exogenous 3, 3'-diindolylmethane increases *Brassica napus* L. seedling shoot growth through modulation of superoxide and hydrogen peroxide content. *J. Plant Physiol.* **2016**, 196, 93-98.
54. Gorinstein, S.; Pawelzik, E.; Delgado-Licon, E.; Haruenkit, R.; Weisz, M.; Trakhtenberg, S. Characterisation of pseudocereal and cereal proteins by protein and amino acid analyses. *J. Sci. Food Agric.* **2002**, 82, 886–891.
55. Gorinstein, S.; Pawelzik, E.; Delgado-Licon, E.; Haruenkit, R.; Weisz, M.; Trakhtenberg, S. Characterisation of pseudocereal and cereal proteins by protein and amino acid analyses. *J. Sci. Food Agric.* **2002**, 82(8), 886–891.
56. Gorinstein, S.; Vargas, O.J.M.; Jaramillo, N.O.; Salas, I.A.; Ayala, A.L.M.; Arancibia-Avila, P.; Toledo, F.; Katrich, E.; Trakhtenberg, S. The total polyphenols and the

- antioxidant potentials of some selected cereals and pseudocereals. *Eur Food Res Technol.* **2007**, 225, 321-328.
57. Grancieri, M.; Martino, H.S.D.; Gonzalez de Mejia, E. Chia seed (*Salvia hispanica* L.) as a source of proteins and bioactive peptides with health benefits: A review. *Compr. Rev. Food Sci F.* **2019**, 18(2), 480-499.
58. Grossman, A.; Takahashi H. Macronutrient utilization by photosynthetic eukaryotes and the fabric of interactions. *Annu. Rev. Plant Physiol. Plant Mol. Biol.* **2001**, 52, 163–210.
59. Gygi, S. P.; Rochon, Y.; Franza, B. R.; Aebersold, R. Correlation between protein and mRNA abundance in yeast. *Mol Cell Biol.* **1999**, 19, 1720-1730.
60. Hasegawa, P.M.; Bressan, R.A.; Zhu, J.K.; Bohnert, H.J. Plant Cellular and Molecular Responses to High Salinity. *Annu. Rev. Plant Physiol. Plant Mol. Biol.* **2000**, 51, 463-499.
61. Heleno, S.A.; Martins, A.; Queiroz M.J.R.; Ferreira, I.C. Bioactivity of phenolic acids: Metabolites versus parent compounds: A review. *Food Chem.* **2015**, 173, 501-513.
62. Hichem, H.; Mounir, D.; Naceur, E.A. Differential responses of two maize (*Zea mays* L.) varieties to salt stress: Changes on polyphenols composition of foliage and oxidative damages. *Ind. Crop Prod.* **2009**, 30(1), 144-151.
63. Hirel, B.; Gallais, A. Rubisco synthesis, turnover and degradation: some new thoughts on an old problem. *New Phytol.* **2006**, 169(3), 445-448.
64. Hollapa, L.D.; U. Blum. Effects of exogeneously applied ferulic acid, a potential allelopathic compound, on leaf growth, water utilization, and endogeneous abscisic acid levels of tomato, cucumber and bean. *J. Chem. Ecol.* **1991**, 17(5), 865-886.

65. Hossain, M.A.; Hoque, M.A.; Burritt, D.J.; Fujita, M. Proline protects plants against abiotic oxidative stress: biochemical and molecular mechanisms. In *Oxidative damage to plants*, Academic Press. **2014**, 477-522.
66. Ixtaina, V.Y.; Nolasco, S.M.; Tomas, M.C. Physical properties of chia (*Salvia hispanica* L.) seeds. *Ind. CROP Prod.* **2008**, 28, 286-293.
67. Jamil A.; Riaz S.; Ashraf M.; Foolad M.R. Gene expression profiling of plants under salt stress. *Crit. Rev. Plant Sci.* **2011**, 30(5), 435–458.
68. Janovicek, K.J.; Vyn, T.J.; Voroney, R.P.; Allen, O.B. Early corn seedling growth response to phenolic acids. *Can. J. Plant Sci.* **1997**, 77, 391-393.
69. Jones, S.; Keyster, M.; Klein, A. Exogenous Caffeic Acid Alters Physiological and Molecular Responses in Chia (*Salvia Hispanica* L.). *S. Afr. J. Bot.* **2017**, 100, 339-340.
70. Joshi, D. C.; Chaudhari, G. V.; Sood, S.; Kant, L.; Pattanayak, A.; Zhang, K.; Fan, Y.; Janovská, D.; Meglič, V.; Zhou, M. Revisiting the versatile buckwheat: reinvigorating genetic gains through integrated breeding and genomics approach. *Planta.* **2019**, 250(3), 783-801.
71. Junge, W.; Lill, H.; Engelbrecht, S. ATP synthase: an electrochemical transducer with rotatory mechanics. *TIBS.* **1997**, 22(11), 420-423.
72. Kalinova, J.; Dadakova, E. Rutin and total quercetin content in amaranth (*Amaranthus spp.*). *Plant Foods Hum Nutr.* **2009**, 64(1), 68-74.
73. Kaur, H.; Bhardwaj, R.D.; Grewal, S.K. Mitigation of salinity-induced oxidative damage in wheat (*Triticum aestivum* L.) seedlings by exogenous application of phenolic acids. *Acta Physiol. Plant.* **2017**, 39, 221–236.
74. Keyster, M.; Klein, A.; Du Plessis, M.; Jacobs, A.; Kappo, A.; Kocsy, G.; Galiba, G.; Ludidi, N. Capacity to control oxidative stress-induced caspase-like activity

- determinates the level of tolerance to salt stress in two contrasting maize genotypes, *Acta Physiol. Plant.* **2013**, 35(1), 31-40.
75. Keyster, M.; Klein, A.; Ludidi, N. Caspase-like enzymatic activity and the ascorbate-glutathione cycle participate in salt stress tolerance of maize conferred by exogenously applied nitric oxide. *Plant Signal. Behav.* **2012**, 7(3), 349-360.
76. Khairy, A. I. H.; Roh, K. S. Effect of salicylic acid, benzoic acid, and *p*-Coumaric acid on growth, chlorophyll, proline, and vitamin C of salinity-stressed tobacco (*Nicotiana tabacum*). *Int. J. Plant. Soil Sci.* **2016**, 9, 1–10.
77. Kiliç, I.; Yeşiloğlu, I.Y. Spectroscopic studies on the antioxidant activity of *p*-coumaric acid. *Spectrochimica Acta Part A: Spectrochim. Acta. A Mol. Biomol. Spectrosc.* **2013**, 115, 719-724.
78. Kim, J.S. Production, separation and applications of phenolic-rich bio-oil—a review. *Bioresour. Technol.* **2015**, 178, 90-98.
79. Kim, K.B.; Jo, B.S.; Park, H.J.; Park, K.T.; An, B.J.; Ahn, D.H.; Kim, M.U.; Chae, J.W.; Cho, Y.J. Healthy functional food properties of phenolic compounds isolated from *Ulmus pumila*. *Korean J. Food Preserv.* **2012**, 19(6), 909-918.
80. Kirakosyan, A.; Seymour, E.; Kaufman, P.B.; Warber, S.; Bolling, S.; Chang, S.C. Antioxidant capacity of polyphenolic extracts from leaves of *Crataegus laevigata* and *Crataegus monogyna* (Hawthorn) subjected to drought and cold stress. *J. Agric. Food Chem.* **2003**, 51, 3973–3976.
81. Klein, A.; Keyster, M.; Ludidi, N. Caffeic acid decreases salinity-induced root nodule superoxide radical accumulation and limits salinity-induced biomass reduction in soybean. *Acta. Physiol. Plant.* **2013**, 35, 3059-3066.
82. Klein, A.; Keyster, M.; Ludidi, N. Response of soybean nodules to exogenously applied caffeic acid during NaCl-induced salinity. *S. Afr. J. Bot.* **2015**, 96, 13-18.

83. Knez Hrnčič, M.; Cör, D.; Knez, Ž. Subcritical extraction of oil from black and white chia seeds with n-propane and comparison with conventional techniques. *J. Supercrit. Fluids*. **2018**, 140:182–187.
84. Kopittke, P.M. Interactions between Ca, Mg, Na and K: alleviation of toxicity in saline solutions. *Plant Soil*. **2012**, 352, 353–362.
85. Krause, D.O.; Denman, S.E.; Mackie, R.I.; Morrison, M.; Rae, A.L.; Attwood, G.T.; McSweeney, C.S. Opportunities to improve fiber degradation in the rumen: microbiology, ecology, and genomics. *FEMS*. **2003**, 27, 663-693.
86. Kruse, E.; Uehlein, N.; Kaldenhoff, R. The aquaporins. *Genome Biol*. **2006**, 7(2), 1-6.
87. Kumar, A.; Agarwal, S.; Heyman, J.A.; Matson, S.; Heidtman, M.; Piccirillo, S.; Umansky, L.; Drawid, A.; Jansen, R.; Liu, Y.; Cheung, K.H. Subcellular localization of the yeast proteome *Genes Dev*. **2002**, 16(6), 707-719.
88. Kwak, J.Y.; Park, S.; Seok, J.K.; Liu, K.H.; Boo, Y.C. Ascorbyl coumarates as multifunctional cosmeceutical agents that inhibit melanogenesis and enhance collagen synthesis. *Arch. Dermatol. Res*. **2015**, 307, 635-643.
89. Lattanzio, V. Phenolic Compounds: Introduction. In Natural Products: Phytochemistry, Botany and Metabolism of Alkaloids, Phenolics and Terpenes; Ramawat, K.G.; Mérillon, J.-M.; Eds.; Springer: Berlin/Heidelberg, Germany, **2013**, 1543–1580.
90. Lee, B.X.; Kjaerulf, F.; Turner, S.; Cohen, L.; Donnelly, P.D.; Muggah, R.; Waller, I. Transforming Our World: Implementing the 2030 Agenda Through Sustainable Development Goal Indicators. *J Public Health Policy*. **2016**; 37, 13-31.
91. Lee, D.; Lim, J.; Woo, K.C.; Kim, K.T. Piperonylic acid stimulates keratinocyte growth and survival by activating epidermal growth factor receptor (EGFR). *Sci Rep*. **2018**, 8, 162.



92. Lee, Y.S.; Park, H.S.; Lee, D.K.; Jayakodi, M.; Kim, N.H.; Koo, H.J.; Lee, S.C.; Kim, Y.J.; Kwon, S.W.; Yang, T.J. Integrated transcriptomic and metabolomic analysis of five *Panax ginseng* cultivars reveals the dynamics of ginsenoside biosynthesis. *Front. Plant Sci.* **2017**, *8*, 1048.
93. Li, S. Q.; Zhang, Q. H. Advances in the development of functional foods from buckwheat. *Crit. Rev. Food Sci. Nutr.* **2001**, *41*(6), 451-464.
94. Li, Y.; Cao, S.; Lin, S.; Zhang, J.; Gan, R.; Li, H. Polyphenolic profile and antioxidant capacity of extracts from *Gordonia axillaris* fruits. *Antioxidants.* **2019**, *8*:150.
95. Lin, D.; Xiao, M.; Zhao, J.; Li, Z.; Xing, B.; Li, X.; Kong, M.; Li, L.; Zhang, Q.; Liu, Y.; Chen, H. An overview of plant phenolic compounds and their importance in human nutrition and management of type 2 diabetes. *Molecules.* **2016**, *21*(10), 1374.
96. Linic, I.; Samec, D.; Gruz, J.; Vujcic Bok, V.; Strnad, M.; Salopek-Sondi, B. Involvement of phenolic acids in short-term adaptation to salinity stress is species-specific among Brassicaceae. *Plants.* **2019**, *8*, 155.
97. Loupassaki, M.H.; Chartzoulakis, K.S.; Digalaki, N.B.; Androulakis, I.I. Effects of salt stress on concentration of nitrogen, phosphorus, potassium, calcium, magnesium, sodium in leaves, shoots, roots of six olive cultivars. *J. Plant Nutr.* **2002**, *25*, 2457–2482.
98. Luceri, C.; Giannini, L.; Lodovici, M.; Antonucci, E.; Abbate, R.; Masini, E.; Dolaro, P. *p*-Coumaric acid, a common dietary phenol, inhibits platelet activity in vitro and in vivo. *BJN.* **2007**, *97*(3), 458–463.
99. Luceri, C.; Guglielmi, F.; Lodovici, M.; Giannini, L.; Messerini, L.; Dolaro, P. Plant phenolic 4-coumaric acid protects against intestinal inflammation in rats. *Scand. J. Gastroenterol.* **2004**, *39* (11), 1128-1133.

100. Mabhaudhi, T.; Chimonyo, V. G. P.; Hlahla, S.; Massawe, F.; Mayes, S.; Nhamo, L.; Modi, A. T. Prospects of orphan crops in climate change. *Planta*. **2019**, 1-14.
101. Macias, F. Allelopathy in the search for natural herbicides model. In: Inderjit, Dakshini KMM, Einhellig FA, editors. Allelopathy, current status and future goals. *J. Am. Chem. Soc.* **1995**, 310-329.
102. Mahajan, S.; Tuteja, N. Cold, salinity and drought stress: an overview. *Arch. Biochem. Biophys.* **2005**, 444, 139-158.
103. Mandal, S.M.; Mandal, M.; Das, A.K.; Pati, B.R.; Ghosh, A.K. Stimulation of indoleacetic acid production in a Rhizobium isolate of Vigna mungo by root nodule phenolic acids. *Arch Microbiol.* **2009**, 191, 389–393.
104. Marchesi, V.T. The relevance of research on red cell membranes to the understanding of complex human disease: a personal perspective. *Annu. Rev. Pathol.* **2008**, 3, 1-9.
105. Marineli, R. D. S.; Lenquiste, S. A.; Moraes, É. A.; Maróstica, M. R. Antioxidant potential of dietary chia seed and oil (*Salvia hispanica* L.) in diet-induced obese rats. *Food Res. Int.* **2015**, 76, 666–674.
106. Marschner H. Mineral nutrition of higher plants, 2nd edn. London: *Academic Press*. **1995** San Diego, CA.
107. Martinez, V.; Bernstein, N.; Lauchli, A. Salt-induced inhibition of phosphorus transport in lettuce plants. *Physiol. Plant.* **1996**, 97,118–122.
108. Mathew, S.; Abraham, T.E.; Zakaria, Z.A. Reactivity of phenolic compounds towards free radicals under in vitro conditions. *J. Food. Sci.Tech.* **2015**, 52, 5790- 5798.
109. Matysik, J.; Alia, Bhalu. B.; Mohanty, P. Molecular mechanisms of quenching of reactive oxygen species by proline under stress in plants. *Curr. Sci.* **2002**, 525-532.

110. Merzlyak, M.N.; Kovrizhnikh, V.A.; Timofeev, K.N. Superoxide mediated chlorophyll allomerization in a dimethyl sulphoxide-water mixture. *Free. Rad. Res. Commun.* **1991**, *15*, 197-201.
111. Minatel, I.O.; Borges, C.V.; Ferreira, M.I.; Gomez, H.A.G.; Chen, C.Y.O.; Lima, G.P.P. Phenolic compounds: Functional properties, impact of processing and bioavailability. Phenolic Compounds Biological Activity. Ed. *InTech. Rijeka, Croatia.* **2017**, 1-24.
112. Mir, N.A.; Riar, C.S.; Singh, S. Nutritional constituents of pseudo cereals and their potential use in food systems: A review. *Trends Food Sci. Technol.* **2018**, *75*, 170–180.
113. Mittler, R. Oxidative stress, antioxidants and stress tolerance. *Trends Plant Sci.* **2002**, *7*, 405-410.
114. Mohd Ali, N.; Yeap, S.K.; Ho, W.Y.; Beh, B.K.; Tan, S.W.; Tan, S.G. The promising future of chia, *Salvia hispanica* L. *J Biomed Biotechnol.* **2012**, 1-9.
115. Mota, C.; Santos, M.; Mauro, R.; Samman, N.; Matos, A.S.; Torres, D.; Castanheira, I. Protein content and amino acids profile of pseudocereals. *Food Chem.* **2016**, *193*, 55–61.
116. Munns, R. Comparative physiology of salt and water stress. *Plant Cell Environ.* **2002**, *25*, 239-250.
117. Munns, R.; Tester, M. Mechanisms of salinity tolerance. *Annu. Rev. Plant Biol.* **2008**, *59*, 651-681.
118. Muthamilarasan, M.; Singh, N.K.; Prasad, M. Multi-omics approaches for strategic improvement of stress tolerance in underutilized crop species: A climate change perspective. *Adv. Genet.* <https://doi.org/10.1016/bs.adgen.2019.01.001> (**2019**).
119. Naikoo, M.I.; Dar, M.I.; Raghieb, F.; Jaleel, H.; Ahmad, B.; Raina, A.; Khan, F.A.; Naushin, F. Role and Regulation of Plants Phenolics in Abiotic Stress Tolerance: An

- Overview. In *Plant Signaling Molecules*; Elsevier: Amsterdam, The Netherlands, **2019**, 157–168.
120. Nakabayashi, R.; Yonekura-Sakakibara, K.; Urano, K.; Suzuki, M.; Yamada, Y.; Nishizawa, T.; Matsuda, F.; Kojima, M.; Sakakibara, H.; Shinozaki, K.; et al. Enhancement of oxidative and drought tolerance in Arabidopsis by overaccumulation of antioxidant flavonoids. *Plant J.* **2014**, *77*, 367–379.
121. Ng, P.L.L.; Ferrarese, M.L.L.; Huber, D.A.; Ravagnani, A.L.S.; Ferrarese-Filho, O. Canola (*Brassica napus* L.) seed germination influenced by cinnamic and benzoic acids and derivatives: effects on peroxidase. *Seed. Sci. Technol.* **2003**, *31*, 39–46.
122. Ngara R. A Proteomic analysis of drought and salt stress responsive proteins of different sorghum varieties. **2009** (Doctoral dissertation, University of the Western Cape).
123. Ngara, R.; Ndimba, R.; Borch-Jensen, J.; Jensen, O.N.; Ndimba, B. Identification and profiling of salinity stress-responsive protein in Sorghum bicolor seedlings. *J. Proteom.* **2012**, *75*:4139-4150.
124. Nkomo, M.; Gokul, A.; Keyster, M.; Klein, A. Exogenous *p*-coumaric acid improves *Salvia hispanica* L. seedling shoot growth. *Plants.* **2019**, *8*, 546.
125. Nxele, X.; Klein, A.; Ndimba, B.K. Drought and salinity stress alters ROS accumulation, water retention, and osmolyte content in sorghum plants. *S. Afr. J. Bot.* **2017**, *108*, 261-266.
126. Oliveira-Alves, S. C.; Vendramini-Costa, D. B.; Cazarin, C. B. B.; Júnior, M. R. M.; Ferreira, J. P. B.; Silva, A. B.; Bronze, M. R. (2017). Characterization of phenolic compounds in chia (*Salvia hispanica* L.) seeds, fiber flour and oil. *Food Chem.* **2017**, *232*(1), 295–305.

127. Orcaray, L.; Igal, M.; Zabalza, A.; Royuela, M. Role of exogenously supplied ferulic and *p*- coumaric acids in mimicking the mode of action of acetolactate synthase inhibiting herbicides. *J. Agric. Food Chem.* **2011**, 59, 10162-10168.
128. Orona-Tamayo, D.; Valverde, M. E.; Paredes-Lopez, O. Chia—The New Golden Seed for the 21st Century: Nutraceutical Properties and Technological Uses. In Sustainable protein sources. *Academic Press.* **2017**, 265-281.
129. Ozfidan-Konakci, C.; Yildiztugay, E.; Kucukoduk, M. Protective roles of exogenously applied gallic acid in *Oryza sativa* subjected to salt and osmotic stresses: effects on the total antioxidant capacity. *Plant Growth Regul.* **2015**, 75(1), 219-234.
130. Padayachee, B.; Baijnath, H. An updated comprehensive review of the medicinal, phytochemical and pharmacological properties of *Moringa oleifera* S. *Afr. J. Bot.* **2020**, 129, 304-316.
131. Pandey, A.; and Mann, M. Proteomics to study genes and genomes. *Nature.* **2000**, 405, 837-846.
132. Pandey, K.B.; Rizvi, S.I. Plant polyphenols as dietary antioxidants in human health and disease. *Oxid. Med. Cell. Longev.* **2009**, 2.
133. Parida, A.K.; Das, A.B. Salt tolerance and salinity effects on plants: a review *Ecotoxicol. Environ. Saf.* **2005**, 60(3), 324-349.
134. Pathak, H.; Aggarwal, P. K.; Singh, S. D. Climate change impact, adaptation and mitigation in agriculture: methodology for assessment and applications. Indian Agricultural Research Institute, New Delhi. **2012**, 1-302.
135. Patterson, D.T. Effects of allelopathic chemicals on growth and physiological responses of soybean (*Glycine max* L.). *Weed Sci.* **1981**, 29, 53-59.

136. Pejaver, V.; Hsu, W.L.; Xin, F.; Dunker, A.K.; Uversky, V.N.; Radivojac, P. The structural and functional signatures of proteins that undergo multiple events of post-translational modification. *Protein Sci.* **2014**, *23*, 1077-1093.
137. Pitel, J. A.; Cheliak, W.M. Effectiveness of protective agents for increasing activity of five enzymes from vegetative tissues of white spruce. *Can. J. Bot.* **1985**, *64*, 39-43.
138. Politycka, B.; Mielcarz, B. Involvement of ethylene in growth inhibition of cucumber roots by ferulic and *p*-coumaric acids. *Allelopathy J.* **2007**, *19*, 451-60.
139. Porras-Loaiza, P.; Jiménez-Munguía, M.T.; Sosa-Morales, M.E.; Palou, E.; López-Malo, A. Physical properties, chemical characterization and fatty acid composition of Mexican chia (*Salvia hispanica* L.) seeds. *Int. J. Food Sci. Tech.* **2014**, *49*, 571-577.
140. Poudyal, H.; Panchal, S.K.; Waanders, J.; Ward, L.; Brown, L. Lipid redistribution by  $\alpha$ -linolenic acid-rich chia seed inhibits stearoyl-CoA desaturase-1 and induces cardiac and hepatic protection in diet-induced obese rats. *J. Nutr. Biochem.* **2012**, *23*, 153-162.
141. Rajendrakumar, C.S.; Suryanarayana, T.; Reddy, A.R. DNA helix destabilization by proline and betaine: possible role in the salinity tolerance process. *FEBS Lett.* **1997**, *410*, 201-205.
142. Reigosa, M.J.; Souto, X.C.; González, L. Effect of phenolic compounds on the germination of six weeds species. *Plant Growth Regul.* **1999**, *28*, 83-88.
143. Reyes-Caudillo, E.; Tecante, A.; Valdivia-López, M. A. Dietary fibre content and antioxidant activity of phenolic compounds present in Mexican chia (*Salvia hispanica* L.) seeds. *Food Chem.* **2008**, *107*(2), 656–663.
144. Rodríguez, J. P.; Rahman, H.; Thushar, S.; Singh, R. K. Healthy and resilient cereals and pseudo-cereals for marginal agriculture: molecular advances for improving nutrient bioavailability. *Front. genet.* **2020**, *11*.



145. Rosegrant, M.R.; Ringler, C.; Sulser, T.B.; Ewing, M.; Palazzo, A.; Zhu, T. Agriculture and food security under global change: prospects for 2025/2050. *IFPRI*. **2009**, Washington, D.C.
146. Roy, S.; Kumar, V. A practical approach on SDS PAGE for separation of protein. *IJSR*. 2014, 3(8),955-960).
147. Salt, D.E. "Update on Ionomics," *Plant Physiol.* **2004**,136(1), 2451-2456.
148. Salt, D.E.; Baxter, I.; Lahner, B. Ionomics and the study of the plant ionome. *Annu. Rev. Plant Biol.* **2008**, 59, 709–733.
149. Sanchez, D.H.; Schwabe, F.; Erban, A.; Udvardi, M.K.; Kopka, J. Comparative metabolomics of drought acclimation in model and forage legumes. *Plant Cell Environ.* **2012**, 35, 136-149.
150. Satismruti, K.; Senthil, N.; Vellaikumar, S.; Ranjani, R. V.; Raveendran, M. Plant Ionomics: a platform for identifying novel gene regulating plant mineral nutrition. *Am. J. Plant Sci.* **2013**, 4, 1309–1315.
151. Schalk, M.; Cabello-Hurtado, F.; Pierrel, M.A.; Atanossova, R.; Saindrenan, P.; Werck-Reichhart, D. Piperonylic acid, a selective, mechanism-based inactivator of the trans-cinnamate 4-hydroxylase: a new tool to control the flux of metabolites in the phenylpropanoid pathway. *Plant Physiol.* **1998**, 118, 209–218.
152. Shabala, S.; Shabala, S.; Cuin, T.A.; Pang, J.; Percey, W.; Chen, Z.; Conn, S.; Eing, C.; Wegner, L.H. Xylem ionic relations and salinity tolerance in barley. *Plant J.* **2010**, 1, 839–853.
153. Shahidi, F.; Yeo, J. Bioactivities of phenolics by focusing on suppression of chronic diseases: A review. *Int. J. Mol. Sci.* **2018**, 19, 1573.
154. Shahzad, N.; Khan, W.; Shadab, M. D.; Ali, A.; Saluja, S. S.; Sharma, S.; Al-Allaf, F.A.; Abduljaleel, Z.; Ibrahim, I.A.A.; Abdel-Wahab, A.F.; Afify, M. A. Phytosterols

- as a natural anticancer agent: Current status and future perspective. *Biomed.* **2017**, 88, 786-794.
155. Sharma, A.; Shahzad, B.; Rehman, A.; Bhardwaj, R.; Landi, M.; Zheng, B. Response of phenylpropanoid pathway and the role of polyphenols in plants under abiotic stress. *Molecules.* **2019**, 24(13), 2452.
156. Shen, Y.; Song, X.; Li, L.; Sun, J.; Jaiswal, Y.; Huang, J.; Liu, C.; Yang, W.; Williams, L.; Zhang, H.; Guan, Y. Protective effects of *p*-coumaric acid against oxidant and hyperlipidemia-an in vitro and in vivo evaluation. *Biomed.* **2019**, 111, 579-587.
157. Sheokand, S.; Bhankar, V.; Sawhney, V. Ameliorative effect of exogenous nitric oxide on oxidative metabolism in NaCl treated chickpea plants. *Braz. J. Plant Physiol.* **2009**, 22, 81-90.
158. Silva, F.L.B.; Vieira, L.G.E.; Ribas, A.F.; Moro, A.L.; Neris, D.M.; Pacheco, A.C. Proline accumulation induces the production of total phenolics in transgenic tobacco plants under water deficit without increasing the G6PDH activity. *Theor. Exp. Plant Physiol.* **2018**, 30, 251–260.
159. Sindhu, M.; T. Emilia Abraham, T.E.; Zainul, A.Z. Reactivity of phenolic compounds towards free radicals under in vitro conditions. *J Food Sci Technol.* **2015**, 52(9):5790–5798.
160. Slama, I.; Abdelly, C.; Bouchereau, A.; Flowers, T.; Savoure, A. Diversity, distribution and roles of osmoprotective compounds accumulated in halophytes under abiotic stress. *Ann. Bot.* **2015**, 115, 433–447.
161. Smirnoff, N. The role of active oxygen in the response of plants to water deficit and desiccation. *New Phytol.* **1993**, 125, 27-58.
162. Stenlid, G. Flavonoids as inhibitors of the formation of adenosine triphosphate in plant mitochondria. *Phytochemistry.* **1970**, 9, 2251-2256.

163. Tang, Y.; Li, X.; Chen, P.X.; Zhang, B.; Liu, R.; Hernandez, M.; Marcone, M.F.; Tsao, R. Assessing the fatty acid, carotenoid, and tocopherol compositions of amaranth and quinoa seeds grown in Ontario and their overall contribution to nutritional quality. *J. Agric. Food Chem.* **2016**, *64*, 1103–1110.
164. Tavakkoli, E.; Fatehi, F.; Coventry, S.; Rengasamy, P.; McDonald, G.K. Additive effects of Na<sup>+</sup> and Cl<sup>-</sup> ions on barley growth under salinity stress. *J. Exp. Bot.* **2011**, *62*, 2189–2203.
165. Tester, M.; Davenport, R. Na<sup>+</sup> tolerance and Na<sup>+</sup> transport in higher plants. *Ann. Bot.* **2003**, *91*, 503–527.
166. Timilsena, Y. P.; Adhikari, R.; Barrow, C. J.; Adhikari, B. Physicochemical and functional properties of protein isolate produced from Australian chia seeds. *Food Chem.* **2016**, *212*, 648–656.
167. Ullah, R.; Nadeem, M.; Khalique, A.; Imran, M.; Mehmood, S.; Javid, A.; Hussain, J. Nutritional and therapeutic perspectives of Chia (*Salvia hispanica* L.): A review. *J. Food Sci. Technol.* **2016**, *53*(4), 1750–1758.
168. Ullah, S.; Kolo, Z.; Egbichi, I.; Keyster, M.; Ludidi, N. Nitric oxide influences glycine betaine content and ascorbate peroxidase activity in maize. *S. Afr. J. Bot.* **2016**, *105*, 218–225.
169. Velikova, V.; Yordanov, I.; Edreva, A. Oxidative stress and some antioxidant systems in acid rain treated bean plants: protective role of exogenous polyamines. *Plant Sci.* **2000**, *151*, 59–66.
170. von Ballmoos, C.; Dimroth, P. Two distinct proton binding sites in the ATP synthase family. *Biochemistry.* **2007**, *46*(42), 11800–11809.

171. Wang, L.; Shan, T.; Xie, B.; Ling, C.; Shao, S.; Jin, P.; Zheng, Y. Glycine betaine reduces chilling injury in peach fruit by enhancing phenolic and sugar metabolisms. *Food Chem.* **2019**, *272*, 530–538.
172. Wang, W.; Vinocur, B.; Altman, A. Plant responses to drought, salinity and extreme temperatures: towards genetic engineering for stress tolerance. *Planta.* **2003**, *218*, 1–14.
173. Wang, Z.; Huang, B.; Xu, Q. Effect of abscisic acid on drought response of Kentucky bluegrass. *J. Am. Soc. Hortic. Sci.* **2003**, *128*: 36-41.
174. Weatherly, H.; Faria, R.; Rollinger, A.; van den Berg, B.; Chiwaula, L.; Kingkaew, P.; Mejia, A.; Seeley, J.; Settumba, S.; Sandanam, S.; Berman, P. Economic Evaluation of Social Care and Informal Care Interventions in Low-and Middle-Income Countries. *World Scientific Series in Global Health Economics and Public Policy.* **2020**, 133.
175. Wong, W.S.; Guo, D.; Wang, X.L.; Yin, Z.Q.; Xia, B.; Li, N. Study of cis-cinnamic acid in *Arabidopsis thaliana*. *Plant Physiol. Biochem.* **2005**, *43*, 929–937.
176. Xu, Y.; Hu, W.; Liu, J.; Zhang, J.; Jia, C.; Miao, H.; Xu, B.; Jin, Z. A banana aquaporin gene, MaPIP1; 1, is involved in tolerance to drought and salt stresses. *BMC Plant Biology.* **2014**, *14*(1), 59.
177. Yamaguchi, T.; Blumwald, E. Developing salt-tolerant crop plants: challenges and opportunities. *Trends Plant Sci.* **2005**, *10*, 615–620.
178. Yan, F.; Liu, Y.; Sheng, H.; Wang, Y.; Kang, H.; Zeng, J. Salicylic acid and nitric oxide increase photosynthesis and antioxidant defense in wheat under UV-B stress. *Biol. Plant.* **2016**, *60*, 686-694.

179. Yancey, P.H. Organic osmolytes as compatible, metabolic and counteracting cytoprotectants in high osmolarity and other stresses. *J. Exp. Biol.* **2005**, 208, 2819-2830.
180. Yang, C.M.; Chang, I.F.; Lin, S.J.; Chou, C.H. Effects of three allelopathic phenolics on chlorophyll accumulation of rice (*Oryza sativa*) seedlings: II. Stimulation of consumption-orientation. *Bot. Bull. Acad. Sin.* **2004**, 45, 119-125.
181. Yang, W.S.; Jeong, D.; Yi, Y.; Park, J.G.; Seo, H.; Moh, S.H.; Hong, S.; Cho, J.Y. IRAK1/4-Targeted Anti-Inflammatory Action of Caffeic Acid. *Mediators Inflamm.* **2013**, 518183.
182. Yasmeen, F.; Raja, N.I.; Razzaq, A.; Komatsu, S. Gel-free/label-free proteomic analysis of wheat shoot in stress tolerant varieties under iron nanoparticles exposure. *Biochim Biophys Acta.* **2016**, 1864,1586–1598.
183. Yoon, S.A.; Kang, S.I.; Shin, H.S.; Kang, S.W.; Kim, J.H.; Ko, H.C.; Kim, S.J. *p*-Coumaric acid modulates glucose and lipid metabolism via AMP-activated protein kinase in L6 skeletal muscle cells. *Biochem Biophys Res Comm.* **2013**, 432: 553 - 557.
184. Zanardo, D.I.L.; Lima, R.B.; Ferrarese, M.D.L.L.; Bubna, G.A.; Ferrarese-Filho, O. Soybean root growth inhibition and lignification induced by *p*-coumaric acid. *Environ. Exp. Bot.* **2009**, 66(1), 25-30.
185. Zhang, H.; Han, B.; Wang, T.; Chen, S.X.; Li, H.Y. Mechanisms of plant salt response: insights from proteomics. *J. Proteome Res.* **2012**,11, 49–67.
186. Zhang, H.; Stephanopoulos, G. Engineering *E. coli* for caffeic acid biosynthesis from renewable sugars. *Appl Microbiol Biotechnol.* **2013**, 97:3333–3341.
187. Zhou, X.; Wu, F. *p*-Coumaric acid influenced cucumber rhizosphere soil microbial communities and the growth of *Fusarium oxysporum* f. sp. *cucumerinum* Owen. *PLoS one.* **2012**, 7(10), 48288.

188. Zhu, J.K. (2002) Salt and drought stress signal transduction in plants. *Annu. Rev. Plant Biol.* **2002**, 53, 247–273.
189. Zhu, J.K. (2003) Regulation of ion homeostasis under salt stress. *Curr. Opin. Plant Biol.* **2003**, 6, 441–445.
190. Zhu, J.K. Plant salt tolerance. *Trends Plant Sci.* **2001**, 6, 66–71.
191. Žilić, S.; Šukalović, V.H.T.; Dodig, D.; Maksimović, V.; Maksimović, M.; Basić, Z. Antioxidant activity of small grain cereals caused by phenolics and lipid soluble antioxidants. *J. Cereal Sci.* **2011**, 54, 417–424.





## SUPPLEMENTARY DATA

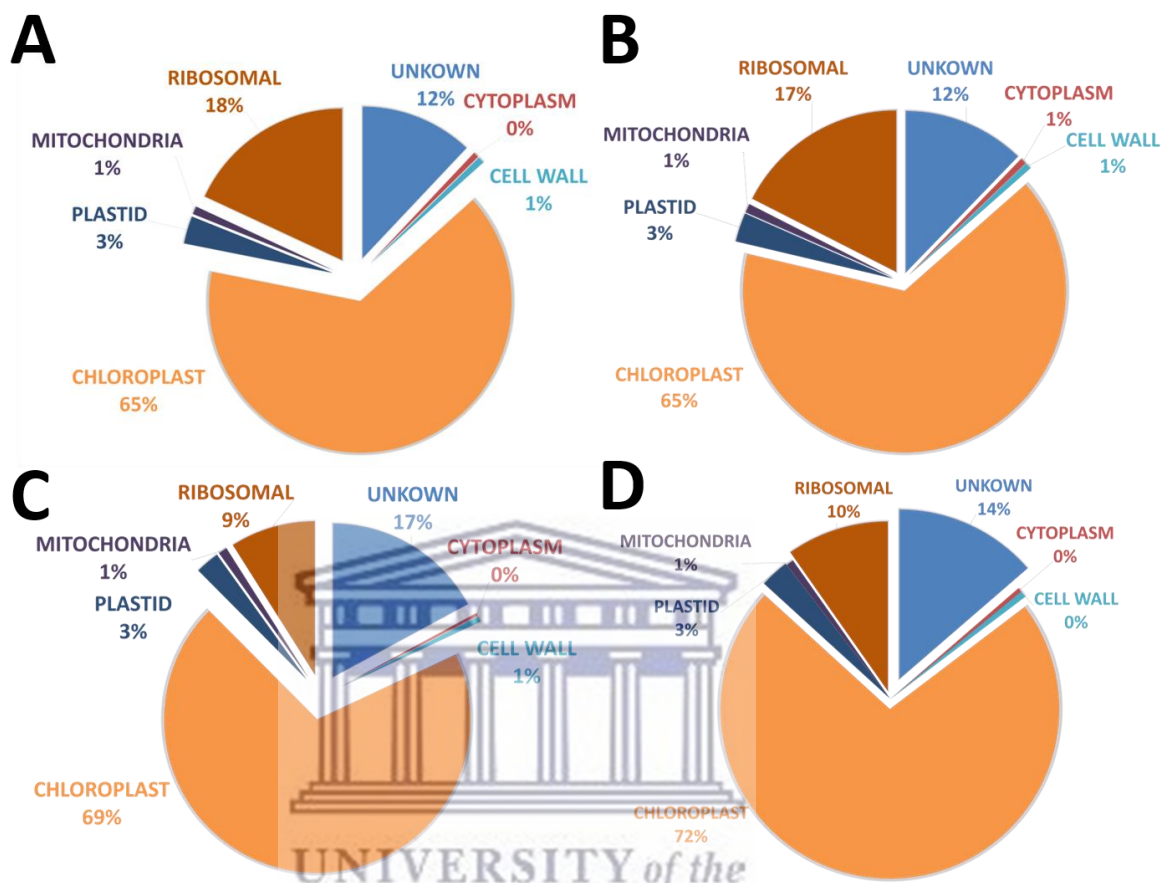


**Figure S1.** Subcellular localisation of positively identified proteins in A) control, B) *p*-CA, C) NaCl and D) *p*-CA + NaCl of chia seedlings.

**Table S1.** Unique proteins identified from different treatments

Entry	Protein names	Gene names	Entry name	Mass
<b>CONTROL Unique Proteins</b>				
A0A4D9B3N3	14_3_3 domain-containing protein	Saspl_020188	A0A4D9B3N3_SALSN	29,002
A0A4D8ZK80	14_3_3 domain-containing protein	Saspl_047008	A0A4D8ZK80_SALSN	31,004
A0A4D8YQ74	15-cis-phytoene desaturase	PDS Saspl_040712	A0A4D8YQ74_SALSN	64,076
A0A4D8Z7K0	1-deoxy-D-xylulose-5-phosphate synthase (EC 2.2.1.7)	dxs Saspl_030225	A0A4D8Z7K0_SALSN	77,170
A0A4D8Z061	1-phosphatidylinositol-3-phosphate 5-kinase (EC 2.7.1.150)	PIKFYVE Saspl_029010	A0A4D8Z061_SALSN	208,536
A0A4D8XSJ7	26S proteasome non-ATPase regulatory subunit 1 homolog	PSMD1 RPN2 Saspl_000185	A0A4D8XSJ7_SALSN	105,422
A0A4D9BAH8	26S proteasome non-ATPase regulatory subunit 2 homolog	PSMD2 Saspl_017108	A0A4D9BAH8_SALSN	100,253
A0A4D8ZYP3	26S proteasome regulatory subunit N3	PSMD3 Saspl_030906	A0A4D8ZYP3_SALSN	63,327
A0A4D9AXS2	26S proteasome regulatory subunit N7	PSMD6 Saspl_015134	A0A4D9AXS2_SALSN	169,508
A0A4D9AGR4	2-oxoglutarate dehydrogenase E1 component	OGDH sucA Saspl_009412	A0A4D9AGR4_SALSN	184,616
A0A4D9A5I4	3-hydroxy-3-methylglutaryl coenzyme A synthase (HMG-CoA synthase) (EC 2.3.3.10)	Saspl_019246	A0A4D9A5I4_SALSN	50,838
A0A4D9AXC2	3-isopropylmalate dehydratase (EC 4.2.1.33)	leuC Saspl_001641	A0A4D9AXC2_SALSN	55,119
A0A4D9BSX4	5-methyltetrahydropteroyltriglutamate--homocysteine S-methyltransferase (EC 2.1.1.14)	metE Saspl_012649	A0A4D9BSX4_SALSN	84,638
A0A4D8Y0C5	Acetyl-CoA carboxytransferase (EC 2.1.3.15)	accA Saspl_005633	A0A4D8Y0C5_SALSN	84,380
A0A4D8YEM5	ADP-ribosylation factor 1	ARF1 Saspl_011122 Saspl_048366	A0A4D8YEM5_SALSN	20,868
A0A4D9ALM0	AIG1-type G domain-containing protein	Saspl_018981	A0A4D9ALM0_SALSN	143,079
A0A4D9BPG2	Alpha-1,4 glucan phosphorylase (EC 2.4.1.1)	Saspl_010930	A0A4D9BPG2_SALSN	111,865
A0A4D9BPS7	Alpha-glucosidase	malZ Saspl_011992	A0A4D9BPS7_SALSN	102,957
R4JQS2	Alpha-terpineol	TPS5	R4JQS2_THYCA	69,605
A0A4D9C7L9	Amylomaltase (EC 2.4.1.25) (Disproportionating enzyme)	malQ Saspl_016347	A0A4D9C7L9_SALSN	102,210
A0A4D8Z8N0	Annexin	Saspl_044237	A0A4D8Z8N0_SALSN	37,197

A0A4D9A8I7	Arginyl-tRNA synthetase (EC 6.1.1.19)	RARS argS Saspl_020698	A0A4D9A8I7_SALSN	156,662
A0A4D9AB47	Aspartyl aminopeptidase	DNPEP Saspl_021530	A0A4D9AB47_SALSN	52,750
A0A4D8Y5Z5	ATP synthase subunit alpha	ATPF1A Saspl_050639 Saspl_051774	A0A4D8Y5Z5_SALSN	55,296
A0A142DPV3	ATP synthase subunit beta, chloroplastic (EC 7.1.2.2)	atpB	A0A142DPV3_9LAMI	53,772
A0A4D9B8U8	ATP-binding cassette, subfamily F, member 2	ABCF2 Saspl_019024	A0A4D9B8U8_SALSN	66,841
A0A4D9A5D4	Beta-adaptin-like protein	Saspl_025591	A0A4D9A5D4_SALSN	99,252
A0A4D8YEE2	CCT-alpha (T-complex protein 1 subunit alpha)	CCT1 Saspl_005737	A0A4D8YEE2_SALSN	59,859
A0A4D8ZN00	CCT-eta	CCT7 Saspl_004183	A0A4D8ZN00_SALSN	114,736
A0A4D9A8V6	Chaperonin GroES	groES HSPE1 Saspl_019406	A0A4D9A8V6_SALSN	26,927
C1K241	Chloroplast ribulose-1,5-bisphosphate carboxylase/oxygenase activase	RCA	C1K241_PLESU	47,508
A0A4D8ZNH1	Clathrin heavy chain	CLTC Saspl_024540	A0A4D8ZNH1_SALSN	193,338
A0A4D9C0J4	Coatomer subunit alpha	COPA Saspl_013325	A0A4D9C0J4_SALSN	136,705
A0A4D9AU66	Coatomer subunit beta'	COPB2 SEC27 Saspl_027953	A0A4D9AU66_SALSN	103,557
A0A4D9BMW9	Coatomer subunit beta'	COPB2 SEC27 Saspl_010774	A0A4D9BMW9_SALSN	105,742
A0A4D8ZSP5	Coatomer subunit beta (Beta-coat protein)	COPB1 SEC26 Saspl_023808	A0A4D8ZSP5_SALSN	105,576
A0A4D9C040	Coatomer subunit delta	Saspl_013252	A0A4D9C040_SALSN	58,123
A0A4D8ZK01	Coatomer subunit gamma	COPG Saspl_035236	A0A4D8ZK01_SALSN	99,212
A0A4D9A0P7	Cullin-associated NEDD8-dissociated protein 1	CAND1 Saspl_031716	A0A4D9A0P7_SALSN	134,687
A0A4D9BBN9	Cystathionine gamma-synthase	metB Saspl_008782	A0A4D9BBN9_SALSN	57,647
A0A4D8Z2K2	Cytoskeleton-associated protein 5	CKAP5 Saspl_034657	A0A4D8Z2K2_SALSN	199,989
A0A4D9AE03	DNA polymerase zeta catalytic subunit (EC 2.7.7.7)	Saspl_004937	A0A4D9AE03_SALSN	223,535
A0A4D9A259	DnaJ-like protein subfamily A member 2	DNAJA2 Saspl_004059	A0A4D9A259_SALSN	46,506
A0A4D8XQI6	DnaJ-like protein subfamily A member 2	DNAJA2 Saspl_042230	A0A4D8XQI6_SALSN	46,636
A0A4D9BA98	Dolichyl-diphosphooligosaccharide--protein glycosyltransferase subunit 1	OST1 Saspl_020097	A0A4D9BA98_SALSN	81,726
A0A4D8YJU3	E1 ubiquitin-activating enzyme (EC 6.2.1.45)	UBE1 UBA1 Saspl_044157	A0A4D8YJU3_SALSN	122,574

A0A4D8Z5A2	Elongation factor G, chloroplastic (cEF-G)	fusA Saspl_031216	A0A4D8Z5A2_SALSN	85,397
A0A4D9AQU7	Enhancer of mRNA-decapping protein 4	EDC4 Saspl_017410	A0A4D9AQU7_SALSN	148,324
A0A4D9BN83	Eukaryotic translation initiation factor 2C	ELF2C AGO Saspl_018644	A0A4D9BN83_SALSN	104,818
A0A4D8XVR8	Eukaryotic translation initiation factor 3 subunit B (eIF3b) (eIF-3-eta) (eIF3 p110)	EIF3B Saspl_000425	A0A4D8XVR8_SALSN	86,116
A0A4D8ZWX6	Eukaryotic translation initiation factor 3 subunit I (eIF3i)	EIF3I Saspl_024684	A0A4D8ZWX6_SALSN	45,436
A0A4D8Z7M3	Exocyst complex component Sec6	Saspl_026810	A0A4D8Z7M3_SALSN	90,339
A0A4D8Z473	Exportin-2 (Importin alpha re-exporter)	CSE1 CAS XPO2 Saspl_045784	A0A4D8Z473_SALSN	109,388
A0A4D8YV56	Exportin-T (Exportin(tRNA)) (tRNA exportin)	XPOT Saspl_040747	A0A4D8YV56_SALSN	105,966
A0A4D8ZCA0	Ferredoxin	RP-L10Ae Saspl_035083	A0A4D8ZCA0_SALSN	44,389
A0A4D9BIQ6	F-type H <sup>+</sup> -transporting ATPase subunit gamma	ATPF1G Saspl_006051	A0A4D9BIQ6_SALSN	35,461
A0A4D8YG24	Glucose-6-phosphate isomerase (EC 5.3.1.9)	GPI pgi Saspl_049570	A0A4D8YG24_SALSN	64,996
A0A4D9BHF2	Glutathione reductase (GRase) (EC 1.8.1.7)	GSR Saspl_016589	A0A4D9BHF2_SALSN	64,221
A0A4D9A2X3	Glutathione reductase (GRase) (EC 1.8.1.7)	GSR gor Saspl_020740	A0A4D9A2X3_SALSN	56,759
A0A4D9A471	HP domain-containing protein	Saspl_027986	A0A4D9A471_SALSN	110,277
A0A4D9AB00	HP domain-containing protein	Saspl_021480	A0A4D9AB00_SALSN	115,441
A0A4D8Y619	Inorganic diphosphatase (EC 3.6.1.1)	ppa Saspl_050908	A0A4D8Y619_SALSN	40,914
A0A4D8XSF1	Inositol-1-monophosphatase (EC 3.1.3.25)	Saspl_052447	A0A4D8XSF1_SALSN	35,996
A0A4D9BG35	Isoleucyl-tRNA synthetase (EC 6.1.1.5)	IARS Saspl_027167	A0A4D9BG35_SALSN	134,007
A0A4D8ZKF6	Kinesin family member C1	KIFC1 Saspl_034911	A0A4D8ZKF6_SALSN	140,478
A0A4D9BRU7	Large subunit ribosomal protein L14e	RP-L14e Saspl_011580 Saspl_012496	A0A4D9BRU7_SALSN	15,315
A0A4D9AGZ0	Leucyl aminopeptidase	CARP pepA Saspl_035323	A0A4D9AGZ0_SALSN	59,841
A0A4D8YYP4	Leucyl-tRNA synthetase (EC 6.1.1.4)	LARS leuS Saspl_042046	A0A4D8YYP4_SALSN	122,569
A0A4D8XXU3	Magnesium chelatase (EC 6.6.1.1)	chlH Saspl_005210	A0A4D8XXU3_SALSN	153,610
A0A4D8Z1T1	Malate dehydrogenase (EC 1.1.1.37)	MDH2 Saspl_040931	A0A4D8Z1T1_SALSN	103,921
A0A4D9BEI5	Malic enzyme	Saspl_026155	A0A4D9BEI5_SALSN	132,508
A0A4D9A9W6	Mannose-1-phosphate guanylyltransferase	GMPP Saspl_004464	A0A4D9A9W6_SALSN	45,644
A0A4D9B6Z4	Methenyltetrahydrofolate cyclohydrolase (EC 3.5.4.9)	folD Saspl_011499	A0A4D9B6Z4_SALSN	31,646

A0A4D9AX74	Methionine S-methyltransferase (EC 2.1.1.12)	Saspl_019227	A0A4D9AX74_SALSN	123,289
A0A4D8YVR7	MHD domain-containing protein	Saspl_041203	A0A4D8YVR7_SALSN	124,060
A0A4D9AML5	NADPH-protochlorophyllide oxidoreductase (EC 1.3.1.33)	Saspl_015280	A0A4D9AML5_SALSN	39,636
A0A4D9BFJ2	NB-ARC domain-containing protein	Saspl_027088	A0A4D9BFJ2_SALSN	210,002
A0A4D8XPU2	Nucleolar protein 58	NOP58 Saspl_051807	A0A4D8XPU2_SALSN	69,319
A0A4D9C3U2	Omp85 domain-containing protein	Saspl_003268	A0A4D9C3U2_SALSN	91,317
A0A3P8MIU4	Pentatricopeptide repeat-containing protein (Fragment)		A0A3P8MIU4_9LAMI	34,990
A0A4D9B876	Peptidylprolyl isomerase (EC 5.2.1.8)	Saspl_013987	A0A4D9B876_SALSN	63,144
A0A4D8YY19	Phage shock protein A	pspA Saspl_032735	A0A4D8YY19_SALSN	29,182
A0A4D9B4K0	Phenylalanyl-tRNA synthetase (EC 6.1.1.20)	FARSA pheS Saspl_010541	A0A4D9B4K0_SALSN	50,321
A0A4D8YJ01	Phosphatidylinositol 4-kinase	PI4K Saspl_051135	A0A4D8YJ01_SALSN	220,219
A0A4D8ZQ53	Phospho-2-dehydro-3-deoxyheptonate aldolase (EC 2.5.1.54)	Saspl_032447	A0A4D8ZQ53_SALSN	73,162
A0A4D9AM91	Phosphoglucomutase (alpha-D-glucose-1,6-bisphosphate-dependent) (EC 5.4.2.2)	pgm Saspl_004865	A0A4D9AM91_SALSN	72,465
A0A4D8ZF59	Phosphoglycerate mutase (2,3-diphosphoglycerate-independent) (EC 5.4.2.12)	gpmI Saspl_036811	A0A4D8ZF59_SALSN	65,655
A0A4D8YS63	Phospholipase D (EC 3.1.4.4)	PLD1_2 Saspl_043837	A0A4D8YS63_SALSN	91,789
A0A4D8ZG72	Pribosyltran domain-containing protein	Saspl_028107	A0A4D8ZG72_SALSN	73,380
A0A4D8ZBK1	Proteasome subunit beta (EC 3.4.25.1)	PSMB1 Saspl_036286	A0A4D8ZBK1_SALSN	24,490
A0A4D9B3B2	Protein kinase domain-containing protein	Saspl_008295	A0A4D9B3B2_SALSN	105,292
A0A4D9AQG2	Protein kinase domain-containing protein	Saspl_022855	A0A4D9AQG2_SALSN	154,957
Entry	Protein names	Gene names	Entry name	Mass
F8TP06	Protein TIC 214 (Translocon at the inner envelope membrane of chloroplasts 214) (Fragment)	ycf1 TIC214	F8TP06_OCIBA	181,707
I1WZA3	Protein TIC 214 (Translocon at the inner envelope membrane of chloroplasts 214) (Fragment)		I1WZA3_MENSP	182,467
A0A4D9B3Z7	Protein TIF31	TIF31 Saspl_010190	A0A4D9B3Z7_SALSN	208,927
A0A4D9B9Y5	Protein transport protein SEC31	SEC31 Saspl_035461	A0A4D9B9Y5_SALSN	128,365
A0A4D8YKJ5	Protein-synthesizing GTPase (EC 3.6.5.3)	EIF2S3 Saspl_042338	A0A4D8YKJ5_SALSN	55,669



A0A4D8Y730	Pyrophosphate--fructose 6-phosphate 1-phosphotransferase subunit alpha (PFP) (6-phosphofructokinase, pyrophosphate dependent) (PPI-PFK) (Pyrophosphate-dependent 6-phosphofructose-1-kinase)	PFP-ALPHA Saspl_000088	A0A4D8Y730_SALSN	69,149
A0A4D8ZW88	Pyruvate kinase (EC 2.7.1.40)	PK Saspl_026441	A0A4D8ZW88_SALSN	59,664
A0A4D8Z0W1	Pyruvate kinase (EC 2.7.1.40)	PK Saspl_032172	A0A4D8Z0W1_SALSN	55,405
A0A4D8ZJI2	Ran GTPase-activating protein 1	RANGAP1 Saspl_030194	A0A4D8ZJI2_SALSN	60,933
A0A482K431	Ribulose biphosphate carboxylase large chain (EC 4.1.1.39) (Fragment)	rbcL	A0A482K431_9LAMI	20,496
A0A1C9HFU5	Ribulose biphosphate carboxylase large chain (EC 4.1.1.39) (Fragment)	rbcL	A0A1C9HFU5_9LAMI	47,905
Q33523	Ribulose biphosphate carboxylase large chain (EC 4.1.1.39) (Fragment)	rbcL	Q33523_HYSOF	52,443
Q36650	Ribulose biphosphate carboxylase large chain (EC 4.1.1.39) (Fragment)	rbcL	Q36650_9LAMI	48,467
Q32728	Ribulose biphosphate carboxylase large chain (EC 4.1.1.39) (Fragment)	rbcL	Q32728_9LAMI	51,776
Q36680	Ribulose biphosphate carboxylase large chain (EC 4.1.1.39) (Fragment)	rbcL	Q36680_PHYVR	49,582
Q36288	Ribulose biphosphate carboxylase large chain (EC 4.1.1.39) (Fragment)	rbcL	Q36288_MENLO	52,320
Q6PZ79	Ribulose biphosphate carboxylase large chain (EC 4.1.1.39) (Fragment)	rbcL	Q6PZ79_9LAMI	41,541
E5RNG5	Ribulose biphosphate carboxylase large chain (EC 4.1.1.39) (Fragment)	rbcL	E5RNG5_9LAMI	47,145
U5N1P9	Ribulose biphosphate carboxylase large chain (EC 4.1.1.39) (Fragment)	rbcL	U5N1P9_9LAMI	43,108
A0A342D2D5	Ribulose biphosphate carboxylase large chain (RuBisCO large subunit) (EC 4.1.1.39)	rbcL DYC0573	A0A342D2D5_9LAMI	54,032
A0A4D9BAP1	Small nuclear ribonucleoprotein-associated protein	SNRPB SMB Saspl_010359	A0A4D9BAP1_SALSN	29,632
A0A4D8YV43	Solute carrier family 25 (Mitochondrial carnitine/acylcarnitine transporter), member 20/29	SLC25A20_29 CACL CACT CRC1 Saspl_045242	A0A4D8YV43_SALSN	30,278
A0A4D8Z7X8	Sterol 14-demethylase	CYP51 Saspl_037965	A0A4D8Z7X8_SALSN	55,321



A0A4D9B6U6	Succinate--CoA ligase [ADP-forming] subunit beta, mitochondrial (EC 6.2.1.5) (Succinyl-CoA synthetase beta chain) (SCS-beta)	LSC2 Saspl_011583	A0A4D9B6U6_SALSN	55,234
A0A4D9C6I3	T-complex protein 1 subunit epsilon	CCT5 Saspl_022666	A0A4D9C6I3_SALSN	59,205
A0A4D9BTB4	TPX2 domain-containing protein	Saspl_013049	A0A4D9BTB4_SALSN	96,367
A0A4D9BQK5	Transaldolase (EC 2.2.1.2)	Saspl_012225	A0A4D9BQK5_SALSN	48,207
A0A4D8ZFF7	Translation initiation factor 4G	EIF4G Saspl_036245	A0A4D8ZFF7_SALSN	188,579
A0A4D8YTV8	Translation initiation factor IF-2	infB MTIF2 Saspl_046157	A0A4D8YTV8_SALSN	108,287
A0A4D9B772	Tubulin alpha chain	TUBA Saspl_008755	A0A4D9B772_SALSN	49,631
A0A4D9A5P5	Tubulin beta chain	TUBB Saspl_048140	A0A4D9A5P5_SALSN	50,324
A0A4D9A2R0	Tubulin beta chain	TUBB Saspl_029906	A0A4D9A2R0_SALSN	50,422
A0A4D8ZH24	Uncharacterized protein	Saspl_040600	A0A4D8ZH24_SALSN	93,003
A0A4D9BN96	Uncharacterized protein	Saspl_010852	A0A4D9BN96_SALSN	131,252
A0A4D8YFX5	Uncharacterized protein	Saspl_005584	A0A4D8YFX5_SALSN	117,936
A0A4D9C639	Uncharacterized protein	Saspl_022584	A0A4D9C639_SALSN	32,993
A0A4D8YUV0	Uncharacterized protein	Saspl_046580	A0A4D8YUV0_SALSN	115,570
A0A4D8YHN0	Uncharacterized protein	Saspl_045861	A0A4D8YHN0_SALSN	33,122
A0A4D9ADR5	Uncharacterized protein	Saspl_027879	A0A4D9ADR5_SALSN	141,128
A0A4D8ZHI1	Uncharacterized protein	Saspl_042724	A0A4D8ZHI1_SALSN	27,899
A0A4D9BXR1	Uncharacterized protein	Saspl_014458	A0A4D9BXR1_SALSN	115,643
A0A4D9C124	Uncharacterized protein	Saspl_013196	A0A4D9C124_SALSN	35,145
A0A4D8Y7K5	Uncharacterized protein	Saspl_005603	A0A4D8Y7K5_SALSN	81,071
A0A4D9AUJ9	Uncharacterized protein	Saspl_025832	A0A4D9AUJ9_SALSN	35,416
A0A4D9C1E4	Uncharacterized protein	Saspl_002454	A0A4D9C1E4_SALSN	102,683
A0A4D9BHE0	Uncharacterized protein	Saspl_016491	A0A4D9BHE0_SALSN	54,500
A0A4D8YSK5	Uncharacterized protein	Saspl_042290	A0A4D8YSK5_SALSN	143,164
A0A4D8XRK1	Uncharacterized protein	Saspl_001102	A0A4D8XRK1_SALSN	135,484
A0A4D8ZH3	Uncharacterized protein	Saspl_034459	A0A4D8ZH3_SALSN	81,576
A0A4D9AAF8	Uncharacterized protein	Saspl_021900	A0A4D9AAF8_SALSN	114,068

A0A4D9BU38	Uncharacterized protein	Saspl_007704	A0A4D9BU38_SALSN	74,364
A0A4D8XTY6	Uncharacterized protein	Saspl_001005	A0A4D8XTY6_SALSN	126,733
A0A4D9ATA5	Uncharacterized protein	Saspl_014909	A0A4D9ATA5_SALSN	102,689
A0A4D8Z9D1	Uncharacterized protein	Saspl_030695	A0A4D8Z9D1_SALSN	47,140
A0A4D9A400	V-type H <sup>+</sup> -transporting ATPase subunit E	ATPeV1E Saspl_030111	A0A4D9A400_SALSN	21,574
A0A4D9A515	V-type proton ATPase subunit C	ATPeV1C ATP6C Saspl_021562	A0A4D9A515_SALSN	42,645
A0A4D9C7P1	WD_REPEATS_REGION domain-containing protein	Saspl_016367	A0A4D9C7P1_SALSN	36,082
A0A4D9BVG8	WD_REPEATS_REGION domain-containing protein	Saspl_008191	A0A4D9BVG8_SALSN	186,120
<b>p-CA Unique Proteins</b>				
A0A4D9AMS5	Photosystem II oxygen-evolving enhancer protein 3	psbQ Saspl_023506	A0A4D9AMS5_SALSN	24,207
A0A4D9BIP2	PDZ domain-containing protein	Saspl_006024	A0A4D9BIP2_SALSN	49,806
Q8MG08	Ribulose biphosphate carboxylase large chain (EC 4.1.1.39) (Fragment)	rbcL	Q8MG08_9LAMI	49,985
A0A4D8ZR36	Dihydrolipoyllysine-residue succinyltransferase (EC 2.3.1.61)	DLST sucB Saspl_031312	A0A4D8ZR36_SALSN	89,553
A0A4D8ZKT6	Aquaporin TIP	TIP Saspl_003952	A0A4D8ZKT6_SALSN	25,936
A0A4D8Z0Z9	Plasminogen activator inhibitor 1 RNA-binding protein	SERBP1 Saspl_036254	A0A4D8Z0Z9_SALSN	36,699
A0A4D9AQ31	Cell division protease FtsH	ftsH Saspl_017145	A0A4D9AQ31_SALSN	73,803
A0A4D8ZFI4	Large subunit ribosomal protein L8e	RP-L8e RPL8 Saspl_033417	A0A4D8ZFI4_SALSN	28,083
A0A4D9ADF3	NADH-cytochrome b5 reductase (EC 1.6.2.2)	Saspl_019463	A0A4D9ADF3_SALSN	35,180
A0A4D8YW15	Large subunit ribosomal protein L27Ae	RP-L27Ae RPL27A Saspl_047250	A0A4D8YW15_SALSN	16,054
A0A4D8ZIQ1	T-complex protein 1 subunit delta	CCT4 Saspl_034927	A0A4D8ZIQ1_SALSN	57,108
A0A4D9BPR2	Large subunit ribosomal protein L15	RP-L15 MRPL15 rplO Saspl_011984	A0A4D9BPR2_SALSN	28,892
A0A4D9B9F1	Photosystem II oxygen-evolving enhancer protein 1	psbO Saspl_018239	A0A4D9B9F1_SALSN	34,411
A0A4D8ZM08	Thioredoxin 1	trxA Saspl_033965	A0A4D8ZM08_SALSN	18,259
A0A4D8YYH0	Suppressor of tumorigenicity protein 13	ST13 Saspl_038600	A0A4D8YYH0_SALSN	52,950

A0A4D9BB76	Uncharacterized protein	Saspl_011734	A0A4D9BB76_SALSN	28,916
A0A142DPS6	Photosystem II protein D1 (PSII D1 protein) (EC 1.10.3.9) (Photosystem II Q(B) protein)	psbA	A0A142DPS6_9LAMI	38,926
A0A4D9AM60	Glyceraldehyde-3-phosphate dehydrogenase (EC 1.2.1.-)	GAPDH gapA Saspl_015129 Saspl_032350	A0A4D9AM60_SALSN	36,706
A0A4D8Z6H9	Proteasome subunit beta (EC 3.4.25.1)	PSMB4 Saspl_046486	A0A4D8Z6H9_SALSN	25,941
A0A4D8YKF7	Large subunit ribosomal protein L23e	RP-L23e Saspl_045371	A0A4D8YKF7_SALSN	16,440
Q32087	Ribulose biphosphate carboxylase large chain (EC 4.1.1.39) (Fragment)	rbcL	Q32087_CONTO	48,826
A0A4D9AX97	Large subunit ribosomal protein L13Ae	RP-L13Ae RPL13A Saspl_014963	A0A4D9AX97_SALSN	117,051
A0A4D8Z802	Serine hydroxymethyltransferase (EC 2.1.2.1)	glyA SHMT Saspl_043218	A0A4D8Z802_SALSN	57,882
A0A4D8YK92	Pectinesterase (EC 3.1.1.11)	Saspl_040718	A0A4D8YK92_SALSN	48,771
A0A4D8Y7X0	Nascent polypeptide-associated complex subunit beta	EGD1 BTF3 Saspl_000453	A0A4D8Y7X0_SALSN	45,120
A0A0K1ZCB5	Ribosomal protein L23	rpl23	A0A0K1ZCB5_NEPCA	10,634
A0A2D0UYT2	Ribulose biphosphate carboxylase large chain (EC 4.1.1.39) (Fragment)	rbcL	A0A2D0UYT2_9LAMI	19,625
F8RGV6	Ribulose biphosphate carboxylase large chain (EC 4.1.1.39) (Fragment)	rbcL	F8RGV6_SALSN	26,266
A0A142DQ30	Photosystem II CP43 reaction center protein (PSII 43 kDa protein) (Protein CP-43)	psbC	A0A142DQ30_9LAMI	51,882
Q6PZB0	Ribulose biphosphate carboxylase large chain (EC 4.1.1.39) (Fragment)	rbcL	Q6PZB0_9LAMI	49,584
Q42662	5-methyltetrahydropteroyltriglutamate--homocysteine methyltransferase (EC 2.1.1.14) (Cobalamin-independent methionine synthase isozyme) (Vitamin-B12-independent methionine synthase isozyme)	MET	METE_PLESU	84,590
A0A4D9BGU8	Enoyl-[acyl-carrier protein] reductase I	fabI Saspl_024310	A0A4D9BGU8_SALSN	41,134
C6FJR5	Ribulose biphosphate carboxylase large chain (EC 4.1.1.39) (Fragment)	rbcL	C6FJR5_ORIVU	12,434
Q8MG06	Ribulose biphosphate carboxylase large chain (EC 4.1.1.39) (Fragment)	rbcL	Q8MG06_9LAMI	49,645
A0A4D9BKM1	Uncharacterized protein	Saspl_022012	A0A4D9BKM1_SALSN	93,727

M9VNN3	Ribulose biphosphate carboxylase large chain (EC 4.1.1.39) (Fragment)	rbcL	M9VNN3_9LAMI	27,558
A0A0D4BP40	Ribulose biphosphate carboxylase large chain (EC 4.1.1.39) (Fragment)	rbcL	A0A0D4BP40_VITNE	29,259
A0A4D9BR91	Large subunit ribosomal protein L34e	RP-L34e RPL34 Saspl_022719 Saspl_032574 Saspl_052867	A0A4D9BR91_SALSN	13,706
A0A0H4SWH4	Ribulose biphosphate carboxylase large chain (EC 4.1.1.39) (Fragment)	rbcL	A0A0H4SWH4_9LAMI	23,231
A0A4D9BWF3	Large subunit ribosomal protein L10e	RP-L10e Saspl_014432	A0A4D9BWF3_SALSN	24,933
A0A4D9AQN2	Phosphoglycerate kinase (EC 2.7.2.3)	PGK pgk Saspl_017349	A0A4D9AQN2_SALSN	52,856
A0A4D9B1M2	Large subunit ribosomal protein L7e	RP-L7e Saspl_008309	A0A4D9B1M2_SALSN	28,488
A0A4D9A077	Glyoxylate/succinic semialdehyde reductase	GLYR Saspl_037487	A0A4D9A077_SALSN	41,757
A0A4D9BKE5	F-type H <sup>+</sup> -transporting ATPase subunit gamma	ATPF1G atpG Saspl_006589	A0A4D9BKE5_SALSN	40,324
A0A4D9AC70	Uncharacterized protein	Saspl_027433	A0A4D9AC70_SALSN	20,078
A0A4D8ZMX2	PKS_ER domain-containing protein	Saspl_036543	A0A4D8ZMX2_SALSN	38,729
A0A4D8YAN0	Multifunctional fusion protein [Includes: Photosystem II reaction center protein Z; Photosystem II D2 protein]	psbD Saspl_049729	A0A4D8YAN0_SALSN	74,976
A0A4D8ZGC2	3-phosphoshikimate 1-carboxyvinyltransferase (EC 2.5.1.19)	aroA Saspl_033765	A0A4D8ZGC2_SALSN	54,624
A0A4D8ZB14	Ribosomal protein L15	RP-L15e Saspl_045421	A0A4D8ZB14_SALSN	24,216
A0A4D9BKD6	UBX domain-containing protein 1	SHP1 NSFL1C UBX1 Saspl_006616	A0A4D9BKD6_SALSN	32,825
A0A4D9ATV9	Large subunit ribosomal protein L26e	RP-L26e RPL26 Saspl_001329	A0A4D9ATV9_SALSN	16,648
A0A4D9AZ83	Large subunit ribosomal protein L18e	RP-L18e Saspl_008243	A0A4D9AZ83_SALSN	21,010
A0A4D8ZSU1	Large subunit ribosomal protein L24e	RP-L24e RPL24 Saspl_021438	A0A4D8ZSU1_SALSN	18,608
A0A4D9AFL9	Histone H2B	Saspl_019666	A0A4D9AFL9_SALSN	15,971
A0A4D8ZNK4	23 kDa subunit of oxygen evolving system of photosystem II (23 kDa thylakoid membrane protein) (OEC 23 kDa subunit)	psbP Saspl_036810	A0A4D8ZNK4_SALSN	28,230

A0A4D9ASV4	Peptidyl-prolyl cis-trans isomerase (PPIase) (EC 5.2.1.8)	PPIB Saspl_004703	A0A4D9ASV4_SALSN	27,882
A0A4D9AIV9	Large subunit ribosomal protein L39e	RP-L39e RPL39 Saspl_021393	A0A4D9AIV9_SALSN	75,801
A0A4D9BZX4	S-adenosylmethionine synthase (EC 2.5.1.6)	metK Saspl_013182	A0A4D9BZX4_SALSN	42,981
A0A4D8ZDI2	Bet_v_1 domain-containing protein	Saspl_042706	A0A4D8ZDI2_SALSN	17,190
A0A4D8Z3R3	Histone H2A	Saspl_009133 Saspl_037750	A0A4D8Z3R3_SALSN	14,426
A0A4D9AN04	ATPase_AAA_core domain-containing protein	Saspl_035590	A0A4D9AN04_SALSN	51,732
O78382	Ribulose biphosphate carboxylase large chain (EC 4.1.1.39) (Fragment)	rbcL	O78382_TEUCH	52,368
Q6PZA2	Ribulose biphosphate carboxylase large chain (EC 4.1.1.39) (Fragment)	rbcL	Q6PZA2_SALDI	43,396
A0A4D8Y5P1	Aquaporin TIP	TIP Saspl_049185 Saspl_049359	A0A4D8Y5P1_SALSN	24,983
A0A4D9C214	Selenium-binding protein 1	SELENBP1 Saspl_002548	A0A4D9C214_SALSN	53,913
Q33198	Ribulose biphosphate carboxylase large chain (EC 4.1.1.39) (Fragment)	rbcL	Q33198_9LAMI	49,136
Q6PZ86	Ribulose biphosphate carboxylase large chain (EC 4.1.1.39) (Fragment)	rbcL	Q6PZ86_9LAMI	41,146
A0A4D8YEU4	CCT-eta	CCT7 Saspl_038031	A0A4D8YEU4_SALSN	124,933
A0A4D8XRD9	Uncharacterized protein	Saspl_000113	A0A4D8XRD9_SALSN	27,481
Q6PZ63	Ribulose biphosphate carboxylase large chain (EC 4.1.1.39) (Fragment)	rbcL	Q6PZ63_9LAMI	43,048
A0A4D9C2I9	Abhydrolase_3 domain-containing protein	Saspl_013421	A0A4D9C2I9_SALSN	38,373
A0A4D9B589	Glutamate-1-semialdehyde 2,1-aminomutase (EC 5.4.3.8)	hemL Saspl_013861	A0A4D9B589_SALSN	50,335
A0A4D9BVM0	Large subunit ribosomal protein L32e	RP-L32e Saspl_029418	A0A4D9BVM0_SALSN	15,726
A0A4D9ARK4	Nascent polypeptide-associated complex subunit beta	EGD1 Saspl_010325	A0A4D9ARK4_SALSN	17,835
A0A4D9AVK6	Uncharacterized protein	Saspl_019183	A0A4D9AVK6_SALSN	22,728
A0A4D9BI60	Chaperonin GroES	groES Saspl_016928	A0A4D9BI60_SALSN	26,851
Q32289	Ribulose biphosphate carboxylase large chain (EC 4.1.1.39) (Fragment)	rbcL	Q32289_9LAMI	51,957



A0A0X9TSM6	ATP synthase subunit alpha, chloroplastic (EC 7.1.2.2) (ATP synthase F1 sector subunit alpha) (F-ATPase subunit alpha)	atpA	A0A0X9TSM6_LAVAN	55,296
A0A4D9B9W4	Phosphoglycerate mutase (2,3-diphosphoglycerate-independent) (EC 5.4.2.12)	gpmI Saspl_015360	A0A4D9B9W4_SALSN	61,214
<b>NaCl Unique proteins</b>				
F8TP30	Protein TIC 214 (Translocon at the inner envelope membrane of chloroplasts 214) (Fragment)	ycf1 TIC214	F8TP30_SALGU	182,499
A0A4D8ZHT5	Uncharacterized protein	Saspl_033835	A0A4D8ZHT5_SALSN	171,913
<b>NaCl + p-CA Unique proteins</b>				
A0A4D8Z026	UDP-glucose 4,6-dehydratase	RHM Saspl_028960	A0A4D8Z026_SALSN	48,388
A0A4D8ZMB7	Uncharacterized protein	Saspl_028356	A0A4D8ZMB7_SALSN	90,152
A0A4D8ZFW5	Histone acetyltransferase (EC 2.3.1.48)	Saspl_028288	A0A4D8ZFW5_SALSN	207,212
A0A4D8Y3H3	Uncharacterized protein	Saspl_051614	A0A4D8Y3H3_SALSN	301,483
A0A4D8XUM7	Uncharacterized protein	Saspl_000154	A0A4D8XUM7_SALSN	389,757
A0A4D8Z0Z4	Non-specific serine/threonine protein kinase (EC 2.7.11.1)	SMG1 Saspl_049915	A0A4D8Z0Z4_SALSN	419,237
A0A4D8XZS0	Uncharacterized protein	Saspl_042223	A0A4D8XZS0_SALSN	133,868
A0A185NWC6	Bornyl diphosphate synthase		A0A185NWC6_LAVAN	70,672
A0A4D8Y1M3	SET domain-containing protein	Saspl_005345	A0A4D8Y1M3_SALSN	93,129
A0A4D9AC78	Transcriptional repressor NF-X1	NFX1 Saspl_025785	A0A4D9AC78_SALSN	241,865
A0A4D9B765	Midasin	MDN1 REA1 Saspl_011805	A0A4D9B765_SALSN	412,445
A0A4D8Z6W0	Lysine-specific histone demethylase 1A	KDM1A Saspl_030360	A0A4D8Z6W0_SALSN	234,123
A0A4D9AQ17	Uncharacterized protein	Saspl_015637	A0A4D9AQ17_SALSN	194,680
A0A4D8YJA8	Myb-like domain-containing protein	Saspl_045641	A0A4D8YJA8_SALSN	218,753
A0A4D9BCL2	SWI/SNF-related matrix-associated actin-dependent regulator of chromatin subfamily A member 2/4	SMARCA2_4 Saspl_009615	A0A4D9BCL2_SALSN	338,595
A0A4D9B5P4	Superkiller protein 3	SKI3 TTC37 Saspl_017072	A0A4D9B5P4_SALSN	133,909
A0A4D8YI34	Histone H2B	NOVA Saspl_041480	A0A4D8YI34_SALSN	50,396



A0A4D8ZNY9	Uncharacterized protein	Saspl_030189	A0A4D8ZNY9_SALSN	163,630
A0A4D9BJ35	PB1 domain-containing protein	Saspl_006180	A0A4D9BJ35_SALSN	76,177
A0A4D8YSZ1	ENDO3c domain-containing protein	Saspl_041496	A0A4D8YSZ1_SALSN	219,872
F8TNT9	Protein TIC 214 (Translocon at the inner envelope membrane of chloroplasts 214) (Fragment)	ycf1 TIC214	F8TNT9_9LAMI	182,494
A0A4D9BS84	Structural maintenance of chromosomes protein	Saspl_012489	A0A4D9BS84_SALSN	140,510
A0A4D8XX72	Uncharacterized protein	Saspl_005679	A0A4D8XX72_SALSN	312,376
A0A4D9C271	Cellulose synthase (EC 2.4.1.12)	CESA Saspl_002799	A0A4D9C271_SALSN	123,778
A0A4D8XW78	Histone acetyltransferase (EC 2.3.1.48)	Saspl_000558	A0A4D8XW78_SALSN	200,709
A0A4D8YQA1	VWFA domain-containing protein	Saspl_040742	A0A4D8YQA1_SALSN	82,440

**Table S2.** Similar proteins identified between different treatments.

Entry	Protein names	Gene names	Entry name	Mass
<b>Shared proteins across all four treatment</b>				
A0A4D8ZVS4	Germin-like protein	Saspl_039583	A0A4D8ZVS4_SALSN	22,024
A0A4D8YGX6	Cytochrome f	Saspl_049645	A0A4D8YGX6_SALSN	32,480
A0A4D8YZD9	Peptidyl-prolyl cis-trans isomerase (PPIase) (EC 5.2.1.8)	Saspl_037966	A0A4D8YZD9_SALSN	17,954
A0A4D9AJQ4	Large subunit ribosomal protein L12e	RP-L12e RPL12 Saspl_019056	A0A4D9AJQ4_SALSN	17,349
A0A4D9BMN0	Photosystem II oxygen-evolving enhancer protein 1	psbO Saspl_018730	A0A4D9BMN0_SALSN	34,350
A0A410KKW0	Photosystem II D2 protein (PSII D2 protein) (EC 1.10.3.9) (Photosystem Q(A) protein)	psbD	A0A410KKW0_9LAMI	39,535
A0A4D9A5S3	ATP synthase subunit beta (EC 7.1.2.2)	ATPeF1B Saspl_019881	A0A4D9A5S3_SALSN	59,168
A0A4D9B987	Carbonic anhydrase (EC 4.2.1.1) (Carbonate dehydratase)	cynT can Saspl_008678	A0A4D9B987_SALSN	34,334
<b>Shared proteins between Control and p-CA</b>				
A0A4D8YR26	Histone_H2A_C domain-containing protein	Saspl_042645	A0A4D8YR26_SALSN	13,290
A0A4D9A2D6	Rhodanese domain-containing protein	Saspl_026456	A0A4D9A2D6_SALSN	25,837

A0A4D8Z3Z7	Clathrin light chain	Saspl_046091	A0A4D8Z3Z7_SALSN	34,115
A0A4D8XP31	Methyltransferase (EC 2.1.1.-)	Saspl_000221	A0A4D8XP31_SALSN	70,135
A0A4D9A923	DnaJ-like protein subfamily A member 1	DNAJA1 Saspl_019467	A0A4D9A923_SALSN	283,070
A0A4D9BAT7	Peptidylprolyl isomerase (EC 5.2.1.8)	Saspl_001371	A0A4D9BAT7_SALSN	49,012
A0A4D8YJ16	Tubulin alpha	TUBA Saspl_045323	A0A4D8YJ16_SALSN	107,976
A0A4D8YK58	Peptidylprolyl isomerase (EC 5.2.1.8)	Saspl_048783	A0A4D8YK58_SALSN	19,500
Q6PZ77	Ribulose biphosphate carboxylase large chain (EC 4.1.1.39) (Fragment)	rbcL	Q6PZ77_9LAMI	43,768
A0A4D8ZZ23	Glutaredoxin-dependent peroxiredoxin (EC 1.11.1.25)	Saspl_031016	A0A4D8ZZ23_SALSN	30,093
A0A4D9C565	T-complex protein 1 subunit zeta	CCT6 Saspl_003220	A0A4D9C565_SALSN	59,020
A0A4D8YPN2	Large subunit ribosomal protein L18Ae	RP-L18Ae RPL18A Saspl_044545	A0A4D8YPN2_SALSN	39,659
A0A4D9A2Y6	TRANSKETOLASE_1 domain-containing protein	Saspl_025229	A0A4D9A2Y6_SALSN	84,193
A0A4D8Y3R6	Uncharacterized protein	Saspl_051450	A0A4D8Y3R6_SALSN	33,253
A0A4D9AHJ0	40S ribosomal protein S24	RP-S24e RPS24 Saspl_009972 Saspl_026928 Saspl_027498 Saspl_038194	A0A4D9AHJ0_SALSN	15,749
A0A4D9BWB0	Small subunit ribosomal protein S10	RP-S10 MRPS10 rpsJ Saspl_008217	A0A4D9BWB0_SALSN	19,865
A0A4D9A4W1	Proteasome subunit alpha type (EC 3.4.25.1)	PSMA3 Saspl_021502	A0A4D9A4W1_SALSN	30,339
A0A4D9C642	Aquaporin PIP	PIP Saspl_016163	A0A4D9C642_SALSN	29,812
A0A4D8YNX1	Uncharacterized protein	Saspl_032207	A0A4D8YNX1_SALSN	25,669
A0A4D9B9B6	Aldose 1-epimerase (EC 5.1.3.3)	galM GALM Saspl_008749	A0A4D9B9B6_SALSN	38,997
A0A4D8YBM5	Proteasome subunit alpha type (EC 3.4.25.1)	PSMA2 Saspl_050498	A0A4D8YBM5_SALSN	27,182
A0A4D8ZKA6	Malate dehydrogenase (EC 1.1.1.37)	MDH2 Saspl_047680	A0A4D8ZKA6_SALSN	36,043
A0A4D9ADL2	PAP_fibrillin domain-containing protein	Saspl_019523	A0A4D9ADL2_SALSN	36,146
A0A4D8XZ09	Large subunit ribosomal protein L21e	RP-L21e RPL21 Saspl_005143	A0A4D8XZ09_SALSN	18,690
A0A4D9C1C9	Formyltetrahydrofolate synthetase (EC 6.3.4.3)	MTHFD Saspl_013667	A0A4D9C1C9_SALSN	68,337
A0A4D9A4K3	Prohibitin	PHB1 Saspl_019707 Saspl_052946	A0A4D9A4K3_SALSN	30,455

A0A4D9BKW6	Lactoylglutathione lyase (EC 4.4.1.5) (Glyoxalase I)	GLO1 Saspl_006594	A0A4D9BKW6_SALSN	40,771
A0A142DQ42	Ribulose biphosphate carboxylase large chain (RuBisCO large subunit) (EC 4.1.1.39)	rbcL	A0A142DQ42_9LAMI	53,388
A0A4D9C572	Peroxin-14	PEX14 Saspl_002988	A0A4D9C572_SALSN	57,927
A0A4D8YEG4	Large subunit ribosomal protein L28e	RP-L28e RPL28 Saspl_047663	A0A4D8YEG4_SALSN	16,014
A0A4D9B632	3-deoxy-8-phosphooctulonate synthase (EC 2.5.1.55)	Saspl_017338	A0A4D9B632_SALSN	36,069
A0A4D9C174	12-oxophytodienoic acid reductase	OPR Saspl_013246	A0A4D9C174_SALSN	40,166
A0A4D8Y933	40S ribosomal protein SA	RP-SAe RPSA Saspl_051610	A0A4D8Y933_SALSN	32,639
A0A4D9A594	4-aminobutyrate--pyruvate transaminase	POP2 Saspl_027880	A0A4D9A594_SALSN	56,652
A0A4D8ZNI3	Small subunit ribosomal protein S18e	RP-S18e Saspl_038193	A0A4D8ZNI3_SALSN	21,152
A0A4D9B3H7	Glutamate dehydrogenase	GLUD1_2 Saspl_011616	A0A4D9B3H7_SALSN	42,546
A0A4D9BSA3	NADH dehydrogenase (Ubiquinone) 1 alpha subcomplex subunit 9	NDUFA9 Saspl_012509	A0A4D9BSA3_SALSN	219,454
A0A4D8ZEW0	Aconitate hydratase (Aconitase) (EC 4.2.1.3)	ACO Saspl_033383	A0A4D8ZEW0_SALSN	105,693
A0A4D8Y111	26S proteasome regulatory subunit T5	PSMC3 Saspl_052096	A0A4D8Y111_SALSN	54,939
A0A4D8ZRG4	Phosphoserine aminotransferase (EC 2.6.1.52)	serC Saspl_035807	A0A4D8ZRG4_SALSN	46,253
A0A4D9C5K4	Phospholipase D (EC 3.1.4.4)	PLD1_2 Saspl_016444	A0A4D9C5K4_SALSN	91,426
A0A4D9BW10	Uncharacterized protein	Saspl_029631	A0A4D9BW10_SALSN	31,097
A0A4D9BIP4	Glucose-6-phosphate 1-dehydrogenase (EC 1.1.1.49)	G6PD Saspl_005989	A0A4D9BIP4_SALSN	55,133
A0A4D9B8W8	Aha1_N domain-containing protein	Saspl_011638	A0A4D9B8W8_SALSN	39,382
A0A4D8ZK74	Germin-like protein	Saspl_041291	A0A4D8ZK74_SALSN	21,958
A0A4D9C5T7	H15 domain-containing protein	Saspl_016363	A0A4D9C5T7_SALSN	42,494
A0A4D9AQL1	Thiamine thiazole synthase, chloroplastic (Thiazole biosynthetic enzyme) (EC 2.4.2.60)	THI4 THI1 Saspl_035620	A0A4D9AQL1_SALSN	36,263
A0A4D9A5B9	Bet_v_1 domain-containing protein	Saspl_036752	A0A4D9A5B9_SALSN	17,522
A0A4D8Z3N1	Uncharacterized protein	Saspl_033504	A0A4D8Z3N1_SALSN	63,550
A0A4D8YV83	PKS_ER domain-containing protein	Saspl_030792	A0A4D8YV83_SALSN	44,953
Q6PZB9	Ribulose biphosphate carboxylase large chain (EC 4.1.1.39) (Fragment)	rbcL	Q6PZB9_9LAMI	43,279

A0A4D8XWI7	PSI-G (Photosystem I reaction center subunit V, chloroplastic)	psaG Saspl_052611	A0A4D8XWI7_SALSN	15,564
A0A4D9ATZ8	Phosphopyruvate hydratase (EC 4.2.1.11)	ENO eno Saspl_005117	A0A4D9ATZ8_SALSN	57,486
A0A4D9C2I1	Large subunit ribosomal protein L28	RP-L28 Saspl_002456	A0A4D9C2I1_SALSN	20,449
A0A4D8ZZ98	H15 domain-containing protein	Saspl_035748	A0A4D8ZZ98_SALSN	17,401
A0A4D9AJE4	Assimilatory sulfite reductase (ferredoxin) (EC 1.8.7.1)	sir Saspl_009424	A0A4D9AJE4_SALSN	77,639
A0A4D9AEP0	Germin-like protein	Saspl_038929	A0A4D9AEP0_SALSN	21,916
A0A4D9B3S1	Seryl-tRNA synthetase (EC 6.1.1.11)	SARS Saspl_004898	A0A4D9B3S1_SALSN	50,868
A0A4D8ZS62	Histone H2A	Saspl_008252 Saspl_028917 Saspl_029313 Saspl_033421	A0A4D8ZS62_SALSN	13,934
A0A4D8YX06	Phosphoribulokinase (EC 2.7.1.19)	PRK prkB Saspl_042519	A0A4D8YX06_SALSN	40,541
A0A4D8Z617	Uncharacterized protein	Saspl_037748	A0A4D8Z617_SALSN	43,251
A0A4D8ZPK1	UDP-arabinopyranose mutase (EC 5.4.99.30)	RGP UTM Saspl_023096	A0A4D8ZPK1_SALSN	42,006
A0A4D8YEZ0	Ubiquitin	RP-S27Ae RPS27A Saspl_050704	A0A4D8YEZ0_SALSN	21,471
A0A4D9AN42	rRNA 2'-O-methyltransferase fibrillarin	NOPI Saspl_004839	A0A4D9AN42_SALSN	33,554
A0A4D9BXN3	Ras-related protein Rab-7A	RAB7A Saspl_006814	A0A4D9BXN3_SALSN	23,037
A0A4D9AKT9	Malate dehydrogenase (EC 1.1.1.37)	MDH1 Saspl_018157	A0A4D9AKT9_SALSN	35,676
A0A4D8ZH06	23 kDa subunit of oxygen evolving system of photosystem II (23 kDa thylakoid membrane protein) (OEC 23 kDa subunit)	Saspl_037767	A0A4D8ZH06_SALSN	33,683
A0A4D8ZLS2	Uncharacterized protein	Saspl_003655	A0A4D8ZLS2_SALSN	62,106
A0A4D9BGG0	Heat shock 70kDa protein 1/8	HSPA1_8 Saspl_024067	A0A4D9BGG0_SALSN	47,670
A0A4D8YVD4	FeThRed_A domain-containing protein	Saspl_050948	A0A4D8YVD4_SALSN	16,660
A0A4D9BHQ0	Serine hydroxymethyltransferase (EC 2.1.2.1)	glyA Saspl_016764	A0A4D9BHQ0_SALSN	51,952
A0A4D9BCW9	Serine hydroxymethyltransferase (EC 2.1.2.1)	glyA SHMT Saspl_009699	A0A4D9BCW9_SALSN	56,862
A0A4D9B813	Tr-type G domain-containing protein	Saspl_014111	A0A4D9B813_SALSN	93,880
A0A4D8YWL8	PEROXIDASE_4 domain-containing protein	Saspl_045094	A0A4D8YWL8_SALSN	46,727
A0A4D9B519	Large subunit ribosomal protein L11	RP-L11 Saspl_013870	A0A4D9B519_SALSN	24,800
A0A4D8ZF56	Uncharacterized protein	Saspl_033503	A0A4D8ZF56_SALSN	63,793

A0A4D9BC73	Plasminogen activator inhibitor 1 RNA-binding protein	SERBP1 Saspl_020454	A0A4D9BC73_SALSN	38,679
A0A4D8YXB4	Uncharacterized protein	Saspl_042007	A0A4D8YXB4_SALSN	29,073
A0A4D8YP84	Proteasome subunit alpha type (EC 3.4.25.1)	PSMA7 Saspl_044206	A0A4D8YP84_SALSN	27,213
A0A4D8ZXX7	Diaminopimelate decarboxylase	lysA Saspl_003742	A0A4D8ZXX7_SALSN	53,017
Q6PZ84	Ribulose biphosphate carboxylase large chain (EC 4.1.1.39) (Fragment)	rbcL	Q6PZ84_9LAMI	35,649
A0A4D8ZSF8	DUF4057 domain-containing protein	Saspl_023267	A0A4D8ZSF8_SALSN	30,670
A0A1B0VAW1	Photosystem I iron-sulfur center (EC 1.97.1.12) (9 kDa polypeptide) (PSI-C) (Photosystem I subunit VII) (PsaC)	psaC	A0A1B0VAW1_9LAMI	9,038
A0A4D9AG76	Uncharacterized protein	Saspl_025429 Saspl_025654	A0A4D9AG76_SALSN	41,744
A0A4D8ZGN9	40S ribosomal protein S27	RP-S27e RPS27 Saspl_026228	A0A4D8ZGN9_SALSN	9,573
A0A4D9AWZ6	Sulfate adenylyltransferase (EC 2.7.7.4)	PAPSS Saspl_011401	A0A4D9AWZ6_SALSN	53,462
A0A4D9AGY5	Glyoxalase I (EC 4.4.1.5)	GLO1 Saspl_019294	A0A4D9AGY5_SALSN	44,014
A0A4D8ZHR0	Non-specific lipid-transfer protein	Saspl_032078	A0A4D8ZHR0_SALSN	11,846
A0A4D9B6U0	Uncharacterized protein	Saspl_008786	A0A4D9B6U0_SALSN	54,645
A0A4D8ZHR3	40S ribosomal protein S8	RP-S8e Saspl_036423	A0A4D8ZHR3_SALSN	24,976
A0A4D8Z0A1	Acetyltransferase component of pyruvate dehydrogenase complex (EC 2.3.1.12)	DLAT Saspl_029070	A0A4D8Z0A1_SALSN	62,698
A0A4D9A9Q5	OMPdecase (EC 2.4.2.10) (EC 4.1.1.23) (Orotate phosphoribosyltransferase) (Orotidine 5'-phosphate decarboxylase) (Uridine 5'-monophosphate synthase)	UMPS Saspl_031477	A0A4D9A9Q5_SALSN	51,986
A0A4D9B740	Serine/threonine-protein phosphatase 2A regulatory subunit B	PPP2R2 Saspl_011765	A0A4D9B740_SALSN	114,369
A0A4D9C2X2	Plastocyanin	petE Saspl_002814	A0A4D9C2X2_SALSN	16,827
A0A4D8YFU3	Ferredoxin-nitrite reductase	nirA Saspl_046198	A0A4D8YFU3_SALSN	64,964
A0A4D8XUM8	Mg-protoporphyrin IX chelatase (EC 6.6.1.1)	chII Saspl_000957	A0A4D8XUM8_SALSN	49,389
A0A4D8YD34	26S proteasome regulatory subunit T4	PSMC6 RPT4 Saspl_044322	A0A4D8YD34_SALSN	44,804
A0A4D9C6A9	CCT-theta	CCT8 Saspl_016224	A0A4D9C6A9_SALSN	63,558
A0A4D8ZIK0	Large subunit ribosomal protein L13	RP-L13 Saspl_047696	A0A4D8ZIK0_SALSN	25,993
A0A4D8XRY5	Tyrosinase_Cu-bd domain-containing protein	Saspl_000894	A0A4D8XRY5_SALSN	61,898



A0A4D8XYB8	Germin-like protein	Saspl_005161	A0A4D8XYB8_SALSN	26,275
A0A4D8ZGJ0	Glyceraldehyde-3-phosphate dehydrogenase (NADP+) (Phosphorylating)	GAPA Saspl_026839	A0A4D8ZGJ0_SALSN	67,849
A0A4D8Y793	Adenosylhomocysteinase (EC 3.3.1.1)	Saspl_000148	A0A4D8Y793_SALSN	53,340
A0A3G2SDB9	30S ribosomal protein S16, chloroplastic	rps16	A0A3G2SDB9_9LAMI	9,035
A0A0X9SEX0	30S ribosomal protein S19, chloroplastic	rps19	A0A0X9SEX0_LAVAN	10,530
A0A4D9B8K2	40S ribosomal protein S6	RP-S6e RPS6 Saspl_039045 Saspl_045216	A0A4D9B8K2_SALSN	28,428
A0A4D8YMR6	Eukaryotic translation initiation factor 3 subunit I (eIF3i)	EIF3I Saspl_041860	A0A4D8YMR6_SALSN	35,810
A0A4D9BED6	Glutamate dehydrogenase	GLUD1_2 gdhA Saspl_025990	A0A4D9BED6_SALSN	44,627
A0A4D8Z835	Xyloglucan endotransglucosylase/hydrolase (EC 2.4.1.207)	Saspl_043239	A0A4D8Z835_SALSN	32,962
A0A4D9BHN6	Acetyl-CoA acyltransferase 1	ACAA1 Saspl_016606	A0A4D9BHN6_SALSN	49,785
A0A4D8XZN7	26S proteasome regulatory subunit T3	PSMC4 Saspl_053349	A0A4D8XZN7_SALSN	50,194
A0A4D9B163	Uncharacterized protein	Saspl_008366	A0A4D9B163_SALSN	82,689
A0A4D9A7X4	Large subunit ribosomal protein L15	RP-L15 Saspl_021690	A0A4D9A7X4_SALSN	28,443
A0A4D9A8Q0	Usp domain-containing protein	Saspl_021975	A0A4D9A8Q0_SALSN	21,206
A0A4D9BFQ1	NADPH-protochlorophyllide oxidoreductase (EC 1.3.1.33)	Saspl_033747	A0A4D9BFQ1_SALSN	42,629
A0A4D8YW33	Translation initiation factor 4A	EIF4A Saspl_008411 Saspl_029072	A0A4D8YW33_SALSN	46,773
A0A4D8Z0Z8	Translocase of chloroplast (EC 3.6.5.-)	Saspl_041914	A0A4D8Z0Z8_SALSN	33,448
A0A4D8XUG1	ATP-dependent Clp protease ATP-binding subunit ClpB	clpB Saspl_044767	A0A4D8XUG1_SALSN	107,332
A0A4D9AYG6	Ferredoxin--NADP reductase, chloroplastic (FNR) (EC 1.18.1.2)	petH Saspl_018381	A0A4D9AYG6_SALSN	40,465
A0A4D8Z540	Chaperonin GroEL	groEL Saspl_039883	A0A4D8Z540_SALSN	67,250
A0A344X9E2	Ribulose biphosphate carboxylase large chain (EC 4.1.1.39) (Fragment)	rbcL	A0A344X9E2_9LAMI	48,122
A0A4D9AKY1	Uncharacterized protein	Saspl_014982	A0A4D9AKY1_SALSN	87,625
A0A4D9A4E8	Uncharacterized protein	Saspl_028058	A0A4D9A4E8_SALSN	28,428
A0A4D9AJ15	ATP synthase subunit d, mitochondrial	ATPeF0D Saspl_019082	A0A4D9AJ15_SALSN	24,669
A0A4D9B5F1	Translation initiation factor 2 subunit 2	EIF2S2 Saspl_042875	A0A4D9B5F1_SALSN	30,913



A0A4D9C1R9	Protein disulfide-isomerase (EC 5.3.4.1)	PDIA6 Saspl_013158	A0A4D9C1R9_SALSN	41,349
A0A0R5QM80	Dihydrolipoamide Dehydrogenase	A0A0R5QM80_SALMI	60,383	
A0A4D9B990	Obg-like ATPase 1	K06942 Saspl_018095	A0A4D9B990_SALSN	46,182
A0A0K0N8B5	30S ribosomal protein S14, chloroplastic	rps14	A0A0K0N8B5_PERFR	11,730
A0A4D9BYW2	Superoxide dismutase (EC 1.15.1.1)	SOD1 Saspl_007032	A0A4D9BYW2_SALSN	23,978
A0A4D8ZM57	Polyadenylate-binding protein (PABP)	PABPC Saspl_003787	A0A4D8ZM57_SALSN	70,711
A0A4D9B6P6	Plasminogen activator inhibitor 1 RNA-binding protein	SERBP1 Saspl_010294	A0A4D9B6P6_SALSN	37,072
A0A4D9ACQ8	26S proteasome regulatory subunit T6	PSMC5 RPT6 Saspl_004493	A0A4D9ACQ8_SALSN	46,862
A0A4D8Z1C8	ATP-dependent Clp protease proteolytic subunit	Saspl_030757	A0A4D8Z1C8_SALSN	32,535
Q6PZC1	Ribulose biphosphate carboxylase large chain (EC 4.1.1.39) (Fragment)	rbcL	Q6PZC1_9LAMI	41,155
A0A4D9C422	Catalase (EC 1.11.1.6)	Saspl_002592	A0A4D9C422_SALSN	53,744
A0A4D8XYP1	Epimerase domain-containing protein	Saspl_052833	A0A4D8XYP1_SALSN	42,181
A0A4D9AS25	Uncharacterized protein	Saspl_009138	A0A4D9AS25_SALSN	40,310
A0A4D9A9D9	Adenosylhomocysteinase (EC 3.3.1.1)	Saspl_019567	A0A4D9A9D9_SALSN	54,316
A0A4D8YF26	D-3-phosphoglycerate dehydrogenase (EC 1.1.1.95)	serA PHGDH Saspl_041828	A0A4D8YF26_SALSN	66,466
A0A4D9AHH9	Small subunit ribosomal protein S13	RP-S13 Saspl_017638	A0A4D9AHH9_SALSN	18,591
A0A4D9B339	Small subunit ribosomal protein S6e	RP-S6e RPS6 Saspl_015032	A0A4D9B339_SALSN	96,553
A0A4D8ZQB0	PEROXIDASE_4 domain-containing protein	Saspl_023771	A0A4D8ZQB0_SALSN	33,180
A0A4D9A8C3	Large subunit ribosomal protein L6e	RP-L6e RPL6 Saspl_020627	A0A4D9A8C3_SALSN	25,307
A0A4D9AUI3	Carbonic anhydrase (EC 4.2.1.1) (Carbonate dehydratase)	cynT can Saspl_001363	A0A4D9AUI3_SALSN	35,677
A0A4D8Y8P5	Uncharacterized protein	Saspl_000789	A0A4D8Y8P5_SALSN	37,140
A0A4D8ZR42	60S ribosomal protein L13	RP-L13e Saspl_026993	A0A4D8ZR42_SALSN	23,529
A0A4D8ZMS7	Peptidylprolyl isomerase (EC 5.2.1.8)	Saspl_003749	A0A4D8ZMS7_SALSN	30,521
A0A4D8Y8T0	F-type H <sup>+</sup> -transporting ATPase subunit delta	ATPF1D Saspl_000127	A0A4D8Y8T0_SALSN	26,240
A0A4D9BSF5	Plasminogen activator inhibitor 1 RNA-binding protein	SERBP1 Saspl_012723	A0A4D9BSF5_SALSN	36,220
A0A4D9A163	Elongation factor 1-alpha	EEF1A Saspl_003674	A0A4D9A163_SALSN	49,392
A0A4D9ANN8	Small subunit ribosomal protein S10e	RP-S10e RPS10 Saspl_009339 Saspl_017602	A0A4D9ANN8_SALSN	19,458

A0A4D9B7T6	Uncharacterized protein	Saspl_001658 Saspl_002141	A0A4D9B7T6_SALSN	25,885
A0A4D9AWV0	Pyr_redox_2 domain-containing protein	Saspl_037592	A0A4D9AWV0_SALSN	47,120
A0A1W6CAC1	Ribosomal protein L14	rpl14	A0A1W6CAC1_SCULA	13,576
A0A4D9A4B2	60S acidic ribosomal protein P0	RP-LP0 Saspl_024512	A0A4D9A4B2_SALSN	34,268
A0A4D9A624	Translation initiation factor IF-3	infC Saspl_019993	A0A4D9A624_SALSN	29,432
A0A4D9B1S7	Large subunit ribosomal protein L8e	RP-L8e RPL8 Saspl_017980 Saspl_046338 Saspl_050418	A0A4D9B1S7_SALSN	28,081
A0A4D8YUM8	Glutamine amidotransferase type-2 domain-containing protein	Saspl_039296	A0A4D8YUM8_SALSN	180,609
A0A4D8Y8S2	Uncharacterized protein	Saspl_048861	A0A4D8Y8S2_SALSN	43,627
A0A4D8ZH72	Actin, other eukaryote	ACTF Saspl_043061 Saspl_048459	A0A4D8ZH72_SALSN	41,784
Q76B03	50S ribosomal protein L16, chloroplastic (Fragment)	rpl16	Q76B03_SCUAT	13,129
A0A4D9A2X4	Large subunit ribosomal protein L10	RP-L10 MRPL10 rplJ Saspl_023892	A0A4D9A2X4_SALSN	25,500
A0A4D8Y46	Uncharacterized protein	Saspl_044166	A0A4D8Y46_SALSN	18,331
A0A4D9C608	Dirigent protein	Saspl_016133	A0A4D9C608_SALSN	21,895
A0A4D9B3B3	Nucleoside diphosphate kinase (EC 2.7.4.6)	ndk Saspl_015132	A0A4D9B3B3_SALSN	25,195
A0A4D9A1E3	UDP-glucuronate decarboxylase	UXS1 Saspl_029845	A0A4D9A1E3_SALSN	41,108
A0A4D8Y9C2	Chaperonin GroEL	groEL Saspl_046435	A0A4D8Y9C2_SALSN	104,477
A0A4D8Z7E4	Coproporphyrinogen oxidase (EC 1.3.3.3)	CPOX Saspl_037314	A0A4D8Z7E4_SALSN	37,953
A0A4D9AGF9	UDP-glucose 4-epimerase	galE Saspl_009290	A0A4D9AGF9_SALSN	51,390
A0A4D9BCM4	Lipoxygenase (EC 1.13.11.-)	LOX2S Saspl_009609	A0A4D9BCM4_SALSN	101,837
A0A4D8YUZ8	ATP-dependent Clp protease ATP-binding subunit ClpB	clpB Saspl_045300	A0A4D8YUZ8_SALSN	115,287
A0A4D8YVZ9	12-oxophytodienoic acid reductase	OPR Saspl_045519	A0A4D8YVZ9_SALSN	44,578
A0A4Y5UFC2	Photosystem II CP47 reaction center protein (PSII 47 kDa protein) (Protein CP-47)	psbB	A0A4Y5UFC2_9LAMI	56,127
A0A4D8Y7S6	Peptidyl-prolyl cis-trans isomerase (PPIase) (EC 5.2.1.8)	Saspl_050079	A0A4D8Y7S6_SALSN	22,251
A0A4D9BF90	Chlorophyll a-b binding protein, chloroplastic	LHCB1 Saspl_033725	A0A4D9BF90_SALSN	28,335
A0A4D8YG96	Acetyl-CoA carboxylase biotin carboxyl carrier protein	accB bccP Saspl_049121	A0A4D8YG96_SALSN	35,180

A0A4D9AJ79	V-type H <sup>+</sup> -transporting ATPase subunit D	ATPeV1D Saspl_033317	A0A4D9AJ79_SALSN	29,268
A0A4D8ZG50	Large subunit ribosomal protein L14e	RP-L14e RPL14 Saspl_042930	A0A4D8ZG50_SALSN	18,663
A0A4D9AU79	4-coumarate--CoA ligase (EC 6.2.1.12)	ACSF3 Saspl_027963	A0A4D9AU79_SALSN	72,498
A0A4D8YFB0	Elongation factor 1-beta	EEF1B Saspl_005328	A0A4D8YFB0_SALSN	23,710
A0A4D8ZIT3	23 kDa subunit of oxygen evolving system of photosystem II (23 kDa thylakoid membrane protein) (OEC 23 kDa subunit)	Saspl_034968	A0A4D8ZIT3_SALSN	28,031
A0A4D8XWL6	Uncharacterized protein	Saspl_052753	A0A4D8XWL6_SALSN	38,622
A0A4D8ZIT6	Solute carrier family 35, member E1	SLC35E1 Saspl_029380	A0A4D8ZIT6_SALSN	45,414
A0A4D9A3A5	Heat shock 70kDa protein 1/8	HSPA1_8 Saspl_031729	A0A4D9A3A5_SALSN	59,442
A0A4D8Z3X2	ERF-3 (ERF2) (Eukaryotic peptide chain release factor GTP-binding subunit) (Polypeptide release factor 3) (Translation release factor 3)	ERF3 GSPT Saspl_039926	A0A4D8Z3X2_SALSN	60,515
A0A4D8ZN65	50S ribosomal protein L5, chloroplastic	RP-L5 Saspl_034183	A0A4D8ZN65_SALSN	38,256
A0A4D9B265	40S ribosomal protein S3a	RP-S3Ae Saspl_013998	A0A4D9B265_SALSN	29,485
A0A4D9AQ61	Glucose-1-phosphate adenyltransferase (EC 2.7.7.27) (ADP-glucose pyrophosphorylase)	glgC Saspl_017175	A0A4D9AQ61_SALSN	56,832
A0A4D9BF14	Pto-interacting protein 1	PTI1 Saspl_033670	A0A4D9BF14_SALSN	44,113
A0A4D9BD15	Small subunit ribosomal protein S20	RP-S20 Saspl_009772	A0A4D9BD15_SALSN	25,333
A0A4D8ZLD9	Vacuolar protein-sorting-associated protein 4	VPS4 Saspl_004016	A0A4D8ZLD9_SALSN	48,119
A0A4D9AL47	ATP citrate synthase (EC 2.3.3.8)	ACLY Saspl_031557	A0A4D9AL47_SALSN	47,302
A0A4D8YBD7	Cell division protease FtsH	ftsH hflB Saspl_001150	A0A4D8YBD7_SALSN	73,246
A0A4D9C4E3	Peptidylprolyl isomerase (EC 5.2.1.8)	Saspl_002655	A0A4D9C4E3_SALSN	23,886
A0A4D8YMU7	Spatacsin	SPG11 Saspl_047787	A0A4D8YMU7_SALSN	367,427
A0A4D8ZIF0	Glyceraldehyde-3-phosphate dehydrogenase (NADP <sup>+</sup> )	gapN Saspl_043322	A0A4D8ZIF0_SALSN	52,931
A0A4D9BNG3	Small subunit ribosomal protein S9e	RP-S9e RPS9 Saspl_010998 Saspl_029764 Saspl_046005	A0A4D9BNG3_SALSN	22,969
A0A4D8ZRZ8	Dihydrolipoamide dehydrogenase	DLD lpd pdhD Saspl_031293	A0A4D8ZRZ8_SALSN	64,160
A0A4D9BVD5	PKS_ER domain-containing protein	Saspl_029419	A0A4D9BVD5_SALSN	65,871

A0A4D8ZRK1	14_3_3 domain-containing protein	Saspl_043108	A0A4D8ZRK1_SALSN	28,620
A0A4D8ZMV7	Photosystem I P700 chlorophyll a apoprotein A1 (EC 1.97.1.12) (PsaA)	psaA Saspl_035918	A0A4D8ZMV7_SALSN	83,034
A0A4D9ASN3	Uncharacterized protein	Saspl_001347	A0A4D9ASN3_SALSN	85,917
A0A4D9AAS6	Uncharacterized protein	Saspl_004359	A0A4D9AAS6_SALSN	50,099
A0A4D9ADV9	23 kDa subunit of oxygen evolving system of photosystem II (23 kDa thylakoid membrane protein) (OEC 23 kDa subunit)	Saspl_024914	A0A4D9ADV9_SALSN	25,051
A0A4D9ANC1	Glucose-6-phosphate isomerase (EC 5.3.1.9)	GPI Saspl_021035	A0A4D9ANC1_SALSN	66,759
E0D9C6	Ribulose biphosphate carboxylase large chain (EC 4.1.1.39) (Fragment)		E0D9C6_9LAMI	46,110
A0A4D9BKG1	Fe2OG dioxygenase domain-containing protein	Saspl_006609	A0A4D9BKG1_SALSN	35,692
A0A4D9BYN9	Peptidylprolyl isomerase (EC 5.2.1.8)	FKBP2 Saspl_007157	A0A4D9BYN9_SALSN	23,695
A0A4D9BV98	40S ribosomal protein S7	RP-S7e RPS7 Saspl_007958 Saspl_007959	A0A4D9BV98_SALSN	21,790
A0A4D9AAG0	Histone H3	Saspl_029541 Saspl_031632 Saspl_034225 Saspl_043109 Saspl_050772	A0A4D9AAG0_SALSN	15,406
A0A4D8ZNJ6	Small nuclear ribonucleoprotein D1	SNRPD1 Saspl_038213	A0A4D8ZNJ6_SALSN	68,360
A0A4D9BFL6	Peptidylprolyl isomerase (EC 5.2.1.8)	Saspl_033733	A0A4D9BFL6_SALSN	55,095
A0A4D8ZZ94	Large subunit ribosomal protein L17e	RP-L17e RPL17 Saspl_021001 Saspl_022656 Saspl_032641	A0A4D8ZZ94_SALSN	19,773
A0A4D8ZP53	Large subunit ribosomal protein L10e	RP-L10e RPL10 Saspl_036678	A0A4D8ZP53_SALSN	25,004
A0A4D8YPB8	40S ribosomal protein S3a	RP-S3Ae Saspl_046618	A0A4D8YPB8_SALSN	83,492
A0A4D9BNL6	3-hydroxyisobutyryl-CoA hydrolase	HIBCH Saspl_018806	A0A4D9BNL6_SALSN	48,711
A0A4D9BM55	Small subunit ribosomal protein S2e	RP-S2e RPS2 Saspl_022296 Saspl_039250	A0A4D9BM55_SALSN	29,727
A0A4D8YRB4	Phosphopyruvate hydratase (EC 4.2.1.11)	ENO eno Saspl_044606	A0A4D8YRB4_SALSN	48,831
A0A4D9C3K2	Large subunit ribosomal protein L4e	RP-L4e RPL4 Saspl_003047	A0A4D9C3K2_SALSN	44,199

A0A4D9ARQ2	Small subunit ribosomal protein S3e	RP-S3e RPS3 Saspl_009004 Saspl_023742 Saspl_038429 Saspl_047580	A0A4D9ARQ2_SALSN	26,046
A0A4D9C5U0	Aldo_ket_red domain-containing protein	Saspl_022413	A0A4D9C5U0_SALSN	46,977
A0A4D9AFS9	Diadenosine tetraphosphate synthetase (EC 6.1.1.14)	GARS glyS1 Saspl_025810	A0A4D9AFS9_SALSN	73,270
A0A4D8YV21	Small subunit ribosomal protein S5e	RP-S5e Saspl_030711	A0A4D8YV21_SALSN	23,650
A0A4D9BZV3	Serine/threonine-protein kinase SRK2	SNRK2 Saspl_006985	A0A4D9BZV3_SALSN	40,665
A0A4D8Z3T3	Potassium voltage-gated channel Shaker-related subfamily A, beta member 2	KCNAB2 Saspl_039876	A0A4D8Z3T3_SALSN	41,215
<b>Shared proteins between Control, p-CA and NaCl</b>				
A0A4D9BZT4	50S ribosomal protein L9, chloroplastic (CL9)	RP-L9 Saspl_007034	A0A4D9BZT4_SALSN	25,170
A0A4D8YPD4	Superoxide dismutase (EC 1.15.1.1)	SOD1 Saspl_043683	A0A4D8YPD4_SALSN	17,858
A0A4D9A8D9	Alanine transaminase	GPT ALT Saspl_021843	A0A4D9A8D9_SALSN	56,616
A0A4D9C4G4	Photosystem II 22kDa protein	psbS Saspl_002744	A0A4D9C4G4_SALSN	26,902
A0A4Y6I5B4	Photosystem I P700 chlorophyll a apoprotein A2 (EC 1.97.1.12) (PSI-B) (PsaB)	psaB	A0A4Y6I5B4_9LAMI	82,411
A0A4D8XZ08	Small subunit ribosomal protein S20e	RP-S20e RPS20 Saspl_051315	A0A4D8XZ08_SALSN	13,578
A0A4D8YBK4	PSI subunit V	psaL Saspl_046450	A0A4D8YBK4_SALSN	22,832
A0A342D2J4	Photosystem II protein D1 (PSII D1 protein) (EC 1.10.3.9) (Photosystem II Q(B) protein)	psbA DSC0004	A0A342D2J4_9LAMI	38,879
A0A4D8YBF6	Ketol-acid reductoisomerase (EC 1.1.1.86) (Acetohydroxy-acid reductoisomerase) (Alpha-keto-beta-hydroxylacyl reductoisomerase)	ilvC Saspl_001170	A0A4D8YBF6_SALSN	62,820
A0A4D8YNQ4	Chlorophyll a-b binding protein, chloroplastic	LHCB1 Saspl_043985	A0A4D8YNQ4_SALSN	28,021
A0A4D9B2B0	Aquaporin PIP	PIP Saspl_002264	A0A4D9B2B0_SALSN	31,406
A0A4D9B4V6	Fructose-bisphosphate aldolase (EC 4.1.2.13)	ALDO Saspl_037580	A0A4D9B4V6_SALSN	38,384
A0A4D9AS13	Uncharacterized protein	Saspl_010118	A0A4D9AS13_SALSN	16,970
A0A4D9A5S1	TPM_phosphatase domain-containing protein	Saspl_021250	A0A4D9A5S1_SALSN	32,556
A0A4D8YR42	Small subunit ribosomal protein S14e	RP-S14e RPS14 Saspl_046297	A0A4D8YR42_SALSN	16,999



A0A4D8YNS5	Fructose-bisphosphate aldolase (EC 4.1.2.13)	ALDO Saspl_044613	A0A4D8YNS5_SALSN	38,365
A0A4D8Z9L5	ATPase_AAA_core domain-containing protein	Saspl_040863	A0A4D8Z9L5_SALSN	51,130
A0A4D8ZQC8	Polyadenylate-binding protein	PABPC Saspl_024020	A0A4D8ZQC8_SALSN	139,362
A0A0B5CUQ7	30S ribosomal protein S7, chloroplastic	rps7	A0A0B5CUQ7_9LAMI	17,361
A0A4D8YUF5	Uncharacterized protein	Saspl_040210	A0A4D8YUF5_SALSN	35,455
A0A4D9AKT2	GDP-D-mannose 3', 5'-epimerase	GME Saspl_024797	A0A4D9AKT2_SALSN	42,605
A0A4D9BC99	Chaperonin GroES	groES HSPE1 Saspl_020467	A0A4D9BC99_SALSN	14,823
A0A4D9AI95	60S ribosomal protein L36	RP-L36e RPL36 Saspl_004842 Saspl_011188 Saspl_032238 Saspl_050561	A0A4D9AI95_SALSN	12,342
A0A4D8YWX1	Ferredoxin--NADP reductase, chloroplastic (FNR) (EC 1.18.1.2)	pethH Saspl_039702	A0A4D8YWX1_SALSN	40,162
A0A4D8Y4L9	Photosystem II oxygen-evolving enhancer protein 3	psbQ Saspl_034594 Saspl_051019	A0A4D8Y4L9_SALSN	23,655
A0A4D8ZGP3	Vacuolar proton pump subunit B (V-ATPase subunit B) (Vacuolar proton pump subunit B)	ATPeV1B Saspl_037917	A0A4D8ZGP3_SALSN	56,228
A0A4D9C1Q5	Abhydrolase_3 domain-containing protein	Saspl_013419	A0A4D9C1Q5_SALSN	34,428
A0A4D8XV74	PAP_fibrillin domain-containing protein	Saspl_000212	A0A4D8XV74_SALSN	32,948
A0A4D8YPZ8	Solute carrier family 25 (Mitochondrial phosphate transporter), member 3	SLC25A3 Saspl_043484	A0A4D8YPZ8_SALSN	33,272
A0A4D9B533	Carbonic anhydrase (EC 4.2.1.1) (Carbonate dehydratase)	cynT can Saspl_015600	A0A4D9B533_SALSN	34,506
A0A4D8YHL8	Fructose-bisphosphate aldolase (EC 4.1.2.13)	ALDO Saspl_044294	A0A4D8YHL8_SALSN	75,084
A0A4D8XXU1	Large subunit ribosomal protein L6	RP-L6 Saspl_053938	A0A4D8XXU1_SALSN	27,421
A0A4D8YJF0	Hydroxypyruvate reductase 1	HPR1 Saspl_050858	A0A4D8YJF0_SALSN	42,836
A0A4D9ALY8	4-diphosphocytidyl-2C-methyl-D-erythritol synthase (EC 2.7.7.60) (MEP cytidyltransferase)	ispD Saspl_004436	A0A4D9ALY8_SALSN	35,092
A0A4D8YBU7	Nucleoside diphosphate kinase (EC 2.7.4.6)	ndk Saspl_048159	A0A4D8YBU7_SALSN	45,861
A0A4D9A9G5	Bet_v_1 domain-containing protein	Saspl_019597	A0A4D9A9G5_SALSN	17,675
A0A4D9B146	Catalase (EC 1.11.1.6)	Saspl_020120	A0A4D9B146_SALSN	59,204
A0A4D9ANY1	Photosystem II 10 kDa polypeptide, chloroplastic	psbR Saspl_023669	A0A4D9ANY1_SALSN	14,275
A0A4D9ANI4	Phosphoribulokinase (EC 2.7.1.19)	PRK Saspl_009278	A0A4D9ANI4_SALSN	44,421



<b>Shared proteins between Control, <i>p</i>-CA and NaCl + <i>p</i>-CA</b>				
A0A4D8ZKY3	Large subunit ribosomal protein L28e	RP-L28e RPL28 Saspl_033108	A0A4D8ZKY3_SALSN	16,019
A0A4D9B365	Large subunit ribosomal protein L30e	RP-L30e RPL30 Saspl_015062	A0A4D9B365_SALSN	147,676
A0A4D8ZPD7	Uncharacterized protein	Saspl_040443	A0A4D8ZPD7_SALSN	449,217
<b>Shared proteins between Control and NaCl + <i>p</i>-CA</b>				
A0A4D9AF75	Sacsin	SACS Saspl_023991	A0A4D9AF75_SALSN	530,641
A0A4D9AVE3	Small subunit ribosomal protein S35	MRPS35 Saspl_001853	A0A4D9AVE3_SALSN	58,307
A0A4D9AR80	PAX-interacting protein 1	PAXIP1 Saspl_010165	A0A4D9AR80_SALSN	152,785
A0A4D8ZMF7	Uncharacterized protein	Saspl_003625	A0A4D8ZMF7_SALSN	185,480
A0A4D9AXJ5	Glyceraldehyde 3-phosphate dehydrogenase	GAPDH Saspl_011394	A0A4D9AXJ5_SALSN	195,327
A0A0U1XN56	ATP binding cassette transporter subfamily B1	ABCB1	A0A0U1XN56_LAVAN	135,814
<b>Shared proteins between Control and NaCl</b>				
A0A4D9A9H2	Beta-D-xylosidase 4	XYL4 Saspl_030018	A0A4D9A9H2_SALSN	82,333
A0A2R4LNR9	Glyceraldehyde-3-phosphate dehydrogenase (EC 1.2.1.-)	GAPDH	A0A2R4LNR9_9LAMI	36,706
A0A4D9BMA3	F-type H <sup>+</sup> -transporting ATPase subunit O	ATPeF0O Saspl_018597	A0A4D9BMA3_SALSN	26,421
<b>Shared proteins between Control, NaCl and NaCl + <i>p</i>-CA</b>				
A0A0H4STL7	Ribulose biphosphate carboxylase large chain (EC 4.1.1.39) (Fragment)	rbcL	A0A0H4STL7_9LAMI	19,065
<b>Shared proteins between <i>p</i>-CA and NaCl + <i>p</i>-CA</b>				
A0A4D9C104	Uncharacterized protein	Saspl_013625	A0A4D9C104_SALSN	211,211
A0A4D9AWI0	SWI/SNF-related matrix-associated actin-dependent regulator of chromatin subfamily A member 2/4	SMARCA2_4 Saspl_002270	A0A4D9AWI0_SALSN	111,164
A0A4D9AD33	Lysine-specific histone demethylase 1A	KDM1A AOF2 LSD1 Saspl_020725	A0A4D9AD33_SALSN	219,517

Shared proteins between <i>p</i> -CA and NaCl				
A0A4D9A7I7	Bet_v_1 domain-containing protein	Saspl_019601	A0A4D9A7I7_SALSN	17,854
A5Y6Z9	Non-specific lipid-transfer protein	A5Y6Z9_SALMI	11,328	
A0A4D9AZ46	Glycine cleavage system H protein	gcvH Saspl_039430	A0A4D9AZ46_SALSN	17,264
A0A4D8ZW97	Uncharacterized protein	Saspl_025097	A0A4D8ZW97_SALSN	12,712
A0A4D8ZWL9	PSI-K (Photosystem I subunit X)	psaK Saspl_027721	A0A4D8ZWL9_SALSN	13,251
A0A4D9AY73	NmrA domain-containing protein	Saspl_001935	A0A4D9AY73_SALSN	33,730

